MOLECULAR ANALYSIS OF LONGEVITY ASSURANCE GENES (LASS)/CERAMIDE SYNTHASES (CerS) 4 AND 5 IN ENDOMETRIAL AND COLON CANCER

Rahaba Makgotso Mojakgomo

A dissertation submitted to the Faculty of Health Sciences, University of the Witwatersrand, in fulfilment of the requirements for the degree of Master of Science in Medicine

Johannesburg 2012

Supervisor: Prof. Margot Hosie

DECLARATION

I Rahaba Makgotso Mojakgomo, declare that this dissertation is my own unaided work. It is being submitted for the Master of Science in Medicine degree at the University of the Witwatersrand, Johannesburg. It has not been submitted before for any degree or examination in any other university.

_____

(Signature of candidate)

_____ day of _____ 2012

DEDICATION

This dissertation is dedicated to the precious Lamb of God, whose love has never failed me

To my parents, Mr and Mrs Mojakgomo. Thank you for believing in me, encouraging and supporting me every step of the way.

To my son, Omolemo Mojakgomo, whose love is amazing

To my fiancé, Owen Marima, for his love, encouragement and support

To my family, both the Mojakgomo and the Makoro family

To my family at Rock of Salvation Community Church

Thank you all for encouraging me during tough times

Jehovah The Most High is faithful

ABSTRACT

Longevity Assurance (LASS) genes also known as Ceramide Synthases (CerS) belong to a family of six related genes. CerS gene products have been shown to produce ceramide, hence their name CerS. Ceramide is a bio-effector molecule, belonging to the family of sphingolipids (SLs), which are important components of cell membranes. Ceramide has been implicated in cancer and apoptosis. Cancer still remains the second leading cause of death, globally and in South Africa. The proper regulation of the balance between cell growth and cell death is essential for cellular homeostasis. Failure to properly regulate this balance may lead to pathologic conditions such as cancer development. CerSes have been implicated in cancer biology, especially apoptosis, through the action of ceramide. The precise roles of CerSes in different cancers is not yet fully understood, especially the role of CerS4 and CerS5 in colon and endometrial cancers.

The broad aim of this study was to investigate the role of CerS4 and CerS5 in apoptosis and, thus in cancers of the endometrium and colon, which are among the top five prevalent cancers globally. Bioinformatics tools (STRING, BioGRID and IntAct databases) were used to determine the CerS4 and CerS5 potential protein-interacting partners, to assess their possible roles in cancer biology. Sequence alignment tools (Multi-Align, Clustal Omega and COBALT) were then used to examine if there was sequence similarity between CerS4 and or CerS5 and their possible protein interacting partners. Total RNA was extracted from cancerous and non-cancerous cells, or calibrator and test samples. Quantitative relative expression of CerS4 and CerS5 was then determined in all cell lines, normalised to β-actin. Apoptosis was induced in cultured colon cells using 5-fluorouracil, while anastrozole was used to induce

apoptosis in endometrial cells. Fluorescence activated cell sorting (FACS) was used to analyse and quantify apoptosis. Quantitative Real-Time Polymerase Chain Reaction (qRT-PCR) was again used to determine change in expression level of CerS4 and CerS5 after apoptosis induction.

Bio-informatics analysis revealed at least 30 proteins that could possibly interact with CerS4 and 12 that may interact with CerS5, and these are involved in apoptosis, cell-cycle regulation, ubiquitination and interestingly in bone and cartilage formation, as well as the central nervous system. Surprisingly, no sequence similarity was revealed between CerS4 and/or CerS5 and the possible interacting partners, when all aligned together. Using quantitative real-time PCR, both LASS4 and 5 were shown to be up-regulated in colon and endometrial cancer cells. Apoptosis induction resulted in down-regulation of LASS 4 and LASS 5 in colon and endometrial cancers. These findings implicate the involvement of these genes in cancer and apoptosis. Whether these genes play a pro- or anti-apoptotic roles in the cancers of the colon and endometrium is not conclusive at this stage. It may also be possible that these genes could exert opposing roles in the same or different tissues. Targeting this family of genes and understanding their precise individual roles in different types of cancer, is a promising therapeutic tool to new anti-cancer drug discovery or improving on the existing ones.

ACKNOWLEDGEMENTS

My sincere thanks to:

- my supervisor Prof Margot Hosie, for her support, enthusiasm and for believing in me.
- Dr Zukile Mbita, for his support and encouragement.
- Dr Raymond Motadi for allowing me to use his laboratory.
- the National Research Foundation (NRF), the South African Medical Research Council (SAMRC) and the Cancer Association of South Africa (CANSA) for funding this project, and all who have contributed towards the success of this project.
- Jenny Seagreen, for attending to the technical quality (layout) of this document.

TABLE OF CONTENTS

Page

LIST OF FIGURES

LIST OF TABLES

LIST OF ABBREVIATIONS

%	Percentage
ºC	Degrees Celcius
5-FU	5 Fluorouracil
Aa	Amino acid
ADP	Adenosine diphosphate
ANOVA	One way analysis of variance
AP-1	Activator protein-1
BioGRid	Biological General Respiratory for Interaction Datasets
BLAST	Basic Local Alignment Search Tool
Bp	Base pair
BSA	Bovine serum albumin
Caco-2	The human Caucasian colon adenocarcinoma cell line
CANSA	Cancer Association of South Africa
cDNA	Complementary deoxyribonucleic acid
CerS	Ceramide synthase
COBALT	Constraint based Multiple Alignment Tool
CT	Threshold cycle
DMEM	Dulbecco's Modification of Eagle's Medium
DMSO	Dimethylsulfoxide
DNA	Deoxyribonucleic acid
dNTP	Deoxyribonucleotide triphosphate
E. coli	*Escherichia coli*
EDTA	Ethylenediaminetetraacetic acid

FA	Fatty acid
FACS	Fluorescence activated cell sorter
FBS	Fetal bovine serum
FITC	Fluorescein isothiocyanate
GMMe	Mink Uterus Endometrium Epithelial Cells
Hec-1A	Human endometrial cancer cells
Hox	Homeobox domain
HT-29	Human colon tumour cells
IntAct	The IntAct molecular interaction database
Kb	Kilo base
LASS	Longevity assurance genes
LB	Luria Bertani Broth
Mg	Milligrams
Ml	Millilitre
mM	Millimolar
mRNA	Messenger ribonucleic acid
NCBI	National centre for biotechnology information
NF-κB	Nuclear factor κB
Ng	Nano grams
PBS	Phosphate buffered saline
PCR	Polymerase chain reaction
PI	Propidium iodide
QRT-PCR	Quantitative Real time polymerase chain reaction
rDNA	Recombinant deoxyribonucleic acid
RNA	Ribonucleic acid

Xg	Revolutions per minute
RT-PCR	Real time polymerase chain reaction
SD	Standard deviation
SEM	Standard Error Mean
SLs	Sphingolipids
SM	Sphingomyelin
STRING	Search Tool for the Retrieval of Interacting Genes/Proteins
TBS	Tris buffered saline
TLC	Tram-Lag-CLN8 domain
TNFR-1	Tumour necrosis factor receptor 1
TNF-α	Tumour necrosis factor – alpha
Tris	Tris(hydroxymethyl)-aminomethane
TS	Thymidylate synthatase
V	Volts
α	Alpha
β	Beta
κ	Kappa
μg	Micro gram
μM	Micro molar

CHAPTER 1

INTRODUCTION

1.1 CANCER

Cancer is one of the leading causes of mortality globally and may be described as the uncontrolled growth of undifferentiated cells in the body (Parkin *et al.*, 2005; Matsumoto *et al*., 2008; Sambo *et al*., 2012). Normal tissue growth and development require prolific cell division, regulated cell differentiation, and appropriately timed cell death or apoptosis (Kronja and Orr-Weaver, 2011). Neoaplastic transformation of a tissue that results in tumour growth generally occurs when abnormal regulatory mechanisms promote excessive cell division, impaired cell differentiation and failure to undergo apoptosis. In most tumour types, this aberrant control originates at the genetic level (Parkin *et al*., 2005).

The life cycle of a cell consists of two alternating stages, interphase and mitosis, shown in figure 1.1. Interphase, which is the longer phase, is further divided into three substages or phases and these are: gap 1 (G1), DNA synthesis (S phase) and gap 2 (G2). During G1, cells use DNA as a template to transcribe mRNA then to translate mRNA into proteins. DNA is replicated in the S phase and this doubles the cellular DNA content. During the G2 phase, the DNA repair mechanism corrects any mutations that occurred during the S phase as the cell makes final preparations for entry into mitosis. On the other hand, mitosis is a shorter stage during which cell division occurs. The end result of mitosis is two identical daughter cells each with a complete set of 23 chromosome pairs (Wang *et al*., 2011).

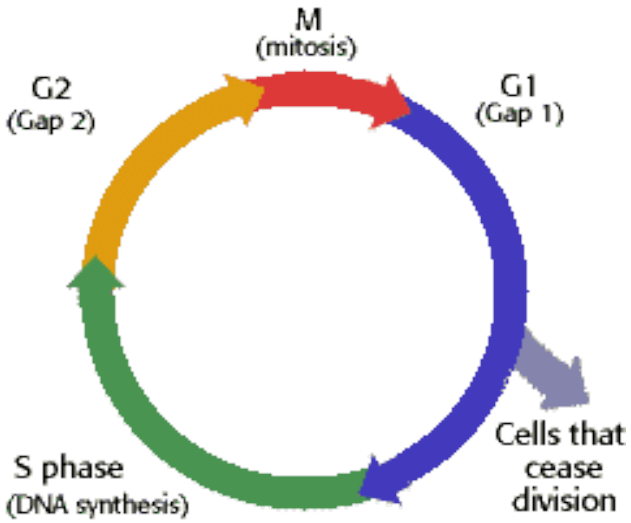

Figure 1.1 – Regulation of the cell cycle: The cell cycle is an ordered set of events and is divided into the Gap 1 (G1) phase, the Synthesis (S)-phase, the G2-phase and the Mitosis (M)-phase. Cells multiply and divide in the cell cycle. Cells double their DNA during the S-phase while nuclear and cytoplasmic division occurs during the M-phase (Parkin *et al*., 2005; Kronja and Orr-Weaver, 2011).

It is hypothesised that failure to properly regulate the cycle, may lead to the survival of damaged cells which can lead to the development of pathological conditions such as cancer. Tumours may develop as a consequence of genetic alterations that occur at the S-phase. These alterations can confer growth advantages to cells as well as the ability to proliferate uncontrollably (King and Cidlowski, 1998; Göhler *et al*., 2005) Compared with normal cells, cancer cells lack contact inhibition, that is, they do not stop growing when they touch one another and therefore may form tumours that can take over and destroy organs (Matsumoto *et al*., 2008).

1.2 WHAT CAUSES CANCER?

Normally, cells have a finite life span, however, sometimes cells acquire genetic changes that make them resistant to cell death. Instead of dying cancer cells grow and multiply infinitely, aggregating together to form tumours (Vogelstein and Kinzler, 2004; Reddel, 2010). Tumours

may be malignant (cancerous) or non-malignant (benign). Malignant tumours have the ability to metastasise and invade other parts of the body (Matsumoto, 2008). Typical features of all forms of cancer include uncontrolled cell proliferation, resistance to apoptosis, metastasis, activation of telomerase, mutation, amplification and re-arrangement of proto-oncogenes and deletion or silencing of tumour suppressor genes (MacKenzie *et al*., 2002; Torkamani *et al*., 2009). The transformation process can be simply divided into initiation (genetic alterations), clone expansion, apoptotic resistance, and tumour invasion to adjacent cells including metastasis to other parts of the body (MacKenzie *et al*., 2002). The majority of organs in the body develop cancer; the endometrium and the colon are also susceptible to cancer. Furthermore, there is evidence to suggest that cancers of the colon and endometrium are linked to genetic alterations (Wu *et al*., 2004; Abe *et al*., 2006).

1.3 GENES AND THEIR PATHWAYS IN CONTROLLING CANCER

Cancer is a metabolic disorder with multi-step genetic alterations. Alterations in three types of genes are responsible for tumourigenesis and these include: oncogenes, tumour-suppressor genes and stability genes (Vogelstein and Kinzler, 2004). Unlike diseases such as cystic fibrosis or muscular dystrophy, where mutations in one gene can cause a disease; no single gene defect ‘causes’ cancer. Mammalian cells have multiple safeguards to protect themselves against potentially lethal effects of cancer gene mutations, and only when several genes are defective does an invasive cancer develop (Vogelstein and Kinzler, 2004). In some instances, oncogenes are mutated in ways that render the gene constitutively active or active under conditions in which the wild-type gene is not. Oncogene activations can result from chromosomal translocations, gene amplifications or from subtle intragenic mutations affecting crucial residues that regulate the activity of the gene product (Davies *et al*., 2002). Tumour-suppressor genes are targeted in the opposite way by genetic alterations where

mutations reduce the activity of the gene product (Santarosa and Ashworth, 2004). Oncogene and tumour-suppressor gene mutations all operate similarly at the physiological level: meaning that they drive the neoplastic process by increasing tumour cell number through the stimulation of cell birth or the inhibition of cell death or cell-cycle arrest. The increase can be caused by the activation of genes that drive the cell cycle, by inhibition of normal apoptotic processes or facilitation of nutrient supply through enhanced angiogenesis (Vogelstein and Kinzler, 2004). A third class of cancer genes, called stability genes or caretakers, promotes tumourigenesis in a completely different way when mutated. This class includes the mismatch repair (MMR), nucleotide-excision repair (NER) and base-excision repair (BER) genes responsible for repairing subtle mistakes made during normal DNA replication or induced by exposure to mutagens (Vogelstein and Kinzler, 2004). Other stability genes control processes involving large portions of chromosomes, such as those responsible for mitotic recombination and chromosomal segregation (for example, BRCA1) (Friedberg, 2003; Vogelstein and Kinzler, 2004). Stability genes keep genetic alterations to a minimum, and thus when they are inactivated, mutations in other genes occur at a higher rate. Most genes are potentially affected by the resultant increased rate of mutation, but only mutations in oncogenes and tumour-suppressor genes affect net cell growth and can thereby confer a selective growth advantage to the mutant cell. As with tumour-suppressor genes, both alleles of stability generally must be activated for a physiologal effect to result (Friedberg, 2003).

Cancer gene mutations enhance net cell growth. For example, several cancer genes directly control transitions from a resting stage (G0 or G1) to a replicating phase (S) of the cell cycle. The products of these genes include proteins as diverse as cdk4 (a kinase), cyclin D1 (which interacts with and activates cdk4), Rb (a transcription factor) and p16 (which interacts with and inhibits cdk4) (Sherr, 2000; Classon and Harlow, 2002; Ortega et al., 2002). The genes encoding Rb and p16 are tumour-suppressor genes inactivated by mutation, whereas those

encoding cdk4 and cyclin D1 are oncogenes activated by mutation. The p53 pathway is another example that highlights the importance of pathways inactivation in the development and the pathogenesis of cancer, rather than individual genes. The p53 protein is a transcription factor that normally inhibits cell growth and stimulates cell death when induced by cellular stresses (Vogelstein *et al*., 2000; Oren, 2003).

Cancer is a multistep genetic process. It has been proven that mutations in a pathway rather than single genes is responsible for tumourigenesis. The p53 and the Rb tumour suppressor genes pathways have been implicated in many types of cancer when inactivated, colon cancer, for example (Prives and Hall, 1999). Rb has been shown to be a down-stream target of ceramide. Activation of Rb by ceramide leads to growth arrest and apoptosis (Ogretmen, 2006). Ceramide is a sphingolipid which has been implicated in cancer biology (Pwezner-Jung *et al*., 2006; Huang *et al*., 2011). Two pathways result in the synthesis of ceramide and these are sphingomyelin (SM) hydrolysis and *de novo* by Ceramide Synthases (CerSes), also known as Longevity Assurance (LASS) genes, which is a family of six related genes (Ogretmen, 2006).

1.4 THE ROLE OF CERAMIDE IN APOPTOSIS

The cellular levels of endogenous ceramide increase in response to stress causing agents such as UV irradiation, hyperthermia (heat stress), or chemotherapeutic agents. The increased concentration of ceramide occurs via the activation of *de novo* synthesis and/or sphingomyelinases (SMases) that hydrolyse sphingomyelin (SM) into ceramide. The high concentrations of ceramide may mediate anti-proliferative pathways, or inhibit prosurvival mechanisms mainly by regulating multiple signaling cascades controlled by protein phosphatase 1 and 2A (also known as CAPPs, ceramide-activated protein phosphatases), kinases, or cathepsin D. Additionally downstream targets of ceramide signaling include

telomeres, which rapidly shorten, and human telomerase reverse transcriptase (hTERT) expression, which is modulated (Ogretmen and Hannun, 2001). Telomerase elongates telomeres at the end of chromosomes and is involved in cellular immortalisation and malignant transformation when other oncogenic signals are present. Transcription of hTERT, which is the catalytic subunit of telomerase, is inhibited by ceramide in a c-Myc dependent mechanism (Ogretmen, 2006). Furthermore ceramide also activates retinoblastoma (RB) and p53-dependent cell death, and regulates the functions of cyclin-dependent kinases and apoptosis related proteins such as Bcl-2, caspases and proteases. Ceramide also induces caspase-independent apoptosis (Ogretmen, 2006). In addition, sphingosine-1-phosphate (S1P) which is also a bioactive sphingolipid, is considered to be a pro-survival lipid, because of its involvement in malignant transformation, cancer proliferation, inflammation, vasculogenesis, and resistance to apoptotic cell death (Ogretmen, 2006). Interestingly, in the recent studies by Senkal *et al*., (2010), it has been shown that ceramide acts as a double-edged lipid, either inhibiting or promoting apoptosis, depending on the ceramide species produced by various CerSes.

1.5 APOPTOSIS ACTIVATORS

Apoptosis also known as programmed cell death (PCD) is characterized by a series of distinct morphological and biochemical changes and plays vital roles in normal cell turnover and development in multicellular as well as in unicellular organisms (Sen *et al*., 2004). One of the hallmarks for cancer is resistance to apoptosis (Chaudhry and Asselin, 2009). DNA topoisomerases are ubiquitous enzymes that catalyse the interconversion of topological isomers of DNA molecules and are involved in many vital processes such as replication, transcription, recombination, integration and chromosomal segregation (Sen *et al*., 2004). These enzymes act by sequential breakage and reunion of either one strand (topo

I) or both the strands of DNA (topo II) (Sen *et al*., 2004). DNA topoisomerases have been shown to be essential as molecular targets for anti-tumour agents like camptothecin (Wang, 1991; Sen *et al*., 2004).

Camptothecin, a class I DNA topoisomerase inhibitor that stabilizes topo I-DNA covalent complex and blocks subsequent rejoining of the DNA break, is widely used as an effective anti-tumour drug (Sen *et al*., 2004). In cultured cells, Camptothecin inhibits both DNA and RNA synthesis, arrests cells in the G2 phase of the cell cycle, stimulates sister chromatid exchanges and chromosomal aberrations, elevates p53 levels, induces multiubiquitination and degradation of topo I and activates signal transduction molecules such as proto-oncogenes and NF-kb (Sen *et al*., 2004). Aromatase inhibitors such as anastrozole have been previously shown to effectively treat endometrial cancer, while 5-FU has been used to treat colon cancer (Ashktorab *et al*., 2005; Meresman *et al*., 2005).

1.5.1 Anastrozole and 5-Fluorouracil (5-FU)

Aromatase is a key enzyme in the synthesis of estrogen that is responsible for binding of testosterone and catalyzes the series of reactions eventually resulting in estrogen production (Jongen *et al*., 2005). Previous reports demonstrated that aromatase is present in endometrial cancer tissue, suggesting that aromatase plays a role in converting testosterone into mitogenic estrogens in endometrial tissue (Lin *et al*., 2009). Anastrozole (Sigma-Aldrich, USA), an aromatase inhibitor (Burstein *et al*., 2010) was used to induce apoptosis in endometrial cells (Meresman *et al*., 2005), and is shown in figure 1.2. Five-Fluorouracil is a potent inhibitor of thymidylate synthatase (TS), (Lu *et al*., 2011) which (TS) is the limiting irreversible step in the synthesis of DNA. Five-FU (Sigma-Aldrich) has been reported to be active against solid tumours like breast, head and neck and cancer of the colon (Wei *et al*., 2006). It has been found that 5-FU induces apoptosis in colon cancer in three ways. Firstly by inhibiting DNA

synthesis, secondly by activating the caspase-8 pathway and finally by inducing the expression of the Fas-ligand and a p-53-dependent increase in cell surface expression of Fas. (Wei *et al*., 2006). The Fas ligand expression in turn activates transcription factors NF-kB and AP-1, which additionally causes tumour cell death via autocrine and paracrine pathways. Interestingly, it has been shown that 5-FU dependent apoptosis in colon cancer cells is blocked by anti-Fas antibodies. (Ashktorab *et al*., 2005). The structure of 5-FU, is shown in figure 1.3.

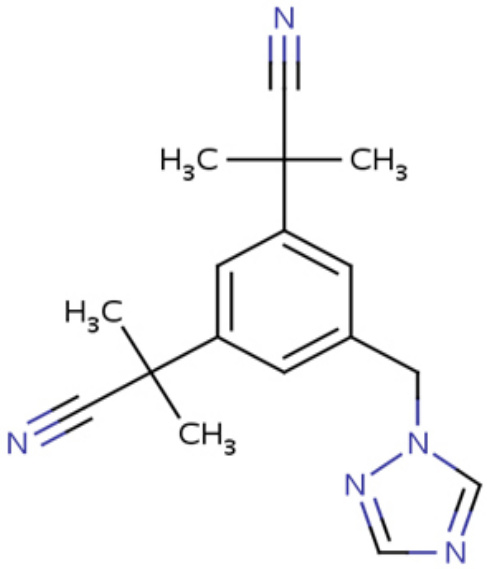

Figure 1.2 - Structure of anastrozole: Anastrozole is an aromatase inhibitor, blocking the synthesis of estrogen and thus blocking proliferation. It was used to induce apoptosis in uterine tissue (www.drugbank.ca.za).

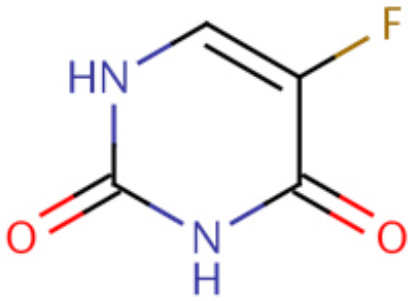

Figure 1.3 - Structure of 5-Fluorouracil (5-FU): 5FU inhibits thymidylate synthatase (TS), which is a key enzyme to DNA synthesis in cancer cells. As a result these cancer cells do not pass the S-phase and therefore cannot divide and multiply, but undergo apoptosis. (www.drugbank.ca.za).

1.6 RATIONALE

Cancer is a multi-step genetic process, being the second leading cause of mortality worldwide (Vogelstein and Kinzler, 2004; Moodley *et al*., 2009). Therefore there is an extensive effort to develop new anti-cancer drugs or to improve the existing ones. As a product of CerSes, ceramide has been implicated in cancer biology. Much data has been reported on ceramide generated by the SM hydrolysis (for example, mutation of SMase in exon 4 in HT-29 colon cells). On contrary, little is known about ceramide produced by CerSes, especially in colon and endometrial cancers, which are amongst the most prevalent in South Africa (CANSA, 2012). Furthermore, CerSes have been shown to produce different ceramide molecules (Pewzner-Jung *et al*., 2006). To complicate matters, distinct ceramide molecules produced by different CerSes have been shown to exert opposing roles in the same or different tissues, i.e CerS1 was shown to play an pro-apoptotic role in head and neck squamous cell carcinoma (HNSCC), while CerS6 promoted growth of these cancer cells (Senkal *et al*., 2007). Additionally, CerS4 and CerS5 have been previously implicated in solid tumours such as breast cancer (Schiffmann *et al*., 2009). However, the precise roles of CerS4 and CerS5 in colon and endometrial cancers are unknown. Understanding the molecular mechanisms

underlying pathways involving CerS4 and CerS5 may significantly contribute towards improving anti-cancer-therapeutics.

1.7 HYPOTHESIS

Resistance to apoptosis is one of the hallmarks of cancer. CerSes (including CerS4 and CerS5) have been implicated in lung and breast cancer (Senkal *et al*., 2007; Panjarian *et al*., 2008). However, little is known about the roles of CerS4 and CerS5 in endometrial and colon cancer. The hypothesis therefore states that CerS4 and CerS5 are involved in the apoptotic regulation of endometrial and colon cancers. Thus failure to properly regulate molecular mechanisms underlying these two genes may play a role in the development and the pathogenesis of endometrial and colon cancer.

1.8 RESEARCH QUESTIONS

- Do CerS4 and CerS5 interact with other proteins shown to be involved in apoptosis?
- Are the expression levels of CerS4 and CerS5 affected in cancerous versus non-cancerous cell lines?
- Is there any relationship between apoptosis regulation and CerS4 or CerS5?
- Does apoptosis induction modulate the expression levels of CerS4 and CerS5 in endometrial and colon cancer?

1.9 BROAD OBJECTIVE

The broad objective of this study was to determine the expression levels of CerS4 and CerS5 in endometrial and colon cancers.

1.9.1 Specific-objectives

- To determine the possible protein-interacting partners of CerS4 and CerS5.
- To determine the expression levels of CerS4 and CerS5 in endometrial and colon cancer relative to non-cancerous (differentiated) cell lines using quantitative real-time PCR (qRT-PCR).
- To induce, quantify and analyse apoptosis in endometrial and colon cells; and determine the expression levels of CerS4 and CerS5 in endometrial and colon cell lines after apoptosis induction.

1.10 RESEARCH APPROACH

The use of bio-informatics to study interactions (including protein-protein interactions) is growing (Prieto and De Las, 2010). Protein-protein interactions are essential in cellular events such as protein and vesicle trafficking, cell-cycle, signal transduction, gene expression and DNA repairs (Pawson and Nash, 2003).

To address the research questions and objectives, we sought bio-informatics to determine CerS4 and CerS5 possible protein interacting partners. STRING, BioGRID and IntAct databases were used to identify the potential interacting protein partners of CerS4 and CerS5. Proteins involved in similar functions may share similar sequences and proteins with similar sequences may share similar functions (Sangar *et al*., 2007). This was then followed by determining sequence similarities between CerS4 and or CerS5 and their interacting partners.

Following the bio-informatics analysis, gene expression analysis was done at mRNA level by qRT-PCR using CerS4 and CerS5 specific primers which were designed using Beacon Software (Bio-Rad). This was done to compare the expression level of CerS4 and CerS5 in endometrial and colon cancer relative to non-cancerous cells.

The change in expression level of CerS4 and CerS5 in endometrial and colon cancer lead to investigating the relationship of these genes and the apoptosis inducing drugs, anastrozole in endometrial cell lines and 5FU in colon cell lines. FACS was used to quantify and analyse apoptosis in endometrial and colon cell lines. Total RNA was extracted from treated and non-treated cells.

QRT-PCR was done to study CerS4 and CerS5 gene expression levels after apoptosis induction, since both of these genes were shown to be up-regulated in endometrial and colon cells, that is (i.e) before apoptosis induction.

These findings implicate a role for CerS4 and CerS5 in the apoptosis regulation of endometrial and colon cancers. The next chapter outlines colon cancer and endometrial cancer, apoptosis as an essential process in cellular homeostasis and a background on Longevity Assurance genes, also known as CerSes, ceramide as a product of CerSes, and its implication in cancer biology.

This thesis is structured in five chapters which are: The introductory chapter (Chapter 1); Chapter 2, which covers the Literature review; Chapter 3, outlining materials and methods; Chapter 4, showing results; and Chapter 5, which includes discussion and conclusion.

CHAPTER 2

LITERATURE REVIEW

2.1 CANCER, APOPTOSIS AND CERS4 AND CERS5 BACKGROUND

Both CerS4 and CerS5 have been implicated in cancer biology. These two genes were found to be up-regulated in breast cancer and correlated with the pathogenesis of the disease (Schiffmann *et al*., 2009). Little is known about the precise roles of CerS4 and CerS5 in colon and endometrial cancer.

2.2 ENDOMETRIAL CANCER

Endometrial cancer is the most common of the female genital tract cancers and overall the fourth most common site for cancer to occur after breast, lung and colorectal cancers globally (Matsumoto *et al*., 2008). This cancer is one of the most common cancers seen in South African women (CANSA, 2012). The uterus is characterised by continuous cycles of endometrial cell growth and apoptosis in response to normal hormonal changes. The apoptotic pathway in female reproductive tissues generally involves a signal transduction pathway of a Fas receptor and its ligand rather than bax-bcl-2 pathway (Abe *et al*., 2006). Fas has been found to be expressed during the menstrual cycle. Estrogen and progesterone have been shown to control the expression of Fas, which is highly expressed during the secretory phase, suggesting a link with progesterone. Estrogen and progesterone represent the two survival factors in the human endometrium. Under the influence of estrogen, endometrial cells proliferate, partly as a result of the activation of anti-apoptotic genes and inhibition of the pro-apoptotic genes (Matsumoto *et al*., 2008). Progesterone on the other hand acts as a

differentiation factor, blocking mitosis and inducing terminal differentiation (Song *et al*., 2002). Withdrawal of these hormones from endometrial cells has been shown to decrease cell viability and thus increase apoptosis, while studies of Fas-mediated apoptosis have shown that this death receptor is important for endometrial cycling and suggests that dysregulation of the Fas/FasL interactions may have an important role in the development of endometrial cancer (Wang *et al*., 2003).

GMMe and Hec-1A endometrial cell lines

In this study, two endometrial cell lines (non-cancerous GMMe and cancerous Hec-1A), were used. GMMe cells are cuboidal in shape and exhibit epithelial characteristics. The Hec-1A cell line is a human endometrial cancer cell line derived from a moderately adenocarcinoma differentiated tumour. This cell line does not produce matrix metalloproteinases (MMPs), which are responsible for the breakdown of extracellular matrix components, and are important in the metastatic phenotype (Schröpfer *et al*., 2010).

2.3 COLON CANCER

Colon cancer is one of the top five most prevalent cancers in both males and females, with the highest incidence found in developed countries such as Australia and New Zealand and the lowest incidence in developing countries, found in Africa and Asia (Jemal *et al*., 2011). However, over the past 20 years, the overall incidence of colon cancer in South Africa has been reported to have increased markedly and currently being in the top five of most common type of cancer in both males and females (Parkin *et al*., 2008; Cronje *et al*., 2009; CANSA 2012).

In normal healthy colon, cellular proliferation, lineage specification differentiation, migration and apoptosis are highly coordinated processes that occur in normally active colonic epithelial

cells. Failure to properly regulate these processes may lead to the development of colon cancer. Three important factors contribute to the pathogenesis of colon cancer, including, the failure of colon epithelial cells to undergo apoptosis; secondly, a mutation in the p53 gene, a tumour suppressor gene involved primarily in cell cycle regulation and associated with initiating apoptosis (Huerta *et al*., 2006). A third possible factor is that Fas mutations are also associated with colon carcinomas (van der Woude *et al*., 2005; Garland *et al*., 2009).

The Caco-2 cells and HT-29 colon cell lines

Because of its great morphological, ultrastructural and biochemical similarity with small intestinal epithelial cells, the Caco-2 cell line has been used to represent a normal colonic cell line, to which the cancerous HT-29 colonic cell line was compared to (Sambuy *et al*., 2005; Geens and Niewold 2010). Normal colon cell lines (CCD-112CoN) have been reported to have a very short life-span and are difficult to maintain over a period of time under cell-culture conditions (Larrosa *et al*., 2006).

2.4 APOPTOSIS

One of the hallmarks of cancer is the failure of cells to undergo apoptosis (Chaudhry and Asselin, 2009). Apoptosis, also named programmed cell death, is a normal component for cellular homeostasis involving embryonic/organ development and health in humans. For tumourigenesis, oncogenic factors are generally involved in activation of anti-apoptotic signaling pathways, whereas tumour suppressor factors are normally pro-apoptotic (Jin and El-Deiry, 2005). Studies of bio-active sphingolipids such as ceramide have gained attention over the past two decades for their important role in the regulation of multiple biological functions, especially in apoptosis. Apoptosis can be induced by adverse conditions such as cellular stress, cross-linking of death receptor, and exposure to anticancer drugs (Chaundry and Asselin, 2009). Apoptosis occurs through two main pathways, that is, extrinsic or death

receptor pathway and the intrinsic or mitochondrial pathway, shown in figure 2.1. Both pathways involve the activation of a cascade of proteases called caspases that interact with other proteins such as the Bcl-2 resulting in the death of the cell (Reed, 2000). Furthermore, apoptosis can also occur independently of caspases (Herbeuval *et al*., 2005).

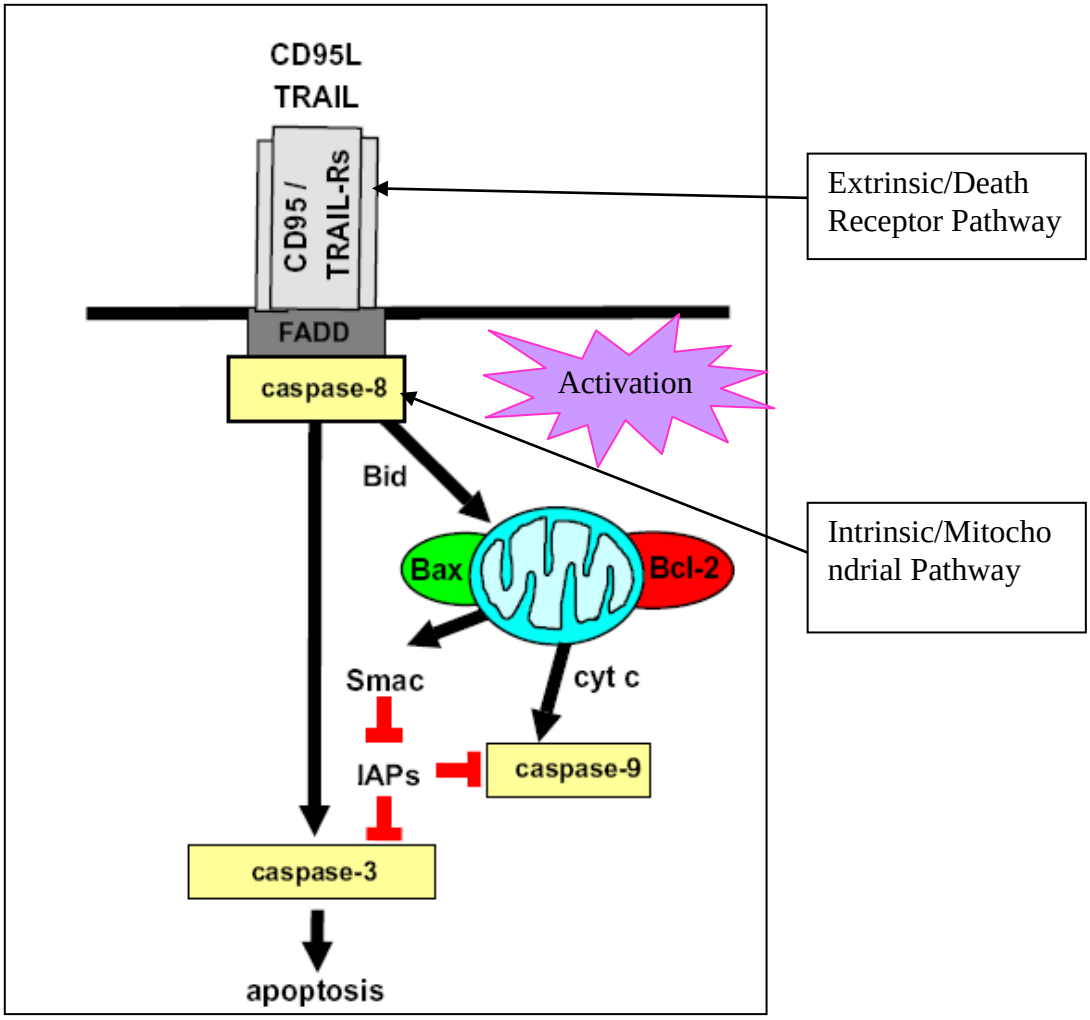

Figure 2.1 – Apoptosis signaling pathways: In the death receptor (extrinsic) pathway, binding of death receptor ligands, e.g. CD95 and TRAIL ligands to death receptors, i.e. CD95 and TRAIL receptors triggers receptor trimerisation, recruitment of FADD and caspase 8 to DISC and activation of caspase 8 at the DISC. In the mitochondrial pathway, the release of cytochrome c from the mitochondria into the cytosol trigger caspase 3 activation, while Smac promotes apoptosis by neutralising Inhibitor of Apoptosis Proteins (IAPs), leading to apoptosis (Fulda, 2009).

Upon induction of apoptosis, caspase 8 (which is present in most cell types as a proenzyme, in an inactive state) becomes activated via oligomerisation in a multimeric complex at activated death receptors (Mohr *et al*., 2005). The ligation of death receptors such as CD95 or TRAIL receptors, by their corresponding ligands, triggers receptor trimerisation and clustering of the receptors' death domains which enables the recruitment of adaptor molecules such as Fas asscociated with a death domain (FADD) via protein-protein interactions through the death domains. Caspase 8 is in turn recruited to this complex via FADD through the interaction of the death-effector-domains (DED), which leads to the formation of the death-inducing signaling complex (DISC). This oligomerisation of caspase 8 in DISC drives its activation through autoproteolysis. Besides its proteolysis at the DISC, caspase 8 can also be activated downstream of the mitochondria upon initiation of the intrinsic apoptosis pathway (Cowling and Downward, 2002). Ceramide which can be produced *de novo* by ceramide synthases or the hydrolysis of sphingomyelin has been shown to induce apoptosis (Schiffman *et al*., 2009).

Smyth *et al*., (1996) showed that Bcl-2 prevents ceramide-induced apoptosis, while Siskind *et al*., (2006) further demonstrated that exogenous ceramide initiates mitochondrial apoptosis by causing an increase of mitochondrial outer membrane permeability which allows cytochrome *c* release. Ceramide can be generated in mitochondria through sphingomyelin (SM) hydrolysis or *de novo* synthesis. Both mitochondrial-overexpressed sphingomyelinase and TNF-stimulation leads to mitochondrial ceramide accumulation, Bax translocation, cytochrome c release, and apoptosis (Birbes, 2001 and 2005). In general, either exogenous ceramides or ceramide-generating death stimuli cause mitochondrial dysfunction, executor caspase activation, and apoptosis (Lin *et al*., 2007). Ceramide has also been shown to trigger apoptotic signaling through two additional pathways namely, the endoplasmic reticulum (ER) pathway and lysosomal pathways, shown in figure 2.2 (Huang *et al*., 2011). Conversely, more

investigations are needed to fully understand how ceramide triggers apoptosis in the latter pathways.

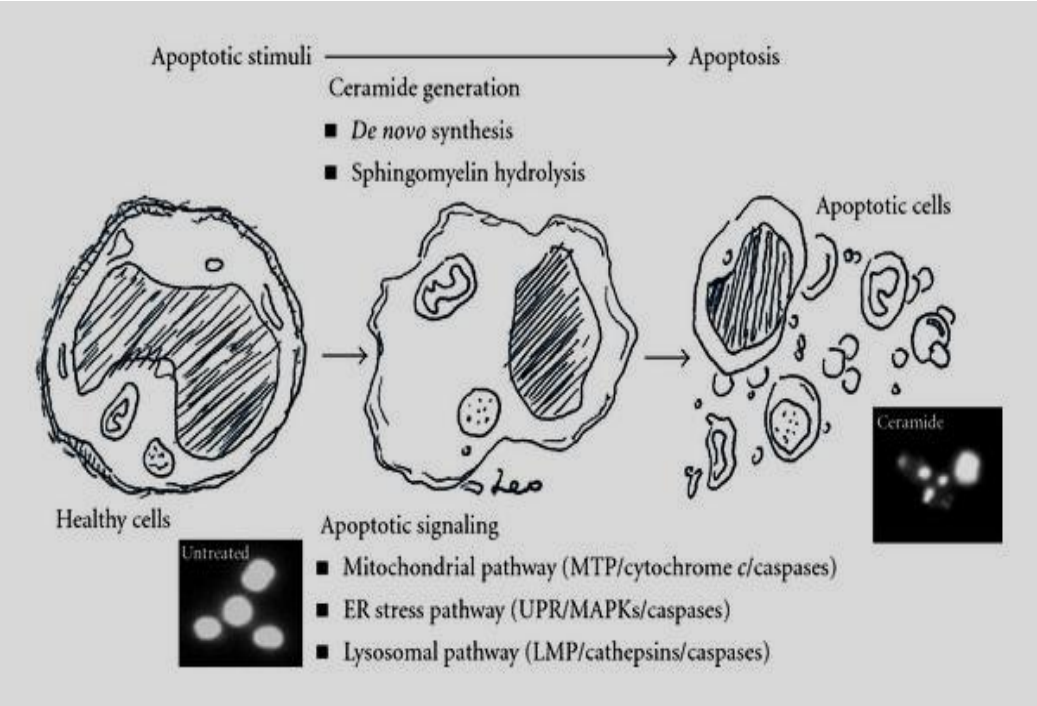

Figure 2.2 - The pro-apoptotic role of ceramide: Ceramide can trigger apoptosis through three different mechanisms which are: the mitochondrial pathway, the ER stress pathway and the lysosomal pathway. Adapted from (Huang *et al*., 2011). Ceramide generation can be through the hydrolysis of sphingomyelin or *de novo* synthesis by ceramide synthases, also known as longevity assurance genes, shown in figure 2.3.

Ceramide is a building block of sphingolipids (SLs) (Ogretmen, 2006). Sphingolipids are major structural components of eukaryotic membranes and fulfill important cellular functions such as signal transduction and intracellular transport (Lahiri and Futerman, 2007; Becker *et al*., 2008). These molecules also play an important role in diverse processes important in cancer biology including apoptosis, cell proliferation, cell migration, senescence and inflammation (Ogretmen and Hannun, 2001; Futerman and Hannun, 2004). These sphingolipid-regulated processes are in turn, crucial in cancer development and progression,

and may also influence the efficacy of anti-cancer therapeutics (Reynolds and Kolesnick, 2004; Fox *et al*., 2006; Modrak *et al*., 2006). A key step in the *de novo* synthesis of sphingolipids is the synthesis of dihydroceramide by (dihydro)ceramide synthases (CerS). Ceramide can also be produced by the hydrolysis of sphingomyelin (SM), which is one of the SLs. In the *de novo* pathway, CerS catalyses the transfer of acyl residues from acyl-CoA to sphinganine, thereby forming dihydroceramide. Dihydroceramide is then converted to ceramide by dihydroceramide desaturase. Ceramide can be further used as a precursor for the synthesis of other SLs (Futerman and Riezman, 2005). Figure 2.3 illustrates the synthesis of ceramide.

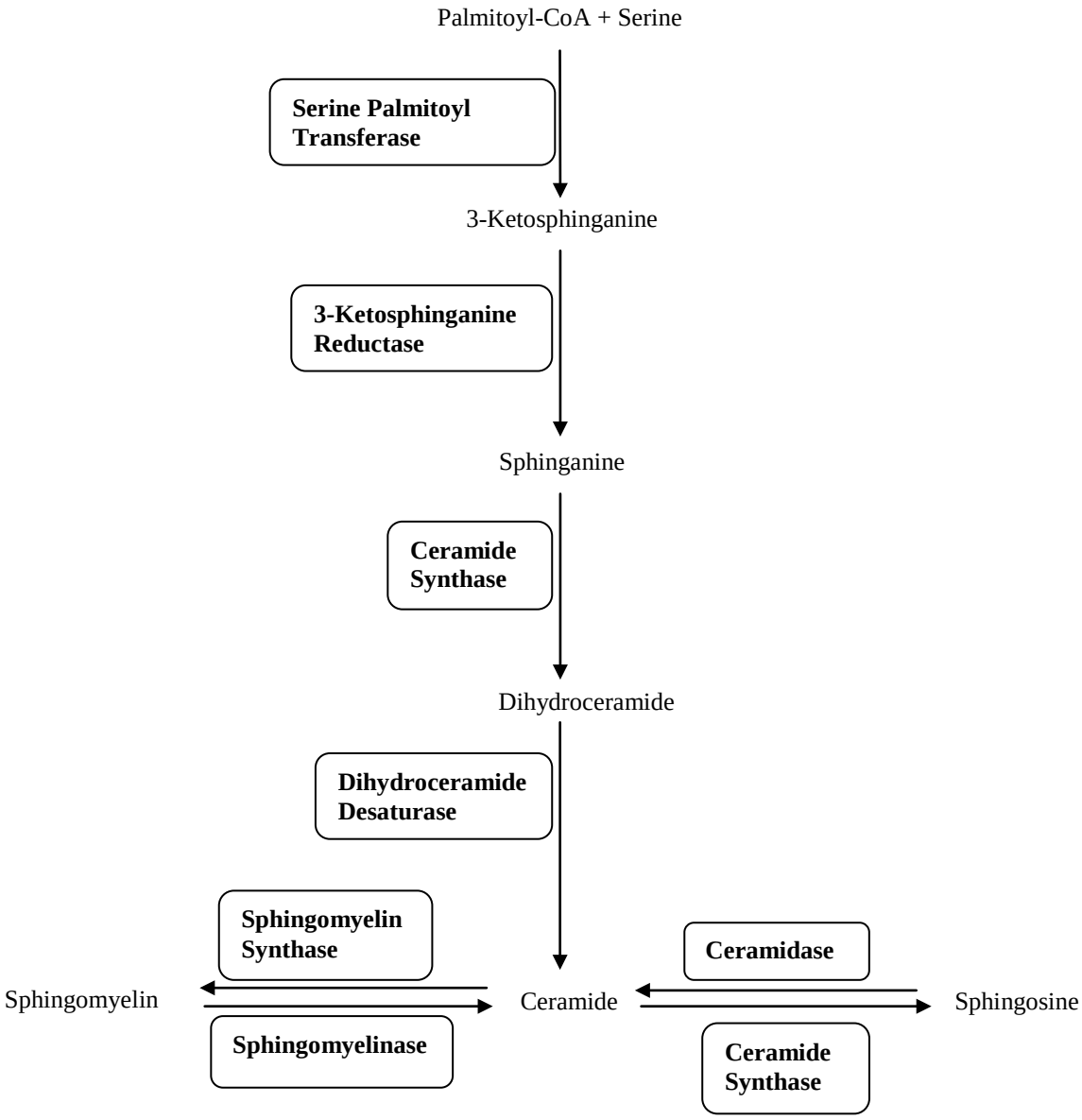

Figure 2.3 - Schematic diagram of ceramide metabolic pathway: This pathway starts by the condensation of Palmitoyl-CoA with serine by serine palmitoyl transferase. The main product of this pathway (ceramide), can be further converted to sphingomyelin by sphingomyelinase or broken down to sphingosine by ceramidase (Levy and Futerman, 2010).

Much has been reported on ceramide produced through SM hydrolysis, compared to reports on ceramide produced *de novo*. However, this area of research is growing. In addition, little is known about the interaction or the relationship between the two pathways that produce

ceramide. Furthermore, CerSes have been implicated in cancer development, progression and metastasis.

2.5 LONGEVITY ASSURANCE GENES (LASS)/CERAMIDE SYNTHASES (CERS)

Longevity assurance genes or Ceramide Synthases are a family of related genes. This family of genes was first discovered in yeast cells and the members are highly conserved as seen in bacteria and humans. (Pewzner-Jung *et al.*, 2006; Masukawa *et al*., 2008; Mizutani *et al*., 2009; Levy and Futerman 2010). To date, at least six paralogs have been identified in mice and humans and at least two members of this gene family have been found in every organism studied so far, as seen in figure 2.4. In yeast, longevity assurance genes are designated LAGs, in mice Lass and LASS in humans. In all LASS family members, LASS1 is most closely related to yeast proteins, while LASS2 to 6 are closely related to each other, as shown in figure 2 (Mizutani *et al*., 2006 and 2009).

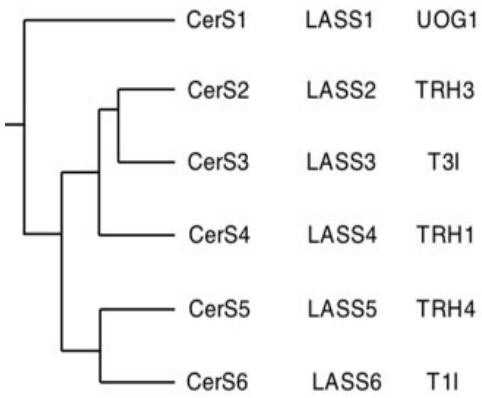

Figure 2.4 - Phylogenetic Tree of Longevity Assurance Genes: This figure shows LASS1 as being furthest from LASS2-6, with LASS 5 and 6 being closely related and furthest from LASS 1. LASS 2 and LASS 3 are shown to share a common origin and LASS 4 being most closely related to LASS2. Adapted from Mizutani *et al*., (2006).

Human and mouse orthologs have been found to have strong similarities, both in sequence and genomic structure (Pewzner-Jung *et al*., 2006). CerS belongs to a large family of endoplasmic reticulum (ER) membrane-associated proteins (Mizutani *et al*., 2006 and Pewzner-Jung *et al*., 2006). Both human and mouse proteins contain two major domains, the Hox domain and the Tram-Lag-CLN8 (TLC) domain as shown in figure 2. 5.

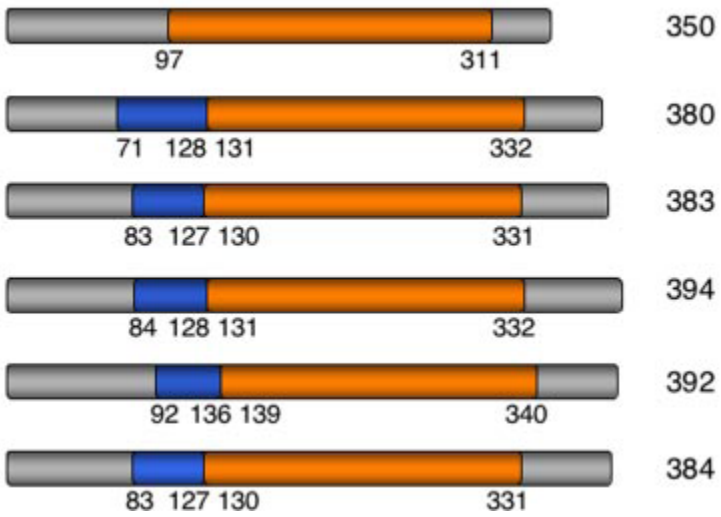

Figure 2.5 - The amino acid conservation of the LASS genes: The two major conserved domains in LASS proteins, the homeobox domain in blue and the TLC domain in orange. The numbers represent the amino acid residues. LASS1 is the shortest isoform due to the absence of the Hox domain. LASS 2-6 contain 30 to 44 amino acids more (Mizutani *et al*., 2006).

The hox domain is derived from homeobox proteins that usually are sequence specific transcription factors regulating development (Venkataraman *et al*., 2002). In LASS genes however there is no evidence to suggest that the Hox domain acts as a transcription factor (Pewzner-Jung *et al.,* 2006). To date, in humans, it has been shown that all members of the LASS family except for LASS3 encode at least two isoforms (Pewzner-Jung *et al.,* 2006). The longer isoform retains both domains, TLC (in orange) domain and the Hox (in blue) domain, while the shorter isoform lacks the hox domain as well as part of the TLC domain, as seen in figure 2.6.

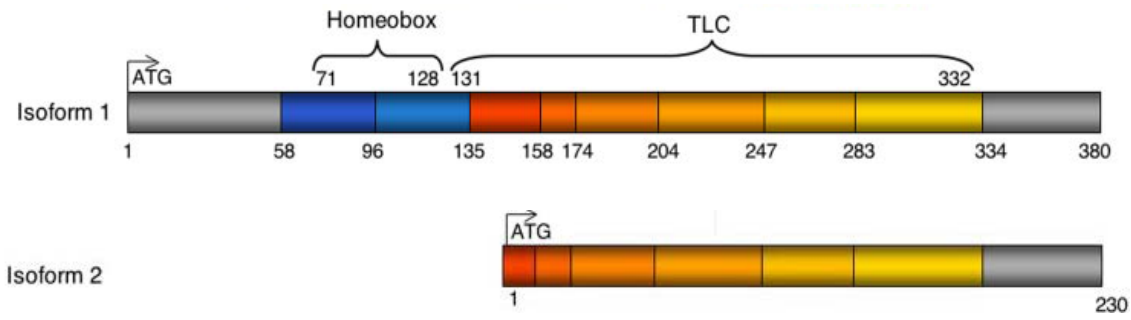

Figure 2.6 - Difference between the isoform 1 and isoform 2: This figure illustrates the difference between the shorter and the longer isoform of LASS genes. The longer isoform retains the two domains while the shorter isoform lacks the Hox domain and part of the TLC domain (Ogretmen, 2006).

It has been reported that the two isoforms seem to be involved in similar mechanisms of transcriptional regulation, suggesting that the Hox domain is not critical for these proteins to function (Pewzner-Jung *et al*., 2006; Ogretmen, 2006; Levy and Futerman, 2010). It has also been documented that the TLC domain is crucial for the main function of LASS proteins, which is the synthesis of ceramide (Ogretmen, 2006; Mizutani *et al*., 2006 and 2009). In addition, the CerS TLC domain consists of a highly conserved Lag1p motif of ~52 amino acids which is essential for the CerS catalytic activity (Spassieva *et al*., 2006; Teufel *et al*., 2009). Furthermore, the Lag1p motif renders CerSes unique from other TLC domain containing proteins which do not produce ceramide (Teufel *et al*., 2009).

2.5.1 LASS genes and their functions

As mentioned above, LASS genes mainly produce ceramide, and different LASS genes are specific for different ceramide species. LASS4 (previously known as Trh1) and LASS5 (formerly known as Trh4) were the first members of the LASS family to be discovered to produce ceramide (Pewzner-Jung *et al*., 2006). The ceramide molecule consists of a sphingoid long chain base linked to a fatty acid chain by an amide bond and the ceramide structure is shown in figure 2.7.

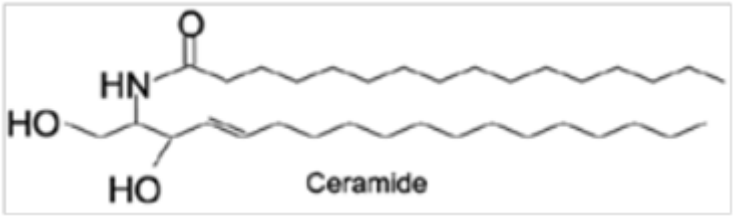

Figure 2.7 - Structure of a ceramide molecule: Ceramide contains a long saturated carbon chain base linked to sphingosine. Adapted from Ogretmen (2006).

The sphingoid base is the same on all ceramide molecules produced by CerSes, but these ceramide molecules differ in fatty acid chain length (Lahiri *et al*., 2007). Some CerSes may share substrate preference, for example, CerS5 and CerS6 both share C-16 fatty acid chain, while others are shown to have a broad substrate specificity, for example, CerS2 (Mizutani *et al*., 2005 and 2006; Laviad *et al*., 2008; Saddoughi *et al*., 2008). Table 2.1 shows CerSes and their substrate preferences.

Table 2.1: The CerS family members with their different substrate preferences

CerS member	Substrate preference
CerS1/LASS1	C18:0
CerS2/LASS2	C20-C26
CerS3/LASS3	C22-C26
CerS4/LASS4	C18-C20
CerS5/LASS5	C16
CerS6/LASS6	C14 and C16

In addition, CerS1-6 have also been shown to have preferential tissue specificity (Mizutani *et al*., 2006; Laviad *et al*., 2008).

2.5.2 Tissue Distribution of LASS Gene Product/CerS

As membrane components, CerS have both the N and C- termini located on the cytosolic leaflet, demonstrated as in figure 2. 9. LASS1 is found predominantly in the brain and LASS5 is found predominantly in lung epithelia (Xu *et al*., 2005; Laviad *et al*., 2008). C-16-ceramides are also found in non-neuronal tissues such as lung, liver and colon and in fibroblasts, endothelial cells and cells of the immune system. LASS5 has also been implicated in prostate cancer (Eto *et al.,* 2003). Additionally, LASS3 is found to be highly expressed in testis, whereas LASS2 was shown to have a broad tissue distribution (Ogretmen, 2006; Levy and Futerman, 2010). Generally little is known about LASS genes and the products with regard to expression levels in different tissues. Furthermore, it has been reported that CerSes can be modified at a posttranslational level, and this posttranslational modification plays a role in cell fate (Stiban *et al*., 2010).

2.5.3 Posttranslational Modification of LASS Gene Products/CerS

There is accumulating evidence to suggest that the CerS family members may undergo posttranslational modification through phosphorylation. Activation of Protein Kinase C (PKC) has been shown to increase the phosphorylation of CerS, and thus increase *de novo* ceramide synthesis, leading to cell death (Becker *et al*., 2005; Kitatani *et al*., 2006). Calcineurin in turn antagonises the phosphorylation of ceramide, and thus promotes proliferation (Stiban *et al*., 2010), as shown in figure 2.8. However, little is known about the CerSes phosphorylation sites. Additionally, the mode of action of ceramide regarding the cell fate depends on the downstream targets of ceramide (Ogretmen, 2006).

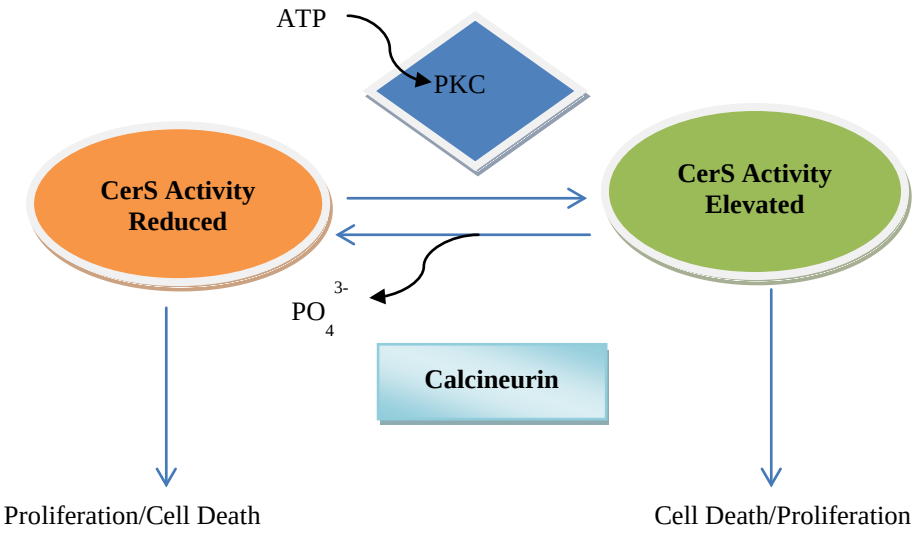

Figure 2.8 - The posttranslational modification of ceramide: The phosphorylation of PKC by ATP in cells increases the production of ceramide through CerS phosphorylation. Contrary to CerS phosphorylation, calcineurin dephosphorylates CerS, and thus leads to decreased ceramide production. Depending on the ceramide species and type of tissue, increased or decreased CerS activity can either lead to cell death or cell proliferation (Stiban *et al*., 2010).

2.5.4 The mode of action of ceramide

The summary of ceramide mode of action is illustrated in figure 2.9. Ogretmen (2006) found that upon various stimuli, ceramide synthesis is activated by either a *de novo* pathway or hydrolysis of SM (1) (sphingomyelin). Ceramide regulates the anti-proliferative responses of cells by regulating its downstream targets such as caspases and telomerases (2). Alternatively, ceramide can be converted to SM, sphingosine-1-phosphate (S1P), sphingosine and glycosylceramide, yielding diacylglycerol (DAG) as a byproduct (3). This reverse pathway of ceramide results in cell survival processes such as drug-resistance (4), malignant transformation (5), cell migration and cell proliferation, including blood vessel formation. This reverse process of ceramide to anti-apoptotic molecules such as S1P (6) occurs through the activation of sphingosine-1-phosphte and its receptor and involves the activation of ERK,

NF-κB (7), while inhibiting caspases and (8) BAX (which is a pro-apoptotic protein). In addition, enzymes which regulate ceramide levels such as ceramidases, exert opposing effects on ceramide and thus increase cell survival by their anti-apoptotic function (Ogretmen, 2006). Furthermore, c-myc (9) and cyclins (and cyclin dependent kinases) were also shown to be downstream targets of the Wnt signaling pathway.

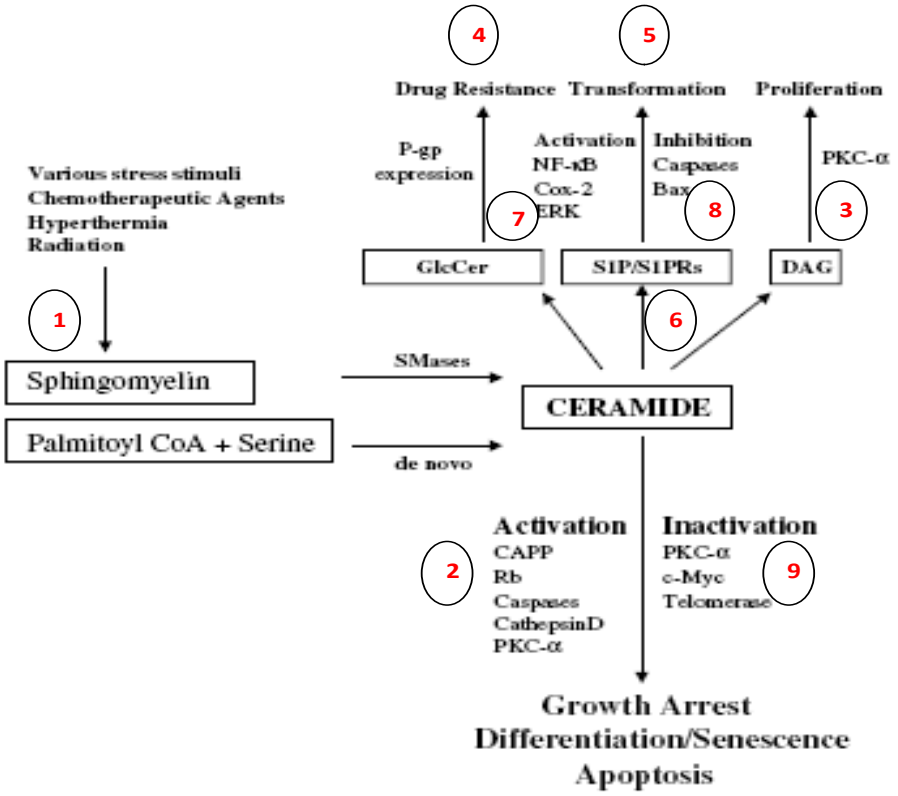

Figure 2.9 - The mode of action of ceramide: Ceramide can either activate or inactivate its downstream targets to induce apoptosis in cells, as described in section 2.5.4 (Ogretmen, 2006).

Interestingly, c-myc and cyclins (and cyclin dependent kinases) were shown to be (indirect) downstream targets of both LASS genes and their products and the Wnt signaling pathway. Targeting the Wnt signaling pathway may help in understanding molecular functions of LASS genes and the impact they have in cancer biology. Furthermore, CerSes have been implicated in other diseases.

2.5.5 The implication of ceramide in diseases

De novo ceramide synthesis has also been implicated in a number of diseases, such as diabetes (Summers 2006), Cystic Fibrosis, (Ito *et al*., 2004; Vilela *et al*., 2006) and chronic obstructive pulmonary disease (COPD) (Petrache *et al*., 2005 and 2006). Ceramide may also play a role in Alzheimers disease where the long ceramide carbon chains abundant in some regions of the brain are vulnerable to Alzheimer's disease (Cutler *et al*., 2004; Wang *et al*., 2008). Ceramide has also been shown to be involved in neuronal death (Schwarz and Futerman, 1997) and white matter dysfunction, cerebral ischemia and stroke (Yu *et al*., 2000; Jana and Pahan, 2004; Lee *et al*., 2004).

The generation of ceramide through SM hydrolysis has been shown to be linked with colon cancer (Wu *et al*., 2004). Loss-of-function mutation of Alkaline Sphingomyelinase (Alk-SMase) has been shown in colon cancer HT-29 cells (Wu *et al.,* 2004) and in liver cancer HepG2 cells (Cheng *et al.,* 2007). The Alk-SMase mutation in HT-29 colon cells occurs at the alternative splicing level, involving the deletion of exon 4, which encodes a critical His (Histidine) that participates in the formation of binding site for SM (Zalatan *et al.,* 2006). This evidence suggests the direct effect of ceramide in colon cancer, produced through the hydrolysis of SM, but what exactly is the role of ceramide produced *de novo* by CerS in colon cancer is still unclear.

While SM, ceramide and sphingosine have antiproliferative and proliferative effects in colon cancer cells, S1P has specifically been shown to stimulate cell proliferation, inhibit apoptosis and promote inflammation, cell migration and angiogenesis. In colon cancer, high levels of S1P correlate to a poor survival rate (Van Brocklyn *et al*., 2005). In colon cancer cells, S1P has been shown to induce COX 2 expression (Hsieh *et al*., 2006), and activate p38, MAPK and Erk (Thamilselvan *et al*., 2002). S1P also increase the production of PDGF and VEGF

and activate growth factor receptor. Visentin *et al*., (2006) showed that neutralising S1P with specific antibody significantly inhibited the cancer progression through inhibiting the cell proliferation and blocking neovascularisation in several cell lines including HT-29 colon cancer cells. Additionally, sphingosine kinase (Sphk), the enzyme responsible for the formation of S1P, is upregulated in many cancer tissues including colonic adenocarcinoma (Kawamori *et al*., 2006). Furthermore, ceramide generated *de novo* has been shown to induce apoptosis through Tumour Necrosis factor α (TNF α) in colon cancer cells as a result of the of the cannabiniod receptor activation. However, the study did not specify which CerS was responsible for the apoptosis induction (Cianchi *et al*., 2008). A balance between ceramide and S1P has been considered as a rheostat mechanism that may determine cell death and cell survival. The normal intestinal epithelial cells have high levels of S1P lyase and S1P phosphatase. However, in colon cancer cells, both S1P lyase and S1P phosphatase are down regulated and thus the catabolism of S1P is inhibited (Duan and Nilsson, 2009). Additionally, ceramide has also been implicated in other types of cancer, including endometrial cancer.

Reports implicating ceramide in endometrial cancer are limited. However, it was demonstrated by Knapp *et al*., (2010) that SL metabolism in the human endometrial carcinoma is markedly elevated compared to the healthy endometrium. They showed that the human endometrial cancer is characterised by increased of ceramide compared to normal endometrium. In addition, they demonstrated that increased levels of ceramide in endometrial cancer were accompanied by high rates of the *de novo* ceramide synthesis pathway. Furthermore, they also showed that endometrial carcinoma was also characterised by increased levels of sphingosine 1 phosphate (S1P). The role of CerSes in limited response of endometrial cancer chemotherapy was also highlighted by Knapp *et al*., (2010), by indicating that doxorubicin and cisplatin (which are commonly used to treat the metastatic endometrial cancer) are largely dependent on the increase levels of intracellular ceramide, including the stimulation of the *de novo* synthesis

pathway. New approaches to improve the response of endometrial cancer cells to chemotherapy are needed as it has been demonstrated that endometrial cancer is characterised by elevated levels of ceramide, at least in part from the *de novo* pathway. (Noda *et al*., 2001; Min *et al*., 2007; Rath *et al*., 2009; Knapp *et al*., 2010). However, unlike in colon cancer, the ratio between S1P and ceramide in endometrial cancer was shown to be stable.

To date, LASS genes have been implicated in cell regulation through the production of ceramide. But the role that these different ceramide species play in cancer development and progression remains to be elucidated. Thus, at present, it is difficult to draw definitive conclusions concerning the role of particular ceramides in defined physiological and pathophysiological events. However, the possibility to experimentally manipulate LASS genes and study their expression, will aid in better understanding the precise roles of specific ceramide species, in different tissues. So far six human CerS have been discovered and their substrate specificity in terms of synthesising ceramides is known. However, the role these ceramide species play in different cancers remains unclear. To complicate matters, it has been shown that the same ceramide species can exert opposing roles in different cancers. (Karahatay *et al*., 2007; Senkal *et al*., 2007). Thus it seems reasonable to investigate the roles of CerS4 and CerS5 in colon and endometrial cancers. The next chapter outlines the materials and the methods used to achieve our goal, as indicated in section 1.7.

CHAPTER 3

MATERIALS AND METHODS

3.1 MATERIALS

Human colon cell lines, Caco-2 and HT-29 were purchased from Highveld Biological (Pty) Ltd (Johannesburg, South Africa). Human endometrial cell lines, GMMe and Hec-1A were purchased from the American Type Culture Collection.

3.1.1 Endometrial Cell lines

3.1.1.1 GMMe cell line

GMMe cell line was established by the stable transfection of endometrial tissue of an adult female mink. A plasmid vector encoding simian virus 40 (SV40) large T-antigen driven by the human β-actin promoter, was used for transfection. The cells were cotransfected with a second plasmid vector to confer neomycin resistance and were selected in medium containing G418. GMMe cells are cuboidal in shape and exhibit epithelial characteristics. This cell line has also been shown to be positive for alkaline phosphatase (www.atcc.org).

3.1.1.2 Human Endometrial cell line-1A (Hec-1A) cell line

Hec-1A is an endometrial epithelial adenocarcinoma cell line, derived from a moderately differentiated tumour. This cell line does not produce matrix metalloproteinases (MMPs), which are responsible for the breakdown of extracellular matrix components, and are important in the metastatic phenotype (Schröpfer *et al*., 2010).

3.1.2 Colon cell lines

3.1.2.1 Caco-2 colon cell line

The study of normal colon cell maturation has been hindered by the inability to maintain normal colonic epithelium cells in culture. For this reason, model systems such as the highly differentiated Caco-2 cell line have proved to be a suitable and highly informative alternative for such studies. (Sambuy *et al*., 2005).

3.1.2.2 HT-29 colon cell line

HT-29 colon cells are highly malignant and poorly differentiated. It has been shown by Wu *et al.*, (2004) that these cells have an exon 4 deletion of alkaline sphingomyelinase (alk-SMase) gene transcript. This enzyme catalyses the hydrolysis of sphingomyelin (SM) to ceramide.

3.1.3 Primer sequences for LASS4, LASS5 and β-actin

Specific primers were designed using the (Beacon software Bio-Rad) to amplify LASS4, LASS5 and β-actin from the synthesised cDNA. The mRNA variant 1 sequences were obtained from NCBI website LASS4 NM_024552.1, LASS 5 NM_147190.1 and β-actin NM_001101.3. The primer sequences were then sent to Inqaba Biotec (SA) for synthesis and 100 µM stocks were dissolved in 1XTE. 10 µM dilutions were prepared as working solutions. Table 3.1 shows the primer sequences for LASS4, LASS5 and β-actin.

Table 3.1: The primer sequences and product sizes for LASS 4, LASS 5 and β-actin

Amplified gene	Sequences	Product size	Annealing Temperature	Melting Temperature
LASS 4	Fw: ctctggtgctgctgttac Rv: gactcgtagtatgtggtgtag	175bp	53°C	83°C
LASS 5	Fw: atggtggctcctcaatgg Rv: aggtggtcacatcttcttcc	124bp	55°C	84°C
β-actin	Fw: gcgggaaatcgtgcgtgacatt Rv: gatggagttgaaggtagtttcgtg	232bp	54°C	89°C

3.1.4 Apoptosis induction

The cells were serum starved for 24h for synchronisation prior to treating with apoptosis drugs (Cooper 2003). Apoptosis was induced in colon and endometrial cells, and then fluorescence-activated cell sorter (FACS) was used to analyse and quantify apoptosis.

3.1.5 Flow Cytometry (FCM)/ fluorescence-activated cell sorter (FACS)

Flow cytometry is an analytical tool that allows for the discrimination of different particles on the basis of size and colour. In this study, flow cytometry, the Flow cytometer Beckton

Dickson Facs Calibur was used to detect apoptosis, differentiating between live and dead cells. The Annexin V kit (BD-BioSciences, USA) was used.

3.1.5.1 Probes for Flow Cytometry

A number of fluorescent probes have been developed for the analysis of cycling cells through flow-cytometry. These include propidium iodide (PI) and Annexin V-Fluorescein isothiocyanate (FITC). The loss of plasma membrane is one of early apoptotic features, in apoptotic cells. The membrane phospholipid phosphatidylserine (PS) is exposed from the inner to the outer leaflet of the plasma membrane, thereby exposing the PS to the external cellular environment. Annexin V is ~36KDa Ca^{2+} dependent phospholipid-binding protein that has high affinity for PS, thus binds to cells with exposed PS. Annexin V may be conjugated to fluorochromes such as FITC. This conjugation retains high affinity for PS and thus Annexin V-FITC serves as a sensitive probe for identifying apoptotic cells. Therefore cells that are in early apoptosis are Annexin V-FITC positive.

PI on the other hand is a fluorescent nucleic acid dye, which stains the total cellular DNA content. PI intercalates into the DNA double helix of fixed and permeabilised cells, but does not cross the intact plasma membrane of viable cells. Furthermore, the dye (PI) can readily enter dead cells, cells in late apoptotic stages, or fixed cells with damaged plasma membrane.

Annexin V-FITC staining is usually used in conjunction with PI staining to permit the identification of cells that are in early apoptosis. Viable cells are Annexin V-FITC and PI negative. Early apoptotic cells are Annexin V-FITC positive and PI negative. Cells that are in late apoptotic stages or already dead stain for both Annexin V-FITC and PI positive.

NB: For each cell line, the following were prepared, blank which constituted of only viable unstained cells. A negative control was composed of untreated but stained cells. These controls

were run in conjunction with the experiment of treated cells. The blank is used to gate the cells with forward and side scatter. The negative control is important in obtaining the true apoptotic signal from the false signal. The DMSO control was not considered necessary as it has been previously shown that it (DMSO) does not influence the cytotoxic effects of anastrozole (Wang and Chen, 2006). The vertical and the horizontal gates of the experiment were placed in the same position as those of the controls.

3.2 METHODOLOGY

Methodology was divided into two sections, the bio-informatics and the gene expression section.

3.2.1 Bio-informatics

3.2.1.1 STRING database and Multi-Align Tool

The use of bio-informatics to discover disease causing genes and how these genes and their products are regulated is growing. As CerS4 and CserS5 have been previously implicated in cancer biology, especially apoptosis, STRING protein-protein interaction database was used to determine CerS4 and CerS5 possible interacting partners and examine if these proteins may be involved in similar cellular functions as CerS4 and CerS5, such as apoptosis. Following this, the amino acid sequences of the possible interacting partners for both CerS4 and CerS5 were obtained from STRING database and verified using NCBI. CerS4/CerS5 and its potential interacting partners' amino acid sequences were aligned using Multi-Align tool, by randomly pasting the amino-acid sequences of these proteins. This was done to examine sequence similarity between CerS4, CerS5 and their protein interacting partners.

In addition to the STRING database, BioGRID and IntAct databases were used to determine protein-protein interactions. Furthermore, Clustal omega and COBALT were used in

conjunction with the Multi-Align database to examine sequence similarity between CerS4/CerS5 and their interacting partners.

NB:

- STRING database protein interactions are experimentally determined as well as predicted interactions.
- IntAct database protein interactions are experimentally determined.
- Bio-GRID database provides comprehensive information (including experimentally determined) protein interactions.

3.2.2 Gene expression analysis

3.2.2.1 Cell culture

The cell lines were maintained in Dulbecco's modified Eagle's medium (DMEM), or HAM'S-F-12 supplemented with 10% fetal bovine serum (FBS) and 1% streptomycin in a humid atmosphere containing 95% air and 5% CO_2 at 37 ºC until the cells reached a required confluency. The cells ($1X10^6$ cells/ml) were further sub-cultured by trypsinisation, using trypsin-EDTA (Sigma-Aldrich), until 70% confluency was reached. Five (5)-Fluorouracil inhibits Thymidylate synthatase, which is a crucial enzyme for DNA synthesis, was then added to the medium, to induce apoptosis, in colon cell lines for 24h and 48h. Anastrozole, which is an aromatase inhibitor, was used to induce apoptosis in endometrial cell lines for 24h. The cultured cells were used for flow cytometry and for RNA extraction.

3.2.2.2 FACS analysis

Apoptosis was induced using apoptosis inducing drugs in colon and endometrial cell lines. Five (5 µM) of 5-Fluorouracil (5-FU) was used to induce apoptosis as demonstrated by Thant *et al*., (2008) to be cytotoxic and was therefore used to induce apoptosis in Caco-2 and HT-29

colon cell lines. Anastrozole has also been shown to induce apoptosis in endometrial cancer (Burnett *et al*., 2004). Meresmas *et al*., (2005) further demonstrated that anastrozole can induce apoptosis in endometrial cell lines from 50nM over 48 hrs, or increased anastrozole concentration over a short period of time. In this study, 2 µM anastrazole was used to induce apoptosis in GMMe and Hec-1A endometrial cell lines. Cells were incubated for a period of 0–48 hrs and the Annexin V-FITC apoptosis detection kit I was used for FACS analysis, with appropriate filter sets (excitation at 488nm; emission at 530nm).

The following controls were used to set up compensation and quadrants:

- Unstained cells
- Cells stained with Annexin V-FITC alone (no PI)
- Cells stained with PI alone (no Annexin V-FITC)
- Both fluorochromes (Annexin V-FITC and PI) were added in one tube and the results were analysed with flow-cytometry.

The Flow Cytometry set-up was as follows:

Different cell lines were maintained and incubated to undergo apoptosis and were trypsinised. This was followed by centrifuging at 2000 xg 5 min. Then the pellet was washed with 1 ml 1X PBS twice and resuspended in 200 µl of 1X binding buffer. 100 µl of each solution was transferred into a 5 ml tube. Then 5 µl of Annexin-FITC and PI were added to different tubes. The cells were then gently vortexed and incubated in the dark at room temperature (25 ºC) for 15 min. 400 µl of 1X binding buffer was then added to each tube and the results were analysed by flow cytometry. Results were represented in a cytogram and figure 3.3 shows a representative cytogram.

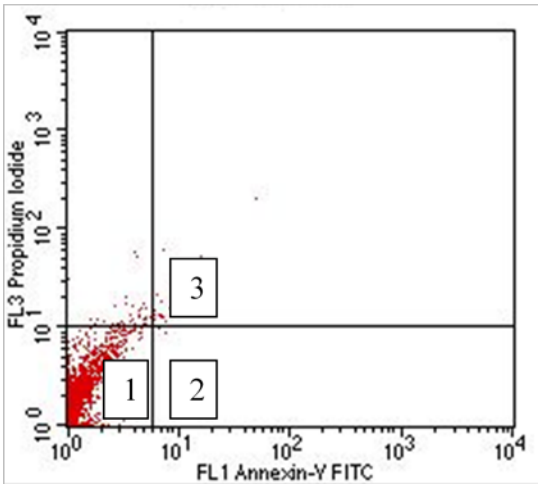

Figure 3.3 - A representation of a cytogram for FACS analysis: Quadrant number 1 constituting of viable cells (Annexin V and PI negative), 2 with cells undergoing early apoptosis (Annexin V positive and PI negative), and 3 with late apoptotic and necrotic cells.

Total RNA was extracted from treated and untreated cell lines.

3.2.2.3 RNA extraction

Prior to cDNA synthesis for quantitative real-time PCR (qRT-PCR), total RNA was extracted from the cultured cells. This was done using the Aurum^{TM} Total RNA Mini Kit (Bio-Rad, USA), following the manufacturer's guide. The floating cells were collected and the adherent cells were washed with 1X PBS and were treated with trypsin-EDTA to detach them from the growth vessel. After the trypsin was poured out, the vessel was then rinsed once with 200 µl of PBS. This was then transferred into a 2 ml microcentrifuge tube and centrifuged for 2 min. The supernatant was discarded and 350 µl of the lysis solution (supplemented with 1% β-mercaptoethanol) was added to each tube. This was pipetted at least 12 times up and down to lyse the cells thoroughly. To this 350 µl of 70% ethanol was added to each tube and was mixed thoroughly by pipetting up and down. The elution solution was then placed into a 70 ºC bath to warm it and use at a later stage. The RNA binding columns (provided) were inserted into 2 ml capless wash tubes and the homogenised lysate was then transferred into

the RNA binding columns. This was centrifuged for 30 sec and the filtrate was removed from the wash tube after removing the binding column. The binding column was then replaced into the same wash tubes. The low stringency wash solution (provided as 5× concentrate, to which 95–100% ethanol was added) was added to the RNA binding column, 700 µl. Following this, the RNase-free DNase I provided as powder was reconstituted by adding 250 µl of 10mM Tris, pH 7.5. Then 5 µl of the reconstituted DNase I was mixed with 75 µl of DNase dilution in a sterile 1.5 ml microcentrifuge tube. The diluted DNase was then added (80 µl) to the membrane stack, to the bottom of each column. This was then incubated at room temperature (RT) for 15 min, to allow the digest. The columns were centrifuged for 30 sec when the digest was complete and the digest buffer was discarded and the column was replaced into the same wash tube. To this 700 µl of high stringency wash solution was added and centrifuged for 30 sec. The column was replaced into the wash tube after discarding the filtrate. Then 700 µl of the low stringency wash solution was added to the RNA binding column and centrifuged for 1 min. The low stringency wash solution was discarded and column was replaced into the same tube. This was then centrifuged for another 2 min to remove the residual wash solution. The columns were then transferred into sterile 1.5 ml capped microcentrifuge tubes and 80 µl of the warmed elution solution was pipetted onto the membrane stack at the bottom of the RNA binding column. This was incubated for 1 min at RT to allow the solution to saturate the membranes. This was then centrifuged for 2 min to elute the total RNA. The eluted total RNA samples were then stored at -80°C for later use. The extracted RNA was then used for reverse transcription.

3.2.2.4 Reverse transcription or cDNA synthesis

Reverse transcription is the technique that synthesises the complementary deoxyribonucleotide nucleic acid (cDNA) from the RNA template. This process uses reverse transcriptase, which reverse transcribes mRNA into cDNA.

A Promega ImProm^{TM} - II Reverse Transcriptase System (A3802) was used to synthesise cDNA from total RNA from the cell lines. The manufacturer's instructions were followed. A total of 1 µg RNA was used as the template for reverse transcriptase. The reverse transcription reaction was carried out in a total volume of 20 µl per RNA sample, and the composition of the reagents is shown in Appendix 2, table 2a. Table 2b shows the conditions for cDNA synthesis. The synthesised cDNA was used for PCR.

3.2.2.5 Polymerase Chain Reaction (PCR)

PCR is a method used to amplify DNA segments through repetitive cycles of DNA synthesis. This process is made possible by the Taq Polymerase which utilises free floating oligonucleotides in reaction solution. Specific primers are required to amplify the fragment of interest as they bind to cDNA through base complementarity to guide the polymerase as to where to begin synthesis. The PCR technique involves 3 temperature steps known as **denaturation**: where the double stranded cDNA is separated out into single strands to allow binding of primers; **annealing**: in this step, the primers anneal to the single stranded DNA through base complementarity guiding the polymerase as to where it should start synthesising and **elongation**: where the amplified products are lengthened to reach the exact size of the fragment of interest.

In addition, as an *in vitro* technique, there can be a number of factors that contribute to the success of PCR. These include pH, salt concentration, temperature and primer: template ratio.

In this investigation, the reagent concentrations and temperatures were optimised in such a way as to allow the optimal conditions and ensure the success of the PCR. The PCR composition reaction is shown in table 2c, and the conditions are shown in table 2d, Appendix 2.

3.2.2.6 Agarose gel electrophoresis

Agarose gel electrophoresis is the technique by which DNA can be separated according to its size. The nucleic acid material is loaded onto the formaldehyde agarose gel, to which an electric current is applied. The DNA migrates towards the positive electrode due to its negative charge rendered by its phosphate molecules on its backbone. The agarose gel, which contain randomly distributed pores acts as a "molecular sieve", separating the molecules by size. The DNA fragments are visualised by staining the gel with ethidium bromide. Ethidium bromide intercalates between the bases of the DNA, which can then be visualised under UV light.

Preparation of 1% agarose gel

This was done to determine the success of PCR and if successful, determine the size of the PCR product. A 1.0% agarose gel was prepared by heating 1.0 g of agarose powder in 100 ml of 1X Tris Borate EDTA (TBE), in a microwave until all powder had dissolved. The mixture was cooled to 4 ºC and 3.5 µl (100 µg/ml) of EtBr was added and mixed. The mixture was poured into a gel casting tray, combs inserted and allowed to set. The PCR products were loaded on the wells and run parallel to a 50bp molecular weight marker in 1X TBE buffer at 70V for 1 hr. The molecular weight marker was loaded for size determination. After running, the gel was viewed using a Bio-Rad Gel. Doc system and the results are shown in the results section.

To verify that the primers had amplified the regions of interest, the PCR products were then cloned into a p-GEM-T-Easy vector (Appendix 2, figure 2a), as described in section 3.2.2.7 below, and then sent for sequencing.

3.2.2.7 Cloning

Cloning is the technique by which the DNA segment of interest is inserted into an autonomously replicating DNA molecule (cloning vector) so that the DNA segment of interest is replicated with the vector. Cloning involves two steps: ligation and transformation.

Ligation

Ligation is the technique by which recombinant DNA (rDNA) molecules are constructed by joining together the vector molecule and the DNA segment of interest using DNA ligase usually, T4 DNA ligase.

The PCR products were ligated into pGEM-T-Easy vector, figure 2a. p-GEM-T-Easy (shown in Appendix 2) vectors are convenient vectors by which PCR products can be cloned into. These vectors are prepared by cutting pGEM-T Easy vectors with *Eco*RV restriction enzyme and adding 3' terminal thymidines (T) to both ends. These 3' T overhangs at the insertion site improves the efficiency of ligation of a PCR product into plasmids by preventing recircularisation of the vector and providing a compatible overhang for certain thermostable polymerases that often add a single adenosine (A), in a template-independent fashion, to the 3' ends of the amplified fragments. Thus, the vector has T tails that can be ligated to the A overhangs of *Taq* polymerase PCR reaction products.

The ligation reactions were carried out using the LigaFast™ Rapid Ligation System (Promega Corporation, Madison WI, USA). Ligation reactions were carried out in a total volume of 10 µl consisting of the reagents indicated in table 2e, Appendix 2. One control was used, a

negative control, where nuclease free water was added instead of the PCR product, all the other ingredients were added. These reactions were then incubated at room temperature for three hours after which transformation was performed.

Transformation

Transformation is the technique that ultimately allows for the selection and propagation of plasmid DNA via competent bacterial cells taking up the plasmid DNA. Positive selection for bacterial cells containing the plasmid DNA is accomplished by growth on medium containing an appropriate antibiotic, since the plasmid DNA is engineered to contain the corresponding antibiotic resistant gene.

Preparation of Competent Cells

Normally *Escherichia coli* cells do not possess the ability to take up DNA from the environment. However, if their cell walls are altered, these bacterial cells become more likely to incorporate foreign DNA and thus these cells are said to be 'competent'. These cells can be made competent by chemical or physical treatment. Chemical treatment includes the calcium chloride method while a physical treatment includes electroporation whereby the bacterial cell is shocked with 2500 V.

The chemical treatment method was used in order to make MC1061 *Escherichia coli* cells (Fermentas Life Sciences, Hanover, MD, USA) competent. These cells were used for cloning of the LASS4 and LASS5 fragments.

1. The night before making competent cells the desired bacterial (MC1061 *Escherichia coli*) strain was plated on Luria-Bertani (LB) Broth plates containing 10 mM Magnesium Chloride (MgCl2).

2. A single colony of the desired strain was added to 20 ml Tryptone Yeast Extract MgCl2 (TYM) Broth in a 500 ml conical flask and grown at 37 ºC overnight, shaking constantly at 300 xg.
3. 1 ml of cells in the TYM Broth were added to 100 ml fresh TYM Broth in a 2 L conical flask. The cells were grown for a further 2–3 hours or until optical density at 550 nm equals 0.2 at 37 ºC, shaking constantly at 300 xg.
4. Thereafter, 400 ml of fresh TYM broth was added to the 2 L conical flask and cells allowed to grow for a further 2–3 hours or until optical density at 550 nm lies between 0.4 and 0.6 at 37 ºC, shaking constantly at 300 xg.
5. Bacterial cells were rapidly cooled in ice water, shaking constantly after which they were centrifuged in two 125 ml propylene tubes at 3000 xg for 10 minutes at 4 ºC using the JA-10 rotor and J2-21 Beckman centrifuge (Beckman Coulter, Inc., Fullerton, CA, USA).
6. The supernatant was discarded and the pellet resuspended in 125 ml Tfb1. This solution was allowed to incubate for 30 minutes on ice after which the bacterial cells were centrifuged at 3000 xg for 10 minutes at 4 ºC using the JA-10 rotor and J2-21 Beckman centrifuge.
7. The bacterial cells were gently resuspended in 80 ml Tfb2 after which 300 µl were aliquoted into 0.5 ml eppendorf tubes. Freeze in liquid nitrogen or dry ice. These aliquoted cells were then stored at -70 ºC for further use.

Transformation steps

1. The ligation mix (containing the vector and insert) was added to 100 µl of E. coli (Fermentas, U.S.A) MC1061 competent cells.
2. This was then incubated on ice for 30 min, followed by 5 min incubation at 37 ºC.
3. The reactions were then immediately placed on ice for 2 min.
4. Luria broth (900 µl) was added and incubated at 37 ºC for 1 hour.

5. 100 µl of each reaction was plated on warmed (0.1mg/ml) ampicillin-containing agar plates as well as on agar plates (containing no ampicillin) and incubated at 37 ºC overnight.
6. An image of the plates was captured using a scanner (Bio-Rad gel Doc machine)

3.2.2.8 Colony PCR

Colony PCR is a technique by which the success of cloning can be evaluated. In this case, colony PCR was used to confirm the presence of the insert.

Ten colonies were picked randomly and mixed with 10 µl of sterile distilled water in each tube, making colony mixes. This was then used as a template and the PCR reactions were run as per table 3 and table 4, Appendix 3, using specific primers to amplify LASS4 and LASS5 fragments.

To check which colonies were carrying the insert, PCR products were ran on a 1.0% agarose gel parallel to a 50bp molecular marker in 1X TBE buffer at 80V for 1.5 hr.

The mixes that contained the insert were each added to 6 ml of LB containing ampicillin to a final concentration of 0.1 g/ml and incubated overnight on a 37 ºC shaking incubator. The incubator was set at 150 xg. This step was done to ensure that all bacterial cells present in the colony mix contained the LASS4 and LASS5 inserts and other contaminating bacteria would die due to the inability to express ampicillin resistant gene. This was also to ensure growth and multiplication of bacterial cells as well as the recombinant plasmids they contain. Sufficient bacterial growth was determined by the medium turning turbid or milky.

3.2.2.9 Plasmid extraction

Plasmid DNA extraction is the method used to extract plasmid DNA from bacterial cells such as *E coli*. The plasmid DNA was purified from the overnight cultures using the WizardPlus™ SV Miniprep DNA Purification System kit (Promega). This was done by following the manufacturer's instructions. All steps were carried out at room temperature.

The first step was to aliquot 0.8 ml (overnight cultures) and 0.2 ml of glycerol into 1.5 ml eppendorf tubes. This was mixed by pipetting and stored at -80 ºC as the glycerol stock. The second step was to centrifuge the overnight culture for 8 min at 12000 xg at room temperature (RT). This was followed by thoroughly resuspending pellet with 250 µl cell resuspension solution. A 250 µl cell lysis solution was then added to the suspension, this was inverted 4–5 times to mix. This was followed by the addition of 10 µl alkaline protease solution, inverted 4–5 times to mix, and incubated at RT for 5 min. A 350 µl neutralising solution was added to the suspension, inverted 4–5 times for mixing. This was followed by centrifuging at 12000 xg for 10 min at RT. The spin column was inserted into the collection tube, where the cleared lysate was decanted. This was centrifuged at 12000 xg at RT for 1 min, the flow through was discarded and the spin column was reinserted back into the collection tube. The plasmid DNA was washed through two steps with wash solution (ethanol added), the first step with 750 µl and the second step with 250 µl, with centrifuging at RT 12000 xg after every wash. The spin column was then transferred into a sterile 1.5 ml eppendorf tube and the collection tube was discarded. The plasmid DNA was then eluted with 70 µl of nuclease free water and this was spun at 12000 xg at RT. The spin column was then discarded and the plasmid DNA was stored at -20 ºC for use.

NB: PCR was run using LASS4 and LASS5 specific primers to confirm the presence of the inserts before sending for sequencing.

3.2.2.10 Sequencing and Data analysis

The purified clone was sent to Inqaba-Biotech Industries (SA) to determine the sequence of the LASS4 and LASS fragments. Results were analysed using Finch Server and BLAST at URL: http://www.ncbi.nlm.nih.gov. This was done to compare the sequence obtained from Inqaba-Biotech, to reference sequences of LASS4 and LASS5, obtained from NCBI.

3.2.2.11 Real-Time PCR

Real-Time PCR is a technique that simultaneously quantifies and amplifies a specific part of a given DNA molecule. Real-Time PCR is used to determine whether or not a specific sequence is present in the sample, and if present, the number of copies present in the sample. Quantitative Real-Time PCR (qRT-PCR) is used to quantify the amount of a target gene in a sample. QRT-PCR can be divided into absolute (measures total amount of target gene in a sample) and relative (compares the amount of target gene between two samples) quantification. The main aim of this project was to determine and compare the expression levels of CerS4 and CerS5 in endometrial and colon cancer, and thus relative qRT- PCR was used.

The primers were designed in such a way as to avoid forming a hairpin-loop and dimers, as these interfere with the accuracy of the results. The primers were then sent to Inqaba-Biotec for synthesis. Quantitative Real-Time (qReal-Time) PCR was done using SYBR Green kit (Bio-Rad). SYBR green is a fluorescent dye that binds to double stranded PCR product and fluoresces. Because multiple SYBR Green molecules bind to a single amplification product, SYBR Green is very sensitive. Thus, the amount of fluorescence is equivalent to the amount of the product accumulated. cDNA synthesised from the non-cancerous and cancerous, treated and untreated cell lines under investigation were used as templates. The gene expression curves were analysed and compared between the normal and cancer samples using Amplicon software (Bio-Rad).

No template was added in the negative control.

cDNA was synthesised and a series of 5X dilutions were used to construct standard curves for LASS4 (using GMMe), LASS5 (using Caco-2) and β-actin (using HT-29) cDNA, shown in table 5a-5c, Appendix 5. The reaction mix was set-up as indicated in table 5d, and table 5e shows the Real-Time PCR conditions, Appendix 5. The Livak Method $2^{-\Delta\Delta CT}$ was used to analyse the results. β-actin was previously shown by (Senkal *et al*., 2007; Jin *et al*., 2009; Schiffmann *et al*., 2009) as a suitable internal control for CerS4 and CerS5. This method was chosen because the amplification efficiencies of target (LASS 4 and/ or LASS 5) and internal control (β-actin) are ± 5% apart.

The Livak method ($2^{-\Delta\Delta CT}$), (Livak and Schmittgen, 2001; Schmittgen and Livak, 2008) was used to calculate the relative expression level of CerS4 and CerS5 in endometrial and colon cell lines. The GMMe and Caco-2 cell lines were used as calibrator samples, whereas Hec-1A and HT-29 were used as test samples. Furthermore, all untreated cells were use as calibrator samples while treated cells were used as test samples.

3.2.2.12 Statistical analysis

The results were expressed as means ± standard error means (SEM) for at least three independent experiments, using Graphpad Prism 5. Significant differences were determined using one-way analysis of variance (ANOVA) followed by Tukey's multiple comparison test. Appendix 4 shows statistical analysis for FACS, while Appendix 5 shows statistical analysis for qRT-PCR. A probability level of $p < 0.05$ was considered significant.

CHAPTER 4

RESULTS

4.1 INTRODUCTION

This chapter addresses the research questions and objectives discussed in section 1.6 and section 1.7, and it is divided into two sections, the bio-informatics analysis section and the gene expression analysis section. As CerSes (4 and 5) have been implicated in cancer biology, we sought to use bio-informatics to investigate how CerS4 and CerS5 activities can be influenced by other proteins. Previous studies show that 70–80% of proteins share at least one identical function with their interacting partners (Deng *et al*., 2003; Letovysky and Kasif, 2003; Zhang *et al*., 2009). Protein-protein interaction databases (STRING, InAct and Bio-GRID) were used to determine possible protein-protein interactions for CerS4 and CerS5. Sequence alignment tools (Multi-Align, Clustal omega and COBALT) were then used to check for domain conservation and sequence similarities between CerS (4 and 5) sequences and their protein interacting partners, as previously reported by Zhang *et al*., (2009) that protein function can be inferred using domain or sequence similarities. QRT-PCR was subsequently used to study gene expression levels of CerS4 and CerS5 in endometrial and colon cancer. FACS analysis was then used to study and quantify apoptosis. This lead to the investigation of the relationship between CerS (4 and 5), and apoptosis, using qRT-PCR, i.e. qRT-PCR was done before and after apoptosis induction in treated and untreated samples, using the Livak method (Livak and Schmittgen, 2001; Schmittgen and Livak, 2008).

4.2 BIO-INFORMATICS ANALYSIS OF PROTEINS THAT POTENTIALLY INTERACT WITH CERS4 AND CERS5

4.2.1 Identification of proteins that potentially interact with CerS4 and CerS5

In using STRING database, at least 30 proteins were discovered to possibly interact with CerS4, shown in figure 4.1. Twelve proteins were discovered to be protein interactors of CerS5, presented in figure 4.2. Only predicted interactions were revealed for both CerS4 and CerS5. These results indicate that little is known about CerS4 and CerS5 protein structure. Furthermore, these results reveal that the CerS4 and CerS5 interacting partners are involved in apoptosis, in cell-cycle regulation and in cell proliferation. Interestingly, some of the protein interactors are involved in bone and cartilage formation, and also in the central nervous system regulation. The results obtained from IntAct and Bio-GRID show that CerS4 and CerS5 interact with proteins involved in ubiquitination. (Results from these databases, IntAct and Bio-GRID are obtained from experimentally determined interactions (Wagner *et al*., 2011; Calderwood *et al*., 2007).

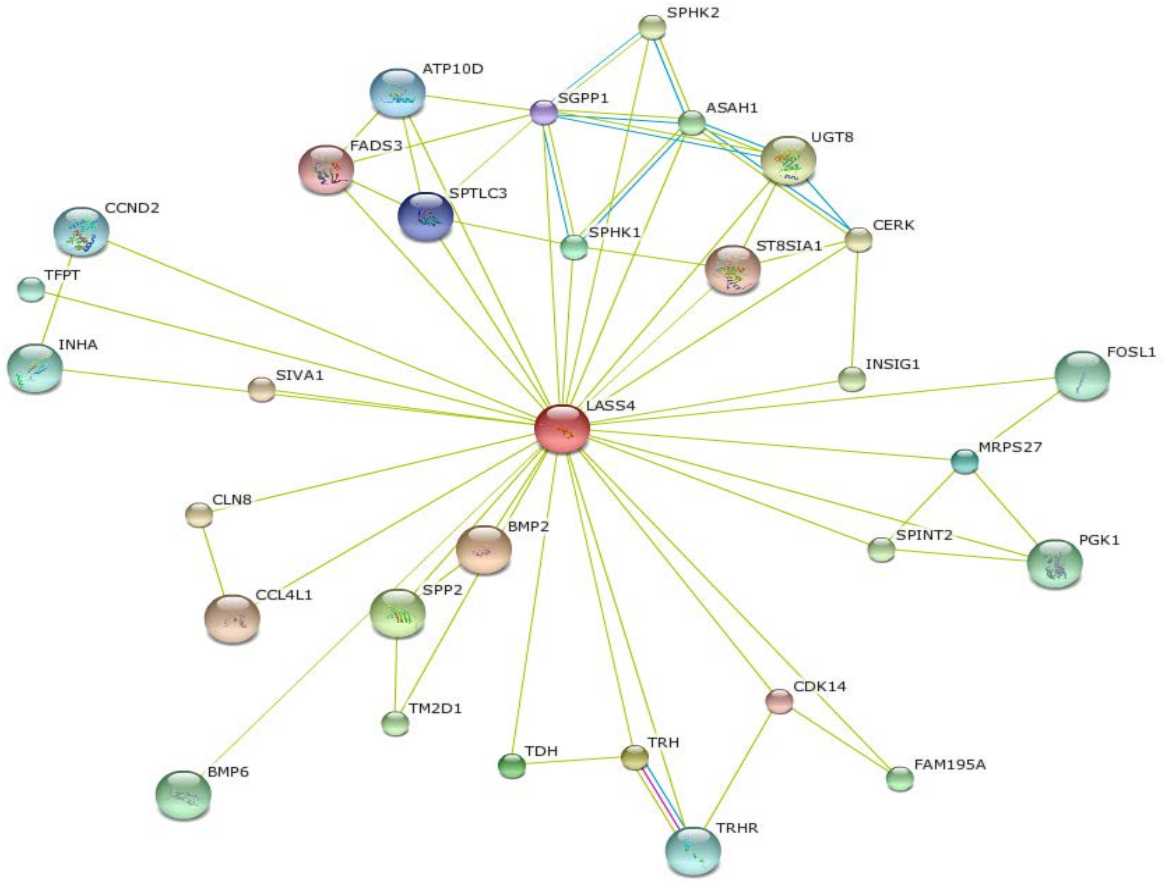

Figure 4.1 - LASS 4 protein interaction network using STRING database: Single lines only show a predicted protein interaction and double lines illustrating a stronger interaction. Triple lines showing an interaction between a ligand and its receptor (STRING-Protein-Interaction Network). The double lines are only observed between CerS4 interacting partners and not directly between CerS4 and its interacting partners. The ligand-receptor interaction is observed between TRH and TRHR. These results indicate that little is known about CerS4 protein structure, and implicates these protein interacting partners as potential interactors.

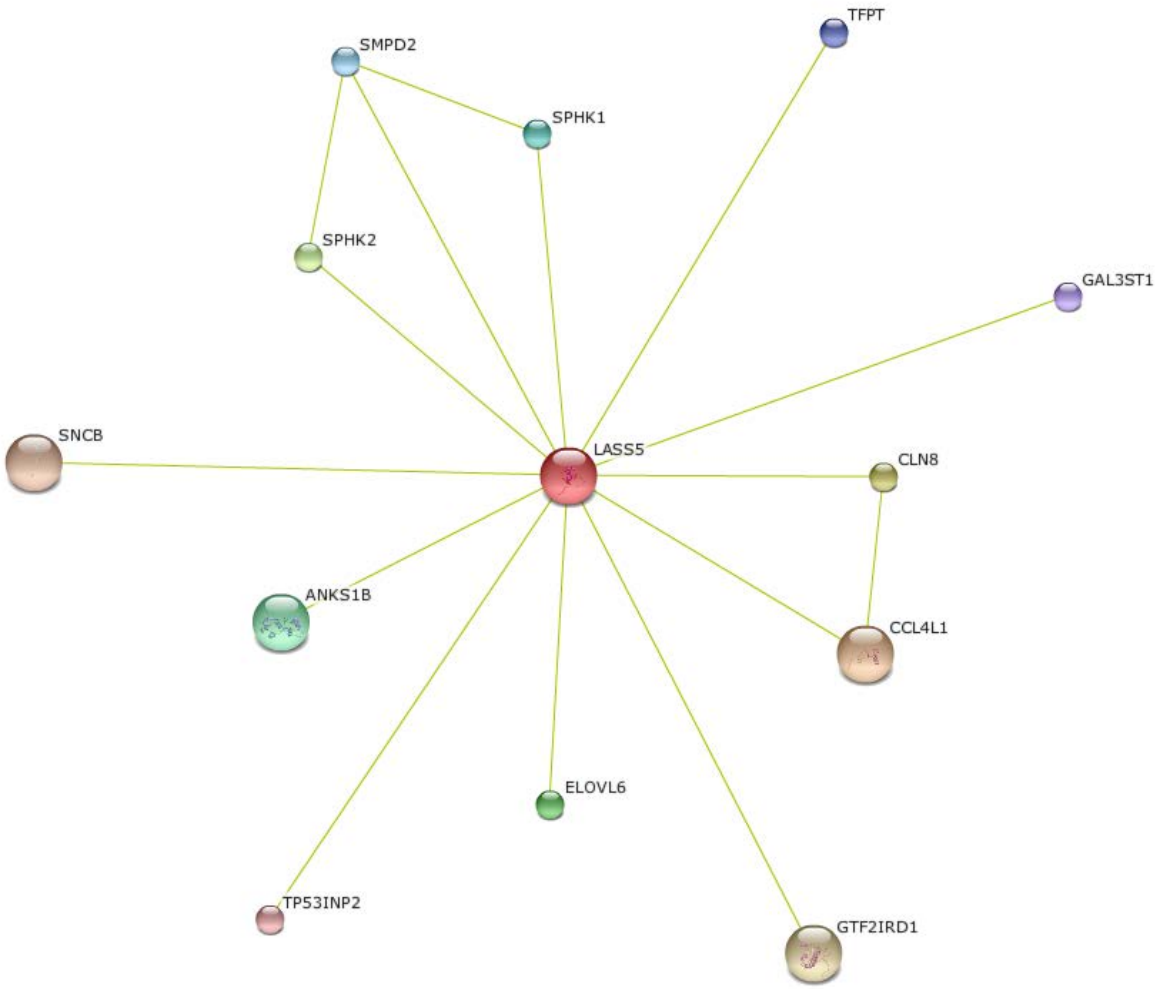

Figure 4.2 - LASS 5 predicted protein interaction network using STRING database: Single lines only showing a predicted protein interaction. (STRING-Interaction Network). Only predicted interactions are observed with CerS5 and there is no strong evidence yet of stronger interactions.

4.2.2 Implication of CerS4 and CerS5 interacting partners in cell-cycle regulation and cellular homeostasis

Table 4.1 and 4.2 summarises the interactions seen in STRING diagrams for LASS4 and LASS5. The information for each protein was obtained from STRING database and NCBI. Accession numbers were also obtained from NCBI. In addition, at least five protein-interacting partners were shown to be shared by CerS4 and CerS5, accession numbers highlighted in red in both table 4.1 and table 4.2.

Table 4.1: CerS4 predicted protein interacting partners

Protein name and Accession number	Function/Information
• SPHK1 Sphingosine kinase 1 ❖ **NP_892010.2**	Catalyses the phosphorylation of sphingosine to form sphingosine 1-phosphate (SPP), a lipid mediator with both intra- and extracellular functions. Also acts on D-erythro-sphingosine and to a lesser extent sphinganine, but not other lipids, such as D,L-threo-dihydrosphingosine, N,N-dimethylsphingosine, diacylglycerol, ceramide, or phosphatidylinositol
• SPHK2 Sphingosine kinase 2 ❖ **NP_064511.2**	Catalyses the phosphorylation of sphingosine to form sphingosine 1-phosphate (SPP), a lipid mediator with both intra- and extracellular functions. Also acts on D-erythro-dihydrosphingosine, D-erythro-sphingosine and L-threo-dihydrosphingosine
• CERK Ceramide kinase ❖ NP_073603.2	Catalyses specifically the phosphorylation of ceramide to form ceramide 1-phosphate. Acts efficiently on natural and analog ceramides (C6, C8, C16 ceramides, and C8-dihydroceramide), to a lesser extent on C2-ceramide and C6-dihydroceramide, but not on other lipids, such as various sphingosines
• ATP10D ATPase, class V, type 10D ❖ AAI31536.1	ATPase, class V, type 10D
• UGT8 UDP glycosyltransferase 8 ❖ AAC51187.1	Catalyses the transfer of galactose to ceramide, a key enzymatic step in the biosynthesis of galactocerebrosides, which are abundant sphingolipids of the myelin membrane of the central nervous system and peripheral nervous system
• FADS3 Fatty acid desaturase 3 ❖ NP_068373.1	Fatty acid desaturase 3
• BMP2 Bone morphogenetic protein 2 ❖ NP_001191.1	Induces cartilage and bone formation
• BMP6 Bone morphogenetic protein 2 ❖ NP_001709.1	Induces cartilage and bone formation

Protein name and Accession number	Function/Information
• SPTLC3 Serine palmitoyltransferase, long chain base subunit 3 ❖ NP_060797.2	Serine palmitoyltransferase (SPT). The heterodimer formed with LCB1/SPTLC1 constitutes the catalytic core. The composition of the serine palmitoyltransferase (SPT) complex determines the substrate preference. The SPTLC1-SPTLC3-SSSPTA isozyme uses both C14-CoA and C16-CoA as substrates, while the SPTLC1-SPTLC3-SSSPTB has the ability to use a broader range of acyl-CoAs without apparent preference
• CDK14 Cyclin-dependent kinase 14 ❖ NP_036527.1	May play a role in meiosis as well as in neuron differentiation
• TRHR Thyrotropin-releasing hormone receptor ❖ NP_003292.1	Receptor for thyrotropin-releasing hormone. This receptor is mediated by G proteins which activate a phosphatidylinositol-calcium second messenger system
• MRPS27 Mitochondrial ribosomal protein S27 ❖ NP_055899.2	Mitochondrial ribosomal protein S27
• PGK Phosphoglycerate kinase 1 ❖ NP_000282.1	In addition to its role as a glycolytic enzyme, it seems that PGK-1 acts as a polymerase alpha cofactor protein (primer recognition protein)
• ST8STA1 ST8 alpha-N-acetyl-neuraminide alpha-2,8-sialyltransferase 1 ❖ NP_003025.1	Involved in the production of gangliosides GD3 and GT3 from GM3; gangliosides are a subfamily of complex glycosphinglolipds that contain one or more residues of sialic acid
• TM2D1 TM2 domain containing 1 ❖ EAX06599.1	May participate to beta-amyloid-induced apoptosis via its interaction with beta-APP42
• INHA Inhibin alpha ❖ NP_002182.1	Inhibins and activins inhibit and activate, respectively, the secretion of follitropin by the pituitary gland. Inhibins/activins are involved in regulating a number of diverse functions such as hypothalamic and pituitary hormone secretion, gonadal hormone secretion, germ cell development and maturation, erythroid differentiation, insulin secretion, nerve cell survival, embryonic axial development or bone growth, depending on their subunit composition. Inhibins appear to oppose the functions of activins.

Protein name and Accession number	Function/Information
• INSIG1 Insulin induced gene 1 ❖ NP_005533.2	Mediates feedback control of cholesterol synthesis by controlling SCAP and HMGCR. Functions by blocking the processing of sterol regulatory element-binding proteins (SREBPs). Capable of retaining the SCAP-SREBF2 complex in the ER thus preventing it from escorting SREBPs to the Golgi. Seems to regulate the ubiquitin-mediated proteasomal degradation of HMGCR. May play a role in growth and differentiation of tissues involved in metabolic control. May play a regulatory role during G0/G1 transition of cell growth
• FOSL1 FOS-like antigen 1 ❖ BAD96622.1	FOS-like antigen 1
• TRH Thyrotropin-releasing Hormone ❖ NP_009048.1	Functions as a regulator of the biosynthesis of TSH in the anterior pituitary gland and as a neurotransmitter/ neuromodulator in the central and peripheral nervous systems
• TFPT TCF3 (E2A) fusion partner (in childhood Leukemia) ❖ **NP_037474.1**	TCF3 (E2A) fusion partner (in childhood Leukemia)
• CLN8 Ceroid-lipofuscinosis, neuronal 8 ❖ **NP_061764.2**	Could play a role in cell proliferation during neuronal differentiation and in protection against cell death
• CCND2 Cyclin D2 ❖ NP_001750.1	Essential for the control of the cell cycle at the G1/S (start) transition
• TDH L-threonine dehydrogenase ❖ CAC82738.1	L-threonine dehydrogenase
• SPP2 Secreted phosphoprotein 2 ❖ AAI06706.1	Could coordinate an aspect of bone turnover
• SPINT2 Serine peptidase inhibitor, Kunitz type, 2 ❖ AAH12868.1	Serine peptidase inhibitor, Kunitz type, 2

Protein name and Accession number	Function/Information
• FAM195A Family with sequence similarity 195, member A ❖ NP_612427.2	Family with sequence similarity 195, member A
• SIVA1 Apoptosis-inducing factor ❖ NP_006418.2	Induces CD27-mediated apoptosis. Inhibits BCL2L1 isoform Bcl-x(L) anti-apoptotic activity. Inhibits activation of NF-kappa- B and promotes T-cell receptor-mediated apoptosis
• CCL4L1 Chemokine (C-C motif) ligand 4-like 1 ❖ **AAI44395.1**	Monokine with inflammatory and chemokinetic properties. Binds to CCR5. One of the major HIV-suppressive factors produced by CD8+ T-cells. Recombinant MIP-1-beta induces a dose-dependent inhibition of different strains of HIV-1, HIV-2, and simian immunodeficiency virus (SIV). The processed form MIP-1-beta (3-69) retains the abilities to induce down-modulation of surface expression of the chemokine receptor CCR5 and to inhibit the CCR5- mediated entry of HIV-1 in T-cells. MIP-1-beta(3-69) is also a ligand for CCR1 and CCR2 isoform B
• SGPP1 Sphingosine-1-phosphate phosphatase 1 ❖ AAK26660.1	Has enzymatic activity against both sphingosine 1 phosphate (S1P) and dihydro-S1P. Regulates intracellular and extracellular S1P levels
• ASAH1 Acid ceramidase 1 ❖ NP_004306.3	Hydrolyses the sphingolipid ceramide into sphingosine and free fatty acid
• BPLF1 Large tegument protein (Epstein Barr Virus) ❖ CAD53402	Involved in deubiquitination activity.

Table 4.2: CerS5 predicted protein interacting partners

Protein name	Function/Information
• SMPD2 Sphingomyelin phosphodiesterase 2, neutral membrane (neutral sphingomyelinase) ❖ NP_003071.2	Converts sphingomyelin to ceramide. Hydrolyse 1-acyl-2-lyso-sn-glycero-3-phosphocholine (lyso-PC) and 1-O-alkyl-2-lyso- sn-glycero-3-phosphocholine
• GAL3ST1 Galactose-3-O-sulfotransferase 1 ❖ NP_004852.1	Catalyses the sulfation of membrane glycolipids. Seems to prefer beta-glycosides at the non-reducing termini of sugar chains attached to a lipid moiety. Catalyses the synthesis of galactosylceramide sulfate (sulfatide), a major lipid component of the myelin sheath and of monogalactosylalkylacylglycerol sulfate (seminolipid), present in spermatocytes (By similarity). Also acts on lactosylceramide, galactosyl 1-alkyl-2-sn-glycerol and galactosyl diacylglycerol (*in vitro*)
• GTF2IRD1 General transcription factor II-Irepeat domain containing 1 ❖ NP_057412.1	May be a transcription regulator involved in cell-cycle progression and skeletal muscle differentiation. May repress GTF2I transcriptional functions, by preventing its nuclear residency, or by inhibiting its transcriptional activation. May contribute to slow-twitch fiber type specificity during myogenesis and in regenerating muscles. Binds troponin I slow-muscle fiber enhancer (USE B1). Binds specifically and with high affinity to the EFG sequences derived from the early enhancer of HOXC8
• ANKS1B Ankyrin repeat and sterile alpha motif domain containing 1B ❖ NP_690001.3	Isoform 2 may participate in the regulation of nucleoplasmic coilin protein interactions in neuronal and transformed cells
• SPHK1 Sphingosine kinase 1 ❖ **NP_892010.2**	Catalyses the phosphorylation of sphingosine to form sphingosine 1-phosphate (SPP), a lipid mediator with both intra- and extracellular functions. Also acts on D-erythro-sphingosine and to a lesser extent sphinganine, but not other lipids, such as D,L-threo-dihydrosphingosine, N,N-dimethylsphingosine, diacylglycerol, ceramide, or phosphatidylinositol
• SPHK2 Sphingosine kinase 2 ❖ **NP_064511.2**	Catalyses the phosphorylation of sphingosine to form sphingosine 1-phosphate (SPP), a lipid mediator with both intra- and extracellular functions. Also acts on D-erythro-dihydrosphingosine, D-erythro-sphingosine and L-threo-dihydrosphingosine

Protein name	Function/Information
• CLN8 Ceroid-lipofuscinosis, neuronal 8 ❖ **NP_061764.2**	Could play a role in cell proliferation during neuronal differentiation and in protection against cell death
• ELOVL6 ELOVL family member 6, elongation of long chain fatty acids ❖ NP_076995.1	Fatty acid elongase specific to C12-C16 saturated and monoinsaturated fatty acids
• TFPT TCF3 (E2A) fusion partner (in childhood Leukemia) ❖ **NP_037474.1**	TCF3 (E2A) fusion partner (in childhood Leukemia)
• TP53INP2 Tumour protein p53 inducible nuclear protein 2 ❖ NP_067025.1	Tumour protein p53 inducible nuclear protein 2
• SNCB Synuclein, beta ❖ NP_003076.1	Non-amyloid component of senile plaques found in Alzheimer disease. Could act as a regulator of SNCA aggregation process. Protects neurons from staurosporine and 6-hydroxy dopamine (6OHDA)-stimulated caspase activation in a TP53/p53-dependent manner. Contributes to restore the SNCA anti-apoptotic function abolished by 6OHDA. Not found in the Lewy bodies associated with Parkinson disease
• CCL4L1 Chemokine (C-C motif) ligand 4-like 1 ❖ **AAI44395.1**	Monokine with inflammatory and chemokinetic properties. Binds to CCR5. One of the major HIV-suppressive factors produced by CD8+ T-cells. Recombinant MIP-1-beta induces a dose-dependent inhibition of different strains of HIV-1, HIV-2, and simian immunodeficiency virus (SIV). The processed form MIP-1-beta(3-69) retains the abilities to induce down-modulation of surface expression of the chemokine receptor CCR5 and to inhibit the CCR5- mediated entry of HIV-1 in T-cells. MIP-1-beta(3-69) is also a ligand for CCR1 and CCR2 isoform B
• UBC Polyubiquitin ❖ NP_066289	This gene represents a ubiquitin gene, ubiquitin C. The encoded protein is a polyubiquitin precursor. Conjugation of ubiquitin monomers or polymers can lead to various effects within a cell, depending on the residues to which ubiquitin is conjugated. Ubiquitination has been associated with protein degradation, DNA repair, cell cycle regulation, kinase modification, endocytosis, and regulation of other cell signaling pathways.

Following the protein interactions and determining their functions, CerS4 and CerS5 amino-acid sequences were aligned with the sequences of their predicted-interacting partners to examine sequence similarity.

4.2.3 Determination of sequence similarity between CerS4 and CerS5 and their interacting partners

The sequence alignment tools (Multi-Align, Clustal Omega and COBALT) reveal that there is no domain or sequence similarity shared between CerS4, CerS5 and their potential interacting partners, when all aligned together. Little sequence similarity is observed when CerS (4 and or 5) is aligned with one of its interacting partners, Appendix 3, figure 3a to figure 3f. Figure 4.3 shows CerS4 amino acid sequence alignment with five of its interacting partners and figure 4.4 shows CerS5 amino acid sequence alignment with five of its interacting partners using Multi-Align tool. As bio-informatics revealed a possible protein-interaction between CerS4 or CerS5 and proteins involved in apoptosis, gene expression studies were implemented to determine the expression level of CerS4 and CerS5 in cancerous versus non-cancerous samples, which also included apoptosis induction and FACS analysis.

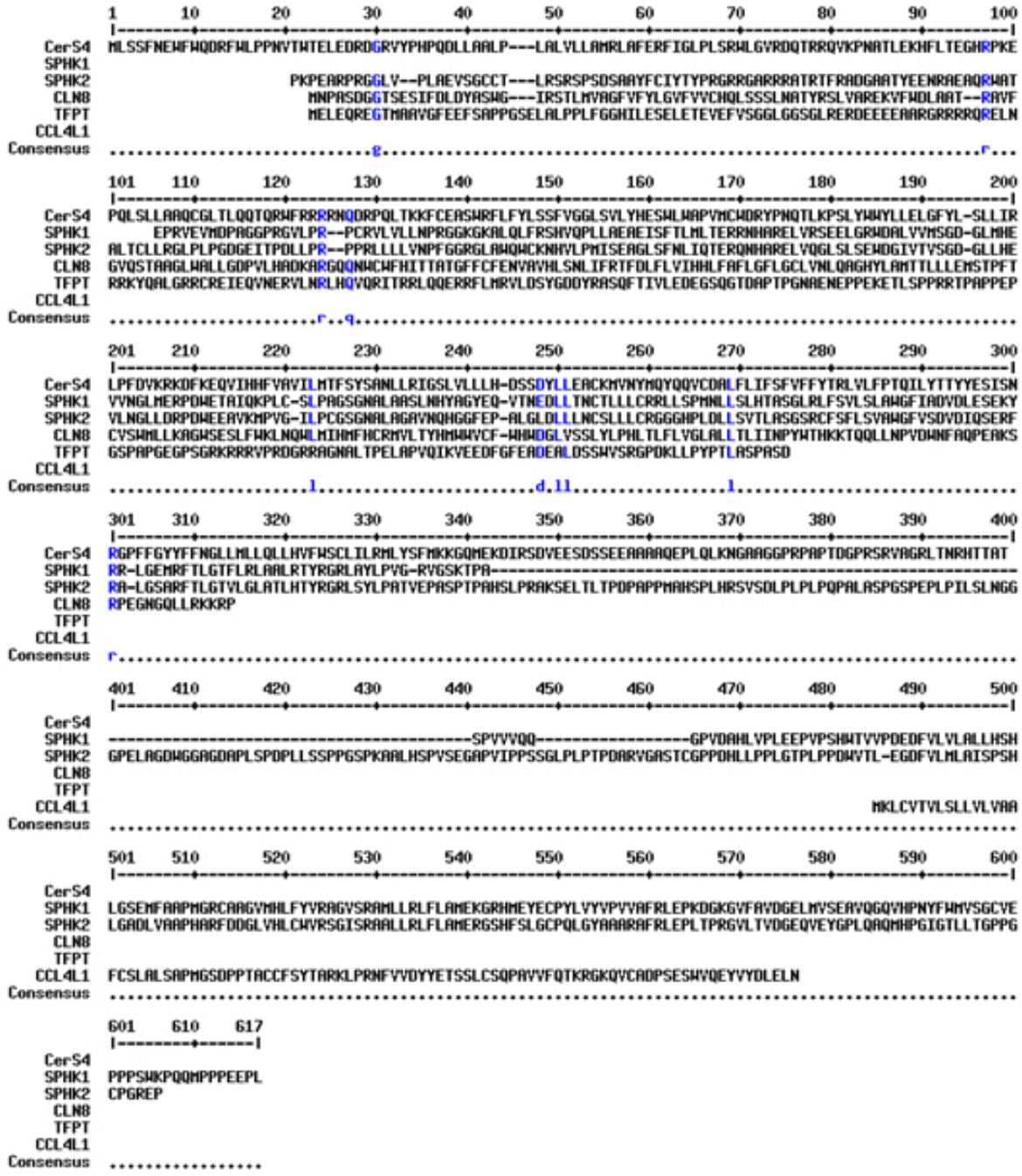

Figure 4.3 - The CerS4 and its protein interacting partners using Multi-Align: These results show an alignment between CerS4 and five of its potential protein interacting partners (also shown to share these protein interacting partners with (CerS5)). Low consensus sequence is shown in blue.

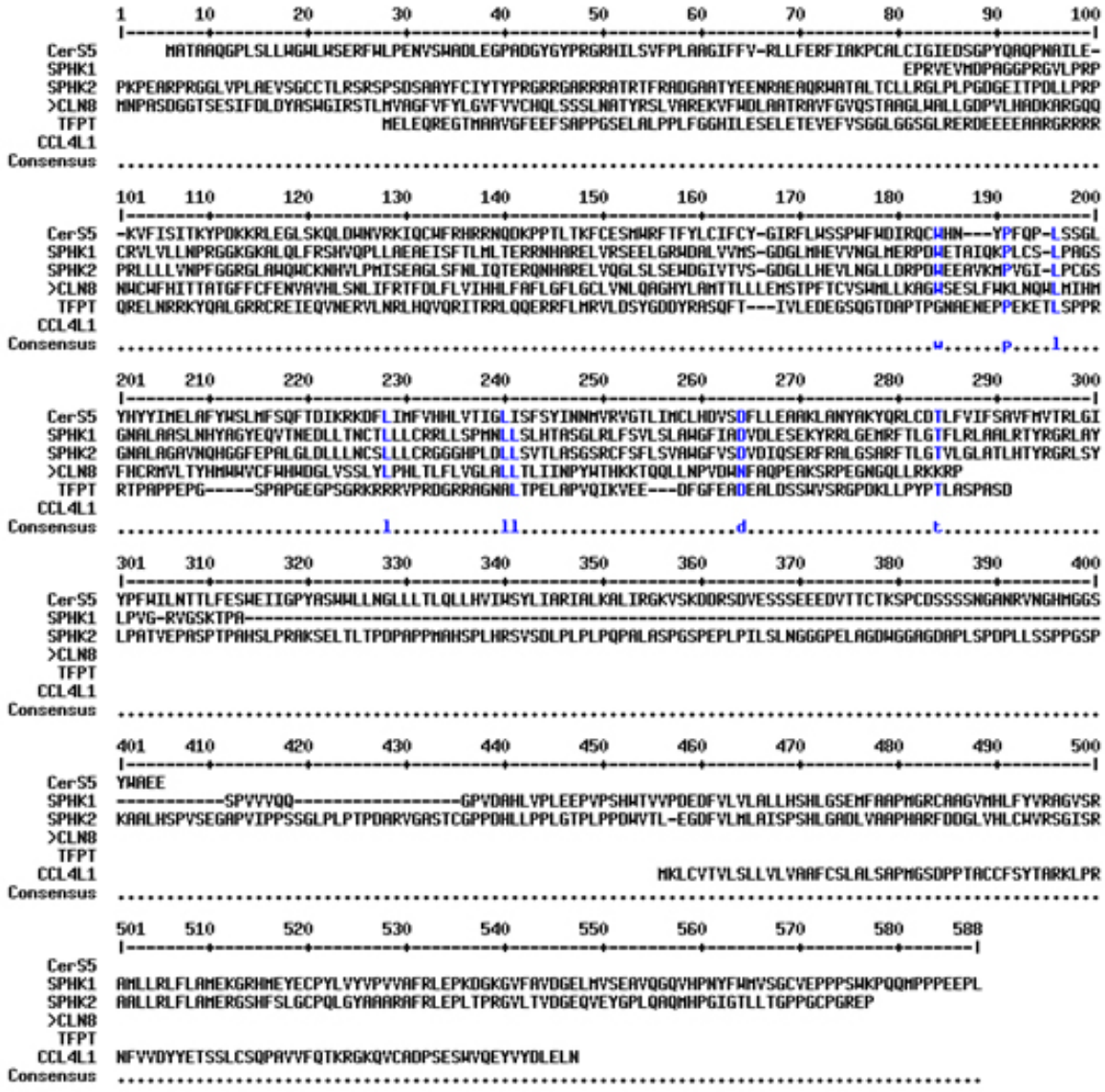

Figure 4.4 - The CerS5 and its protein interacting partners using Multi-Align: These results show an alignment between CerS5 and five of its potential protein interacting partners (also shown to share these protein interacting partners with (CerS4)). Low consensus sequence is shown in blue.

Protein-protein interactions are important in cellular functions such as signal transduction and apoptosis (Pawson and Nash, 2003). Using STRING database, only predicted interactions were revealed for both CerS4 and CerS5. However, using BioGRID database, polyubiquitin (UBC) was found to interact with CerS5 (This study was conducted and proven by Wagner *et al*., 2011). Furthermore, using IntAct database, CerS4 was shown to interact with the BFLP1 protein of the EBV virus through virus-human protein interactions, a mechanism used by this

virus to replicate and persist in the body (This study was determined and proven by Calderwood *et al*., 2007). Figure 3g and 3h (Appendix 3) show sequence alignment of CerS4 and CerS5 from IntAct and BioGRID databases, using MultiAlign. Additionally, little is known about the fundamental structure of the human CerS4 and CerS5 (LASS monomer, homodimer, heterodimer and higher order structure with additional accessory proteins), (Teufel *et al*., 2009), and this remains the same to date. However, results shown by the STRING interaction protein network implicate a role of CerS4 and CerS5 in cell-cycle regulation and apoptosis. Interestingly, our findings indicate that CerS4 and CerS5 share no sequence similarity with their protein interacting partners. It was also revealed in this study that there was no potential protein interaction between the LASS proteins, as they share high sequence similarity. These findings may implicate distinct biological roles of CerSes, as previously demonstrated by Senkal *et al*., (2010). As previously shown that proteins interacting together share at least one identical function (Zhang *et al*., 2009), our Bio-informatics results revealed that CerS4 and CerS5 interact with proteins involved in apoptosis and cell cycle regulation.

4.3 GENE EXPRESSION ANALYSIS OF CERS4 AND CERS5 IN COLON AND ENDOMETRIAL CANCERS

Following the Bio-informatics analysis, gene expression analysis was done to determine the expression level of CerS4 and CerS5 in colon and endometrial cancers. Total RNA was extracted from all cell lines, and then was subjected to reverse transcription for cDNA synthesis, which was used as a template for qRT-PCR. The expression levels of CerS4, CerS5 were determined in malignant (test) compared to their non-malignant (calibrator) samples. Flow cytometry (FCM)/ fluorescence-activated cell sorter (FACS) was then used to analyse apoptosis. QRT-PCR was repeated to compare CerS4, CerS5 expression levels in treated and untreated samples.

4.3.1 Induction of apoptosis by 5FU and anastrozole

Both endometrium and colon cell lines were cultured and apoptosis was induced. FACS was used to determine and analyse apoptosis induced by 5 µM of 5-FU in colon cell lines and 2 µM of anastrozole in endometrial cell lines. For each experiment/cell-line, blank (Untreated and Unstained), and a negative control (Untreated and Stained with annexin-V and/or propidium iodide (PI)), were used. The blank was used to localise the population of a particular cell-line. The negative control was used to determine the true apoptotic signal from the false background/ necrosis. Results are represented in cytograms and bar graphs. The vertical and the horizontal gates were consistent for each experiment and its controls.

4.3.2 Apoptosis analysis using Flow cytometry (FCM)/ fluorescence-activated cell sorting (FACS) analysis

Experiments were done on three independent occasions, each in triplicate. Figue 4.5 , 4.6 (GMMe) and figure 4.7, 4.8 (Hec-1A) show FACS analysis and graphs resulting from statistical analysis for endometrial cell lines.

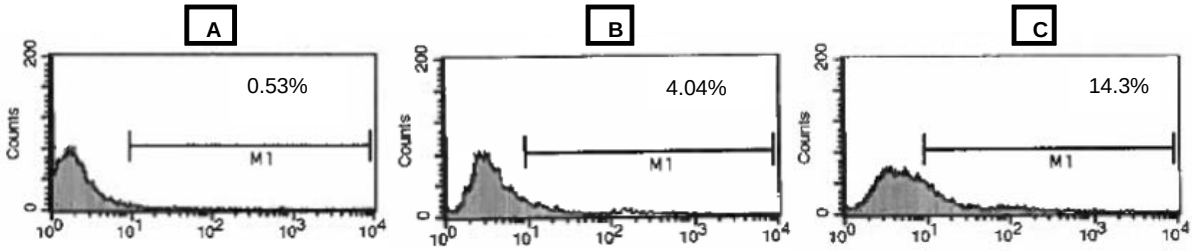

Figure 4.5 - FACS analysis of GMMe endometrial cell-line: **A** represents the blank (untreated cells), **B** represents the negative control (untreated but stained) and **C** represents the 24h treated cells, stained with annexin-V and PI. This demonstrates the exposure of phophatidylserine from the cytosolic side to the surface in the endometrium cells (GMMe), treated with 2 µM of anastrozole for 24h. Annexin-V FITC apoptosis detection assay results are represented in histograms, denoting the percentage of cells staining positive for annexin-V in the M1 region.

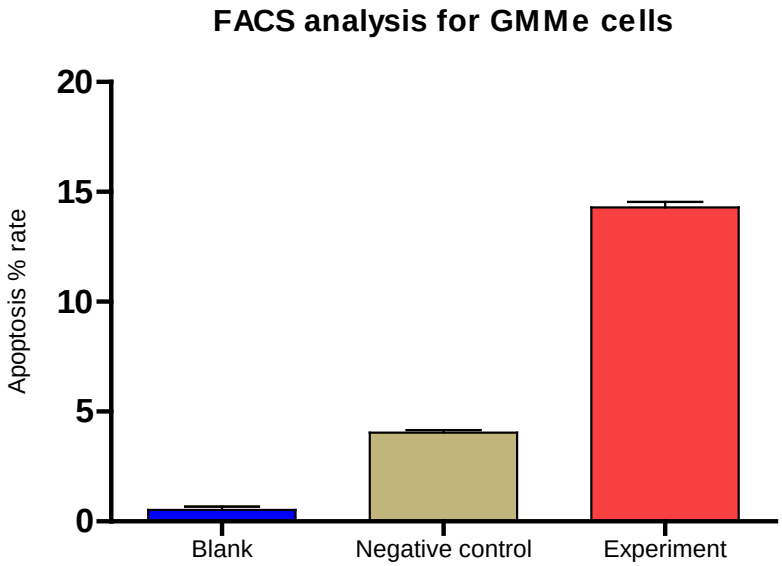

Figure 4.6 - ANOVA and Tukey's multiple comparison test for GMMe endometrial cells: The 2 µM anastrozole treated cells (GMMe experiment) show a higher apoptosis percentage rate compared to the untreated cells. Statistical differences were determined with one-way ANOVA followed by the Tukey's post comparison test. P <0.05 was considered significant.

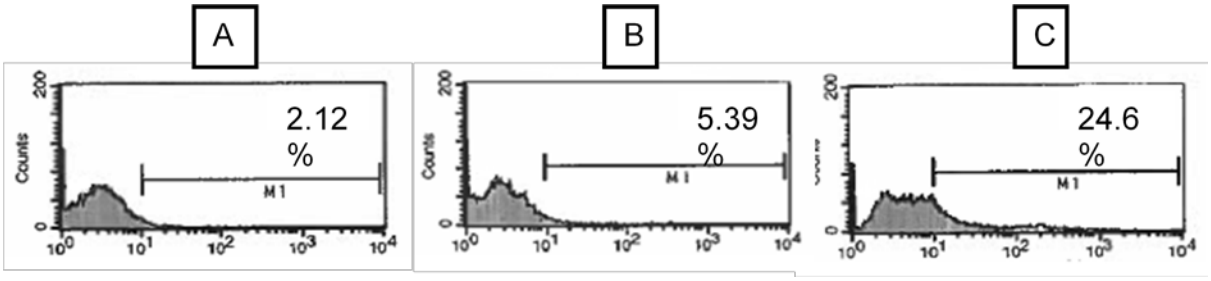

Figure 4.7 - FACS analysis of Hec-1A cell-line: **A** represents the blank (untreated cells), **B** represents the negative control (untreated but stained) and **C** represents the 24h treated cells, stained with annexin-V and PI. This represents the exposure of phophatidylserine from the cytosol to the surface in the endometrium cells (Hec-1A), treated with 2 µM of anastrozole for 24h. Annexin-V FITC apoptosis detection assay results are represented in histograms, denoting the percentage of cells staining positive for annexin-V in the M1 region.

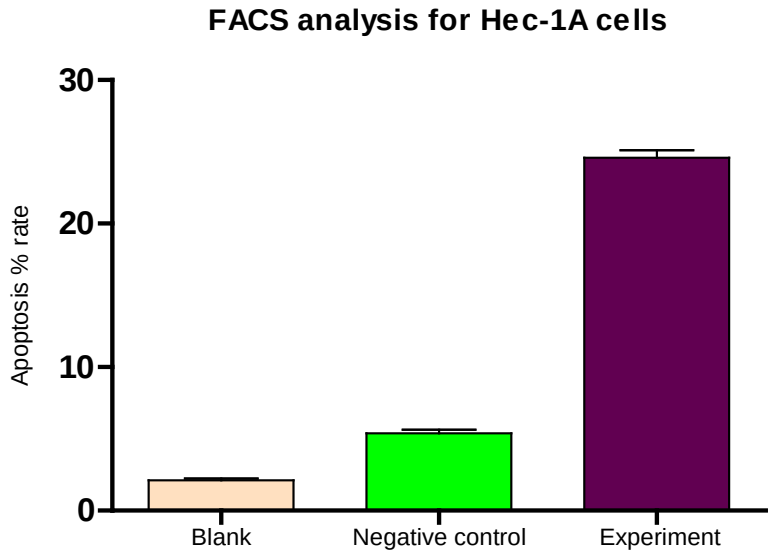

Figure 4.8 - ANOVA and Tukey's multiple comparison test for Hec-1A cells treated with 2 µM anastrozole: The Hec-1A treated (experiment) cells exhibit almost a three -fold of apoptosis percentage rate compared to the negative control. Statistical differences were determined with one-way ANOVA followed by the Tukey's post comparison test. $P < 0.05$ was considered significant.

Results for FACS and statistical analysis in colon cells are shown below. Figure 4.9, 4.10 (Caco-2) and figure 4.11, 4.12 (HT-29) illustrate analysed results for FACS and statistics in colon cell lines respectively. The FACS values for ALL cell lines and their statistical analysis are shown in Appendix 4. Table 4a–4d show FACS and statistical analysis for endometrial cell lines, while table 4e–4h show FACS and statistical analysis for colon cell lines.

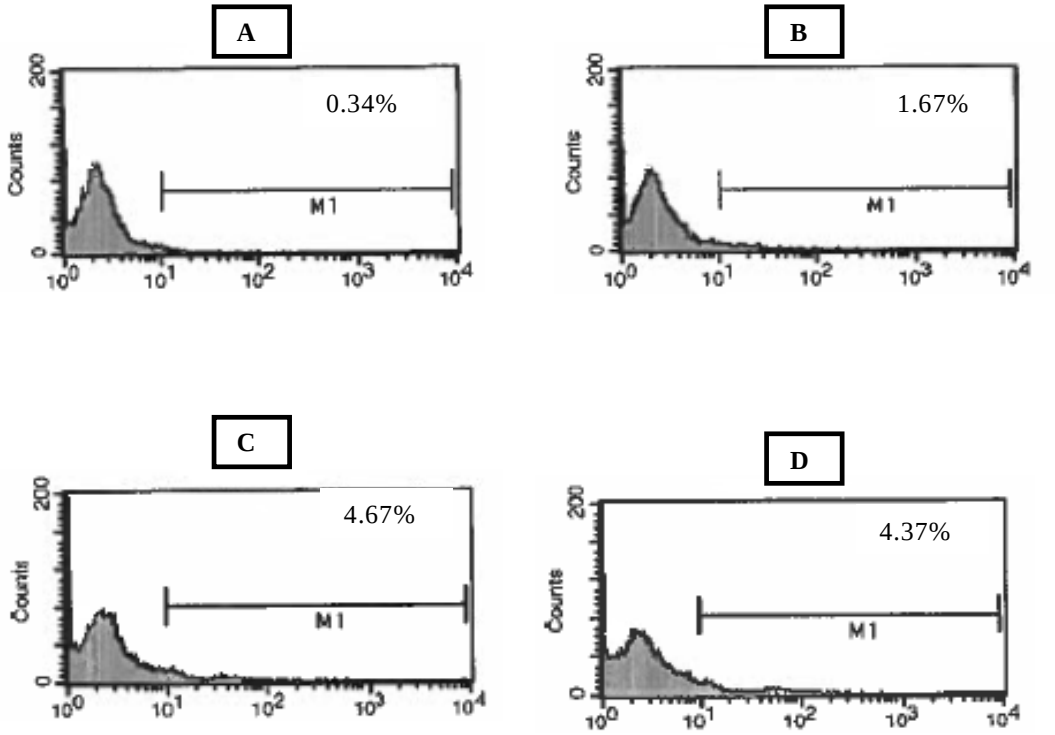

Figure 4.9 - FACS analysis of Caco-2 cells treated with 5 µM of 5FU: **A** represents the blank (untreated cells), **B** represents the negative control (untreated but stained), **C** represents the 24h treated cells and **D** represents the 48h treated cells, stained with annexin-V and PI. The histograms show the exposure of phophatidylserine from the cytosolic side to the surface in the colon cells (Caco-2), treated with 5 µM of 5-FU for 24h and 48h. Annexin-V FITC apoptosis detection assay results are represented in histograms, denoting the percentage of cells staining positively for annexin-V in the M1 region.

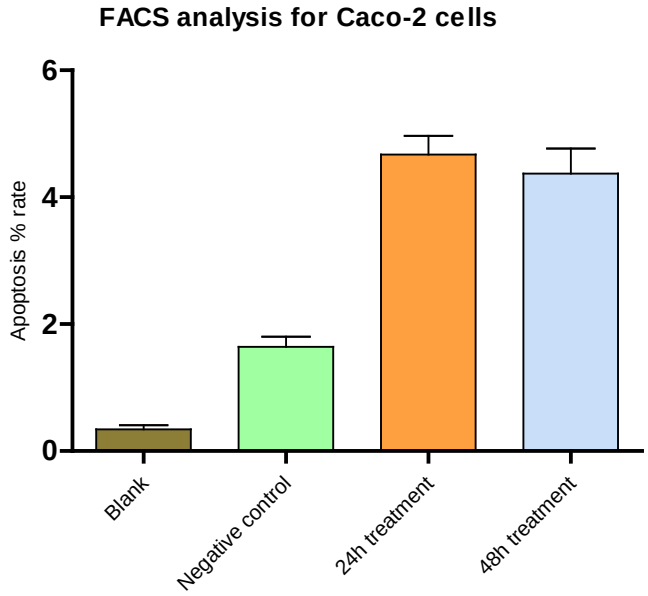

Figure 4.10 - ANOVA and Tukey's multiple comparison test for Caco-2 cells: The Caco-2 24h and 48h treatment show an elevated apoptosis percentage rate compared to the two controls. Using the one-way ANOVA test and the Tukey's multiple post comparison test, $p < 0.05$ was considered significant.

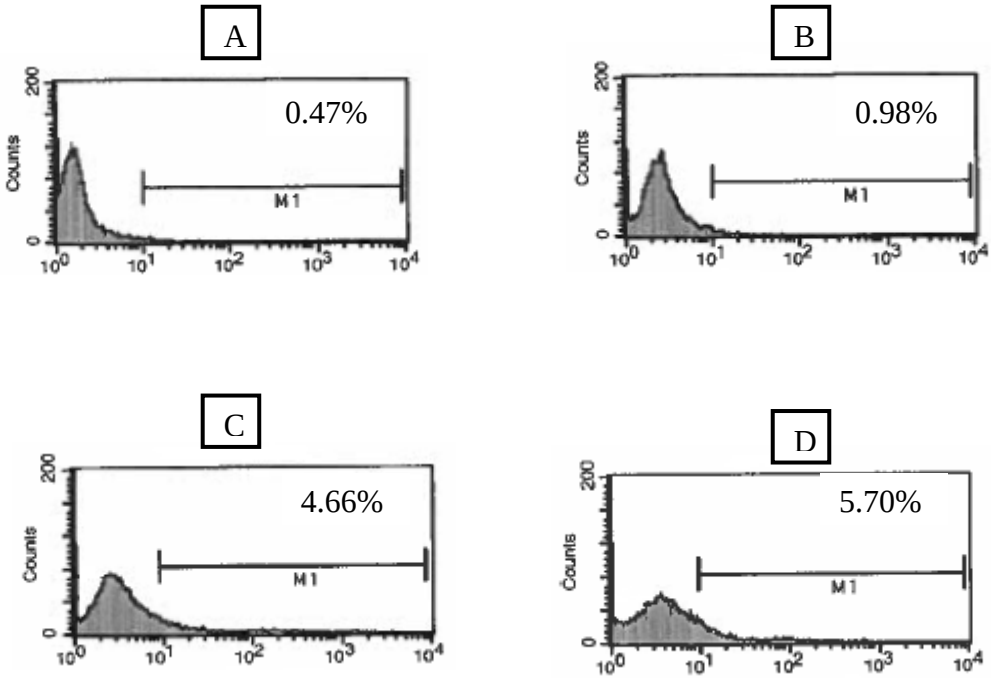

Figure 4.11 - FACS analysis of HT-29 colon cells treated with 5 µM of 5FU: A represents the blank (untreated cells), B represents the negative control (untreated but stained), C represents the 24h

treated cells and D represents the 48h treated cells, stained with annexin-V and PI. The results demonstrate the exposure of phophatidylserine from the cytosolic side to the surface in the colon cells (HT-29), treated with 5 μM of 5-FU for 24h and 48h. Annexin-V FITC apoptosis detection assay results are represented in histograms, denoting the percentage of cells staining positive for annexin-V in the M1 region.

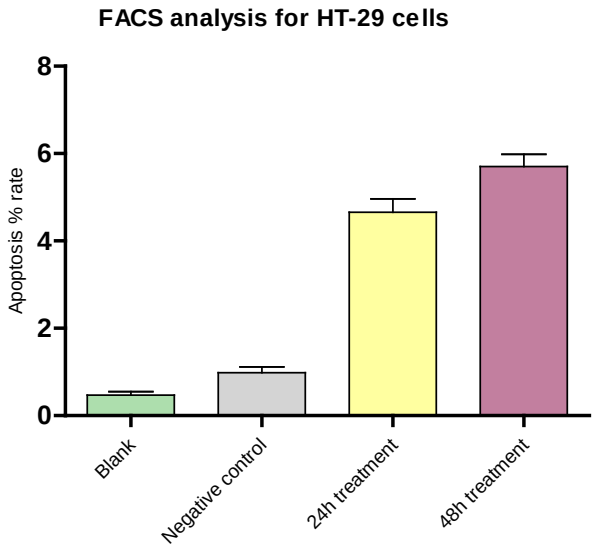

Figure 4.12 - ANOVA and Tukey's multiple comparison test of HT-29 cells: Both of the treated groups illustrate an increased apoptosis percentage rate. 5 μM of 5FU was more effective after 48h with more apoptotic cells compared to 24h. Using the on-way ANOVA test and the Tukey's multiple post comparison test, $p < 0.05$ was considered significant.

Following FACS analysis, the same cell culture and apoptosis induction conditions were followed. Total RNA was extracted from all cell lines when confluence was reached. RNA was then subjected to reverse transcription polymerase reaction.

4.3.3 Polymerase Chain Reaction (PCR) and Insert Confirmation

PCR was carried out to verify the correct insert size and this was then followed by sequencing to verify correct target sequence. PCR was done for both LASS 4 and LASS 5 genes. A

temperature gradient was first run for each primer set and the optimum annealing temperature was determined for each primer set. For more accurate results, it has been suggested that Real-Time PCR primers yield products of 50bp to 250bp. The annealing temperature for LASS 4 was 53°C and 55°C for LASS5. The PCR products were analysed by gel electrophoresis using a parallel molecular weight marker, and resulted in a single band for specificity. The PCR products were then cloned into a pGEM-T Easy vector and sent for sequencing, for insert confirmation. The results were then aligned with reference sequences on NCBI. LASS4 matched 100% and LASS 5 matched 99%. Figure 4.13 and 4.14 show the PCR product and sequence alignment for LASS4. Figure 4.15 and 4.16 show the PCR product and sequence alignment for LASS5.

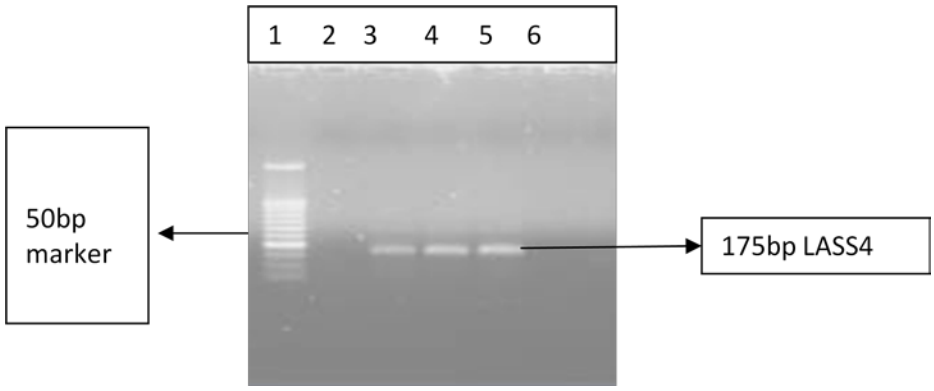

Figure 4.13 - LASS 4 PCR products: The LASS 4 inserts show a size of 175bp run parallel to a 50bp molecular weight marker. Lane 1 is a marker, lane 3 to 5 being LASS4 175bp PCR products.

```
Score = 324 bits (175), Expect = 2e-92
Identities = 175/175 (100%), Gaps = 0/175 (0%)
Strand=Plus/Plus

Query  1171  TCCTCTACACCACATACTACGAGTCCATCAGCAACAGGGGCCCCTTCTTCGGCTACTACT
1230
             ||||||||||||||||||||||||||||||||||||||||||||||||||||||||||||
Sbjct  83    TCCTCTACACCACATACTACGAGTCCATCAGCAACAGGGGCCCCTTCTTCGGCTACTACT
142

Query  1231  TCTTCAACGGGCTTCTGATGTTGCTGCAGCTGCTGCACGTGTTCTGGTCTTGCCTCATTC
1290
             ||||||||||||||||||||||||||||||||||||||||||||||||||||||||||||
Sbjct  143   TCTTCAACGGGCTTCTGATGTTGCTGCAGCTGCTGCACGTGTTCTGGTCTTGCCTCATTC
202

Query  1291  TGCGCATGCTCTATAGCTTCATGAAGAAGGGCCAGATGGAGAAGGACATTCGTAG
1345
             |||||||||||||||||||||||||||||||||||||||||||||||||||||
Sbjct  203   TGCGCATGCTCTATAGCTTCATGAAGAAGGGCCAGATGGAGAAGGACATTCGTAG
257
```

Figure 4.14 - LASS 4 cloned product in reference to the NCBI sequence (NM_024552.1): The results show 100% sequence alignment.

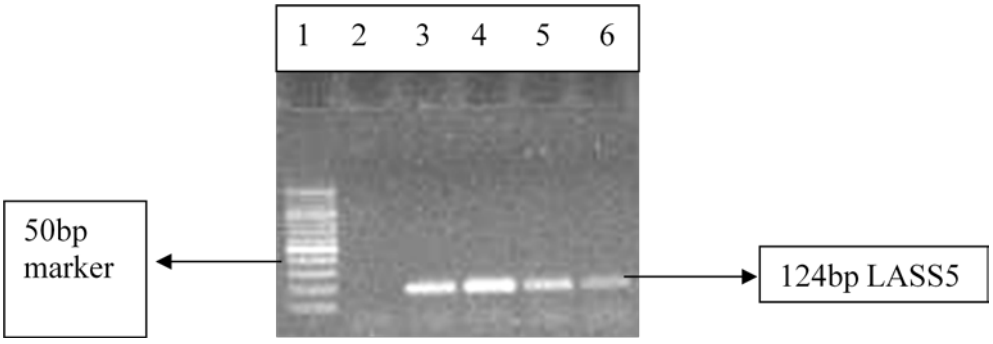

Figure 4.15 - LASS 5 PCR products: The LASS 5 inserts illustrate a size of 124bp, the PCR products were run parallel to a 50bp marker. Lane 1, a 50bp molecular weight marker, lane 3 to 6 being 124 LASS 5 PCR product.

```
Score = 224 bits (121), Expect = 1e-62
Identities = 123/124 (99%), Gaps = 0/124 (0%)
Strand=Plus/Plus

Query  401  TCGGAGGAATCAGGACAAGCCCCCAACGCTTACTAAATTCTGTGAAAGCATGTGGAGATT
460
            ||||||||||||||||||||||||||||||||||||||||||||||||||||||||||||
Sbjct  40   TCGGAGGAATCAGGACAAGCCCCCAACGCTTACTAAATTCTGTGAAAGCATGTGGAGATT
99

Query  461  CACATTTTATTTATGTATATTCTGCTATGGAATTAGATTTCTCTGGTCGTCACCTTGGTT
520
            |||||||| ||||||||||||||||||||||||||||||||||||||||||||||||||||
Sbjct  100  CACATTTTGTTTATGTATATTCTGCTATGGAATTAGATTTCTCTGGTCGTCACCTTGGTT
159

Query  521  CTGG  524
            ||||
Sbjct  160  CTGG  163
```

Figure 4.16 - LASS 5 cloned product in reference to the NCBI sequence (NM_147190.1): The sequence alignment results show 99% identity between the two sequences.

4.3.4 Gene expression using Real-Time polymerase Chain Reaction

Following conventional PCR (which was used to optimise and amplify the target sequences of CerS4 and CerS5), Real-Time PCR (which has been proven to be more sensitive than the conventional method of amplification (Sanguinetti *et al*., 2003) was used for quantification purposes.

4.3.5 Quantitative Real-time Polymerase Reaction (QRT-PCR)

The optimised primers for LASS4 and LASS5 (designed using the Bio-Rad Beacon software) through conventional PCR, were then used for qRT-PCR. The primers were run at a temperature gradient (50°C to 60°C) for LASS4, LASS5 and β-actin. The optimum temperatures were determined from the melting curves and they were as follows: 55°C for LASS4 and 53°C for LASS5 and 54°C for β-actin. Single peaks for melting curves showed the specificity of each primer set. Standard curves were then constructed using known cDNA concentration. Results were analysed using quantitation curves from the Bio-Rad Mini-Opticon version 3.

4.3.6 The Melting Curves

The single peaks in the melting curves denote primer specificity. The melting curve for LASS4 is shown in figure 4.17, and the melting curves for LASS5 and β-actin are demonstrated in Appendix 5, figure 5a and figure 5d.

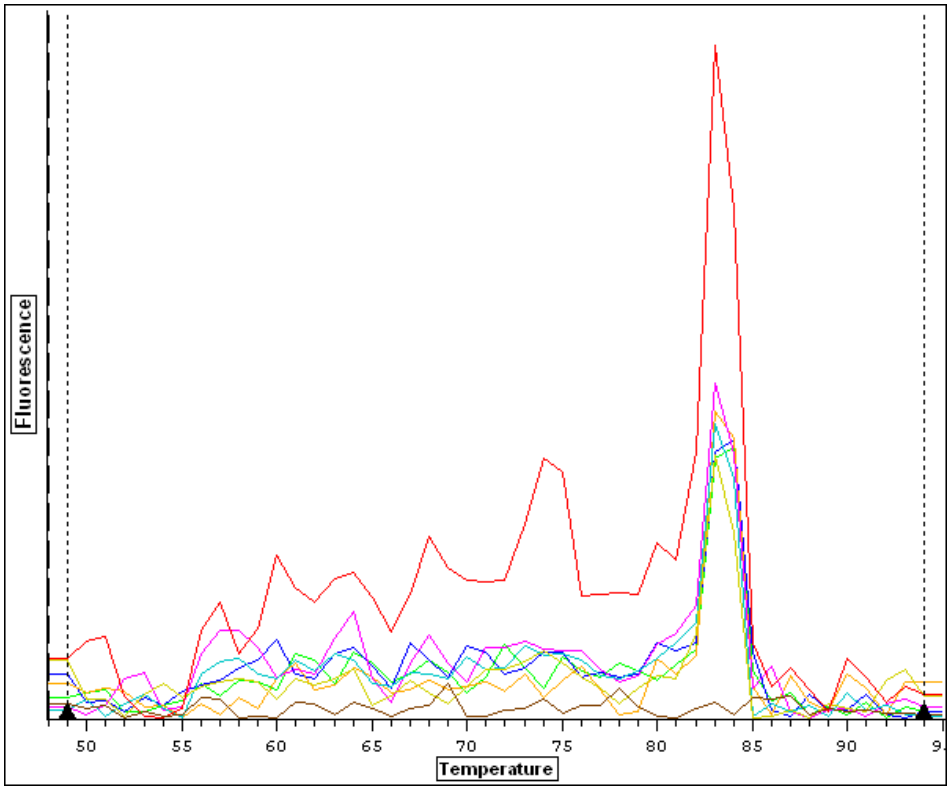

Figure 4.17 - The LASS4 melting curves with a melting temperature of 83°C: The single peak shows product specificity. (---) represents a negative control where no template was added, but both primers were added to the reaction mixture.

Following the correct amplification of the targets, standard curves were constructed to determine the efficiency of the primers.

4.3.7 Primer Efficiency Assessment using standard curves

Unlike conventional PCR primers, real-time PCR primer efficiency has to be assessed using standard curves. The efficiency is expressed in a percentage and the standard efficiency range

is between 90% and 100%. The standard curves of the genes under investigation were constructed using serial dilutions (5X) from the original cDNA, template. The CT-values were obtained from the quantitation curves and the log concentration of each dilution was determined. The standard curves were then plotted, i.e, the log concentration versus the CT-values, and the slope was determined from the curve. Furthermore, the percentage efficiency (%E) for each primer set was determined using the standard curve and the following formula was used:

$$\%E = (10^{(-1/slope)}-1) \text{ X } 100$$

NB: For perfect amplification, % E >90 and r^2 should be -3

4.3.8 Standard Curves

The following standard curves were constructed using MS-Excel, and the slope was directly calculated from the graphs. The CT-values were obtained from the quantitation curves. Figure 4.18 shows the quantitation curves and figure 4.19 shows the STD curve constructed for LASS 4. Table 4.3 shows the log concentrations of the cDNA and the CT-values, which were used to draw-up the standard curve for LASS4. The quantitation curves and STD curves for LASS 5 and β-actin are shown in Appendix 5, figure 5b, 5c and table 5f for LASS 5 and figure 5e, 5f and table 5g for β-actin, Appendix 5.

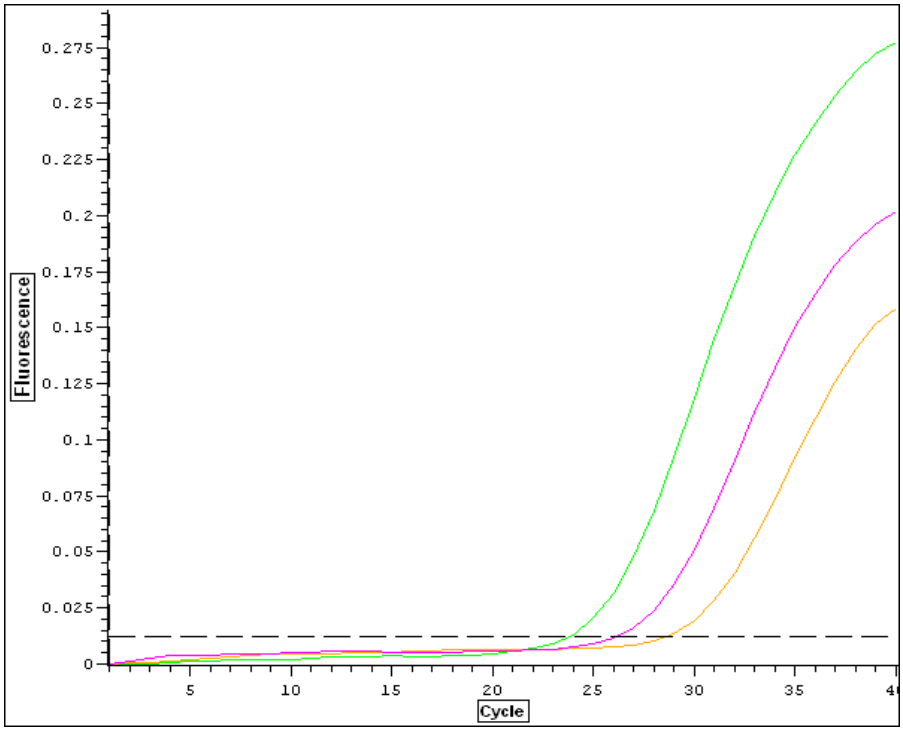

Figure 4.18 - Amplification curves for LASS4: The CT values with the corresponding concentrations were used to construct the STD curve.

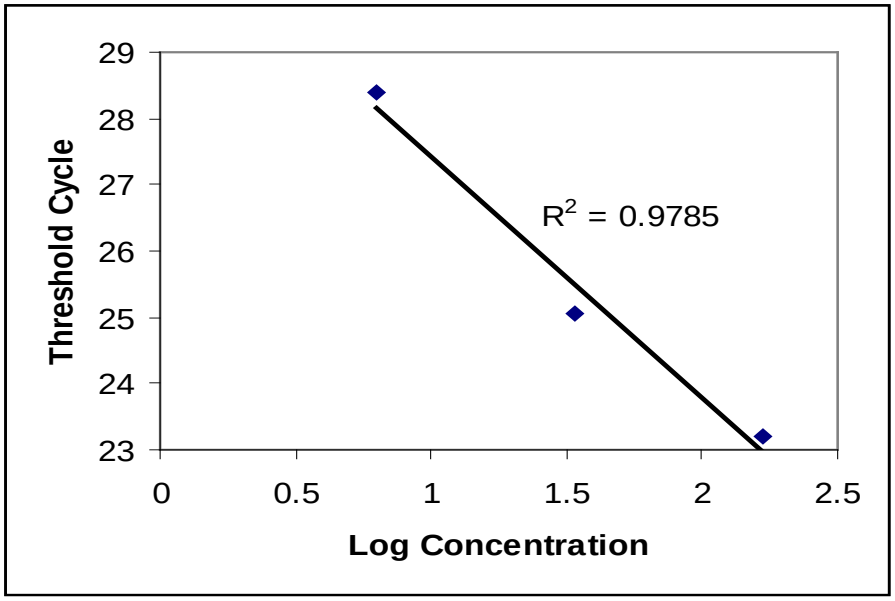

Figure 4.19 - Standard curve for LASS4: The slope was calculated to be -3.6 and the r^2 value is 0.9785. Table 4.3 shows the Log concentrations from the start concentration of 168.5ng/µl of the cDNA from the GMMe cell line, using a 5X dilution.

The percentage efficiency for LASS 4, LASS 5 and β-actin were calculated and were all between 90% and 100%. Calculations are shown in Appendix 4.

Table 4.3: Shows the log concentrations with the corresponding threshold cycle for LASS4

Log Concentration	Threshold Cycle
2.22	23.2
1.53	25.05
0.8	28.38

4.3.9 Relative Quantification RT-PCR of LASS4 and LASS5 expression normalised against an endogenous control (reference gene)

Relative quantification or comparative quantification measures the relative change in mRNA expression levels. It determines the changes in steady state mRNA levels of a gene across multiple samples and expresses it relative to the levels of another RNA, in this study cancerous samples (colon and endometrial) were compared to non-cancerous samples. The expression level for each gene was determined and calculated as an expression ratio. This was calculated using the Livak method ($2^{-\Delta\Delta CT}$).

NB: $\Delta CT = CT\ (Test_{target} - Test_{ref})$

$\Delta CT = CT\ (Calibrator_{target} - Calibrator_{ref})$

$= 2^{-[\Delta CT\ (test) - \Delta CT\ (calibrator)]}$

The expression level of a target gene in the calibrator is assumed to remain constant, hence equals to 1 (Livak and Schmittgen, 2001; Schmittgen and Livak, 2008). The fold ratio above one was considered and an up-regulation of a target gene in the test sample, and a ratio value below one was considered a down-regulation, hence it was calculated as -1/fold ratio below one (Livak and Schmittgen, 2001; Schmittgen and Livak, 2008).

4.3.10 QRT-PCR analysis

Each experiment (non-cancerous and cancerous, treated and untreated), was done three times independently in triplicate. Results were expressed as means ± standard error means (SEM). To examine the relationship between LASS4 and/or LASS5 and apoptosis, using apoptosis inducing drugs, LASS4 and LASS5 mRNA expression levels were compared in endometrial and colon cells before and after apoptosis treatment. The Livak method was still used to compare the expression levels of LASS4 and LASS5 in treated and untreated cells, normalised to β-actin. Figure 4.20 shows LASS4 in endometrial cell lines normalised to β-actin.

LASS4 mRNA expression level analysis

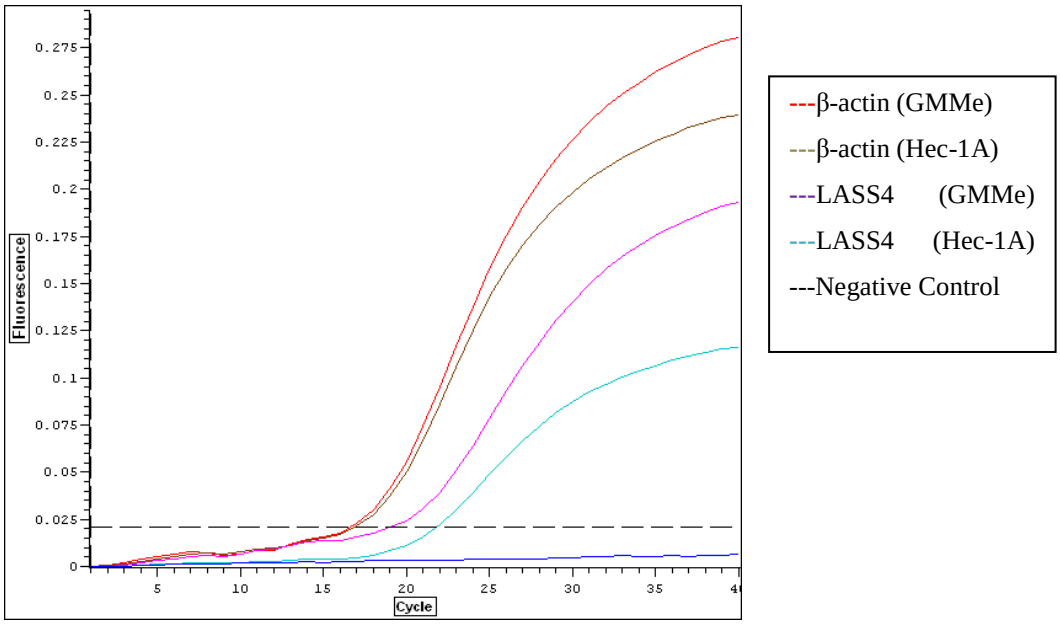

Figure 4.20 - Amplification curves for LASS 4 (with β-actin) in endometrial cell lines GMMe and Hec-1A: The average ΔCT values for the three independent experiments were, 21.32 in GMMe and 18.89 in Hec-1A cells. β-actin average ΔCT values for the three independent experiments in GMMe and Hec-1A cells were 16.46 and 16.09 respectively.

NB: The CT values for the three independent experiments are shown in Appendix 5, table 5h and figure 4.20 is a representative diagram of the three experiments.

The equation described above, section 4.3.9 was used and results are expressed as means ± SEM. Appendix 5 shows Table 5h for LASS4 CT values in endometrial cell lines before apoptosis treatment. The CT-values for LASS4 in GMMe and Hec-1A after apoptosis induction are shown in table 5i and 5j. Table 5k-5o shows the CT-value readings for LASS4 in colon cell lines before and after apoptosis treatment.

NB: Different annealing temperatures were used for each primer set (i.e for β-Actin and LASS 4), as running a temperature gradient using a Mini-Opticon Version 3 (Bio-Rad) was possible. Below are the statistically analysed (ANOVA and Tukey's multiple comparison test) results for LASS4 and LASS5 in fold change expressed as means ± standard error mean (SEM) for at least three independent experiments. Figure 4.21 and 4.22 show statistically analysed results for LASS4 in endometrial cell lines.

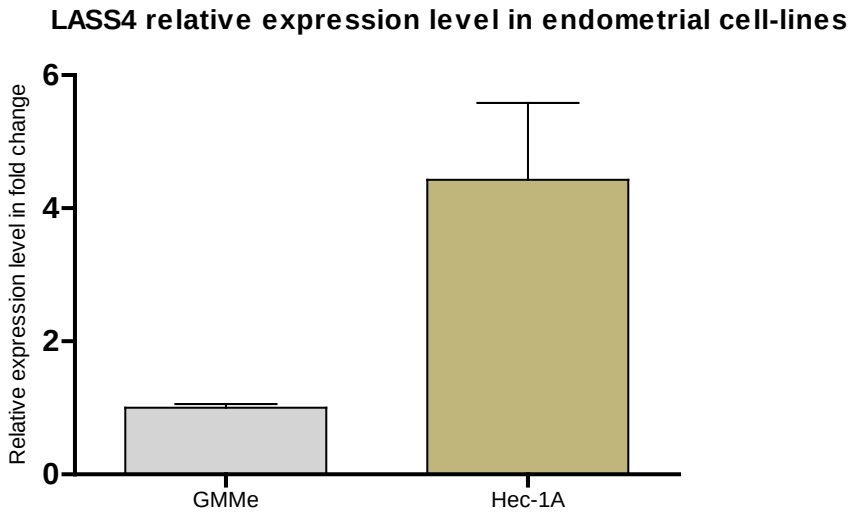

Figure 4.21 - Graph showing LASS4 relative expression level in Hec-1A cells compared to GMMe prior to apoptosis treatment: The expression level of LASS4 in endometrial cancerous cell-line is ~4-fold up-regulated compared to the non-cancerous counterpart (GMMe).

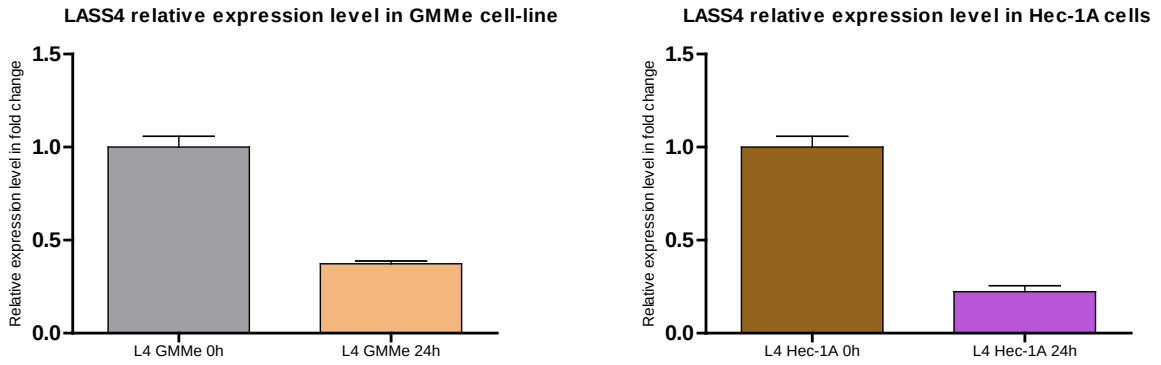

Figure 4.22 - Graphs showing the relative expression level of LASS4 in endometrial cells before and after apoptosis treatment: The induction of apoptosis in both GMMe (left) and Hec-1A (right) cells resulted in the down regulation of LASS4 in both cell lines, more especially in Hec-1A cells, 4.5 fold, and 2.7 fold in GMMe.

Figure 4.23 to 4.25 graphs show results expressed as mean ± SEM for LASS4 in colon cell lines, for at least three independent experiments.

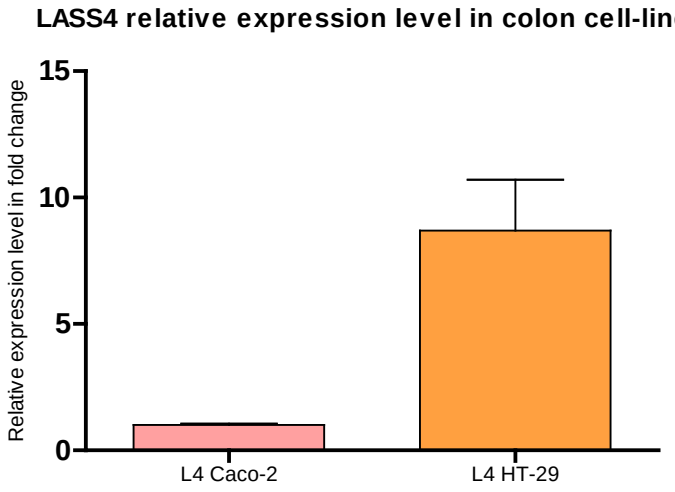

Figure 4.23 - Graph showing LASS4 relative expression level in HT-29 compared to Caco-2 cells before apoptosis induction: LASS4 is shown to be ~10 fold up-regulated in the highly malignant HT-29 cells compared to Caco-2 colon cells.

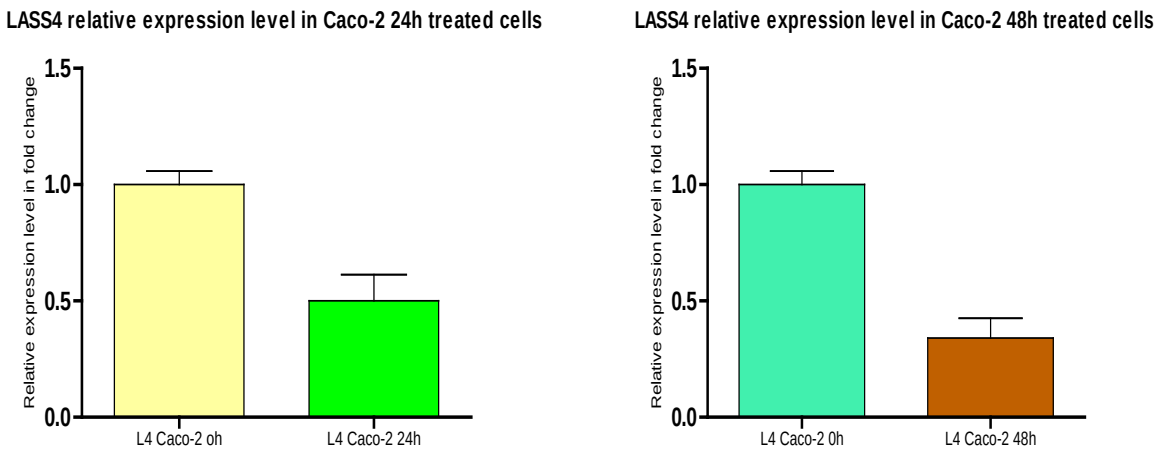

Figure 4.24 - Graphs showing the expression level of LASS4 in Caco-2 colon cells after 24h and 48h apoptosis induction: LASS4 expression level was observed to be down-regulated after 24h (left) and 48h (right). There was no significant difference between 24h (2 fold) and 48h (2.9 fold) treatment.

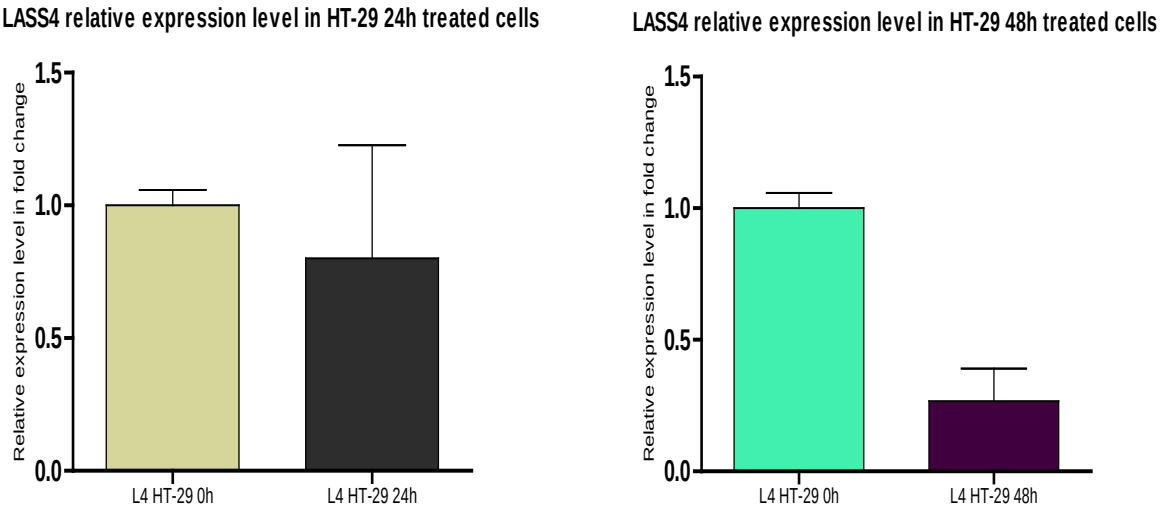

Figure 4.25 – Graphs showing LASS4 relative expression level in HT-29 cells after 24h and 48h induction of apoptosis: A decline in LASS4 mRNA expression level was shown after 24h, 1.25 fold (left) and significantly after 48h, 3.7 fold (right) of the treatment for apoptosis. The down regulation of LASS4 mRNA level was almost 3X after 48h, compared to 24h.

LASS5 mRNA expression level analysis

Appendix 5, Table 5p shows the CT-values of LASS5 with β-actin in GMMe and Hec-1A cells before apoptosis induction. The readings for GMMe and Hec-1A CT-values after apoptosis induction are shown in Appendix 5, table 5q and table 5r of LASS5. The LASS5 CT-values in colon cells before and after apoptosis treatment are seen in Appendix 5, table 5S-5w. Figure 4.26 and 4.27 show the relative expression level of LASS5 in endometrial cell lines, expressed as means ± SEM for at least three independent experiments.

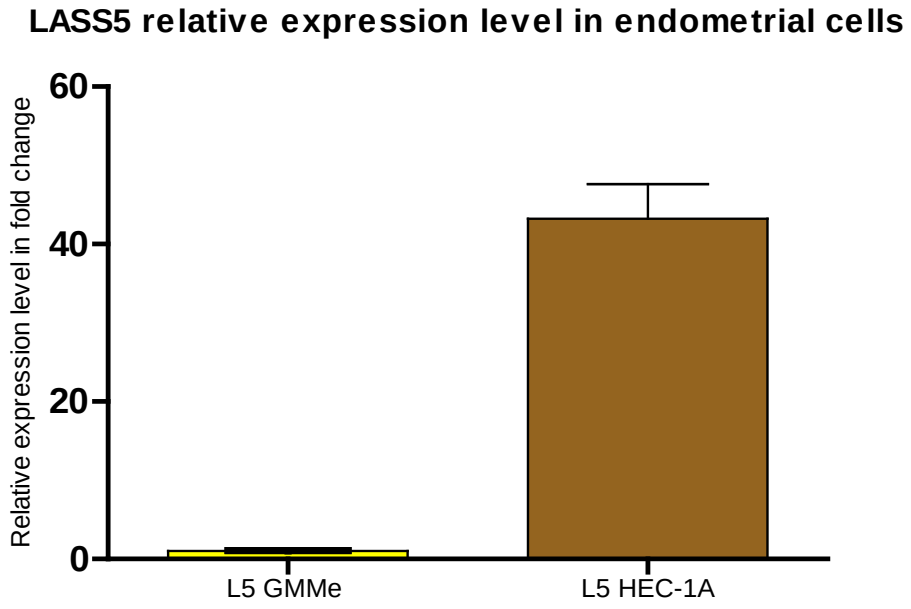

Figure 4.26 - Graph illustrating LASS5 relative expression level in Hec-1A cells compared to GMMe cells: An up-regulation of ~50 fold of LASS5 mRNA expression level is demonstrated in endometrial cancer (Hec-1A) relative to its non-cancerous counterpart.

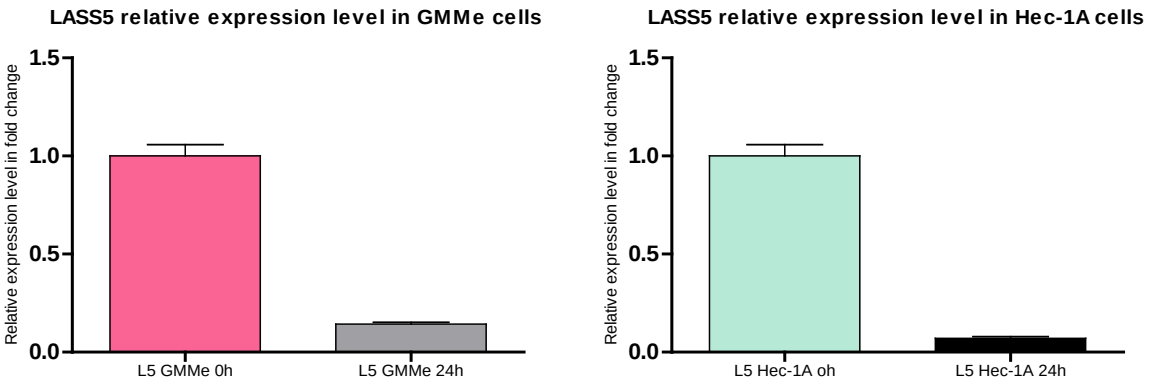

Figure 4.27 - Graphs illustrating the relative expression level of LASS5 in endometrial cell lines after apoptosis induction: A down-regulation of LASS5 mRNA was observed in GMMe, 7 .14 fold (left) and Hec-1A, 14.29 fold (right) after inducing apoptosis. The reduction in LASS5 mRNA in Hec-1A cells doubles, compared to GMMe.

The expression level of LASS5 in colon cell lines was also determined. Figure 4.28 showing amplification curves is a representation of all three independent experiments of LASS5 in colon cell lines normalised to β-actin.

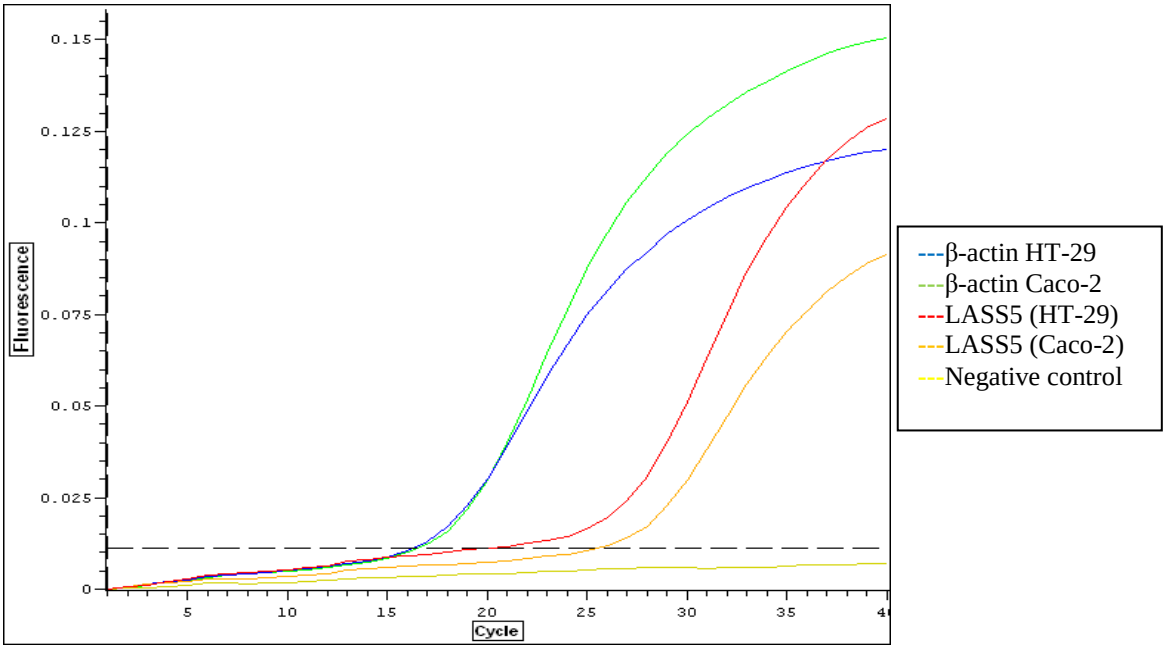

Figure 4.28 - Amplification curves for LASS 5 (with β-actin) in colon cell lines Caco-2 and HT-29: The average CT values for the three independent experiments for Caco-2 were 25.29 and 20.19 for

HT-29. β-actin amplification curves are also illustrated in this figure with average CT values of 16.46 for Caco-2 and 16.09 for HT-29, calculated from three independent experiments.

Figure 4.29 to 4.31 graphs show the relative expression levels of LASS5 in colon cell lines expressed as means ± SEM for at least three independent experiments.

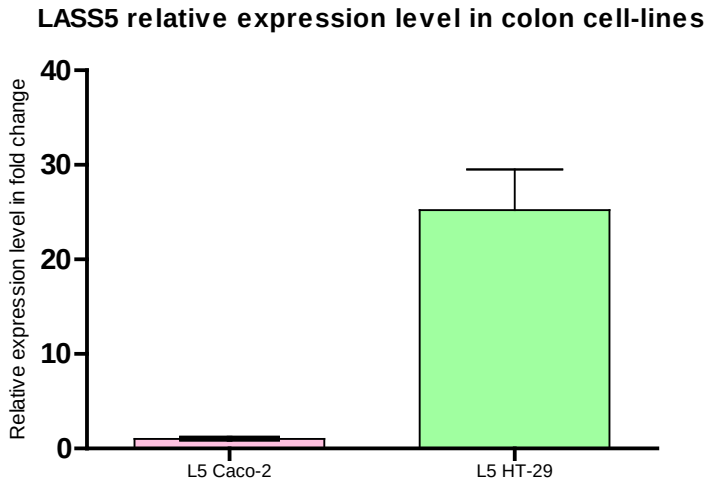

Figure 4.29 - Graph illustrating the relative expression level of LASS5 in HT-29 and Caco-2 colon cell lines before apoptosis treatment: LASS5 mRNA expression level was shown to be ~25-fold up-regulated in colon cancer.

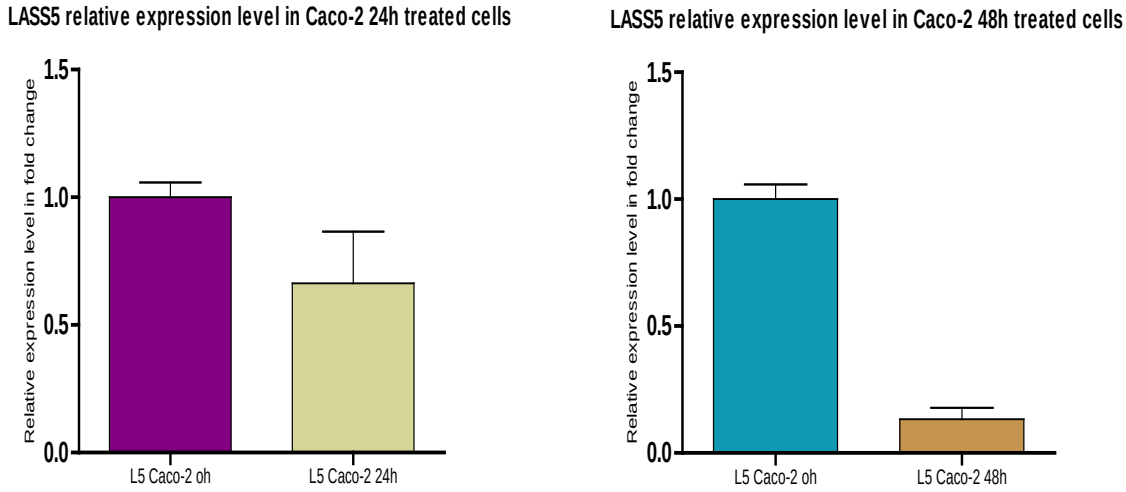

Figure 4.30 - Graphs illustrating LASS5 mRNA relative expression level in Caco-2 cells treated for apoptosis: A more significant decline in LASS5 mRNA is seen after 48h, 7.7 fold (right)

compared to 24h, 1.5 fold (left) apoptosis treatment. A 5X decline in LASS5 mRNA is seen after 48h compared to 24h apoptosis induction.

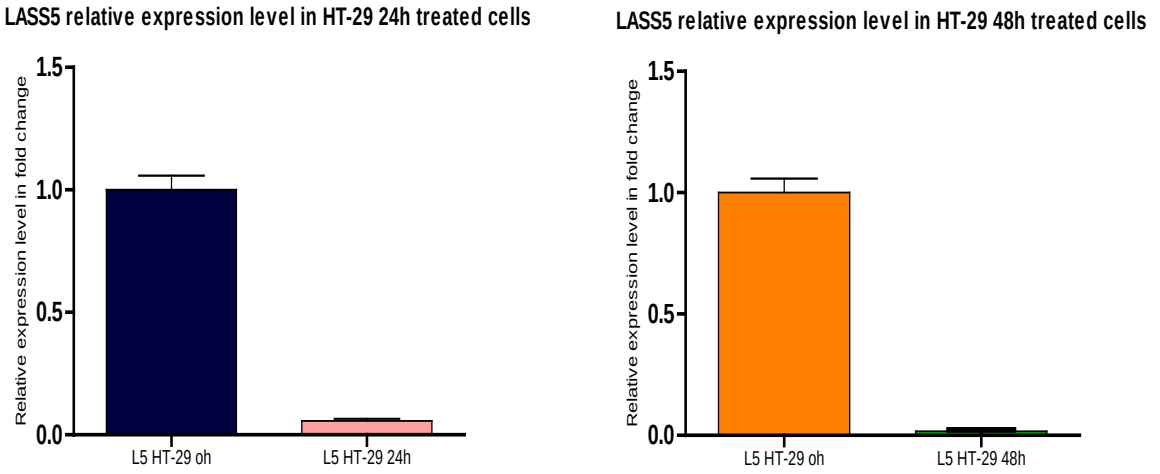

Figure 4.31 - Graphs illustrating the relative expression level of LASS5 in HT-29 cells after apoptosis induction: LASS5 was shown to be more significantly down-regulated in HT-29 cells, with 17.86 fold down-regulation after 24h (left) 58.82 fold down-regulation after 48h (right) induction of apoptosis. After 48h, the decline in LASS5 mRNA level was three-fold, compared to 24h treatment.

4.3.11 Statistical analysis for CerS4 and CerS5 in endometrial and colon cancers

Statistical analysis for LASS4 in endometrial cells is shown in Appendix 5, table 5i–5iii, and table 5iv–5vii, show statistical analysis of LASS4 in colon cells. Appendix 5, table 5viii–5x shows statistical analysis for LASS5 in endometrial cells while table 5xi–5xv shows LASS5 statistical analysis in colon cancer cells.

CHAPTER 5

DISCUSSION AND CONCLUSION

5.1 GENERAL DISCUSSION

Understanding the regulation of CerSes is important since this family of genes has not just been implicated in cancer development, but in cancer progression and targeted in cancer therapy (Teufel *et al*., 2009). Currently, the main function of LASS genes is to produce ceramide (Mizutani *et al*., 2005; Huang *et al*., 2011). However, it is still possible that LASS proteins containing the Hox domain may have an additional novel function in addition to the ceramide synthase activity, in which the entire domain plays a critical role, as the Hox domain containing proteins have been shown to be transcription regulators (Gehring *et al*., 1994). In contrast, it was previously shown by Mesika *et al*., (2007) that the first 15 amino acids of the Hox domain which contain the key residue (N51) involved in DNA binding are missing in CerSes. Mesika *et al*., (2007) further demonstrated that CerS5 and CerS6 contain a conserved region of 12 amino acids at the C-terminus of the Hox domain, which is essential for their catalytic activity. Previously it was shown that the TLC domain only is critical for CerSes function (Ogretment, 2006), now part of the Hox-domain plays a vital role in the activity of CerS5 and CerS6 (Mesika *et al*., 2007). These findings could implicate distinct biological roles for the CerSes isoforms, as the shorter isoform completely lacks the Hox-domain and part of the TLC domain, while the longer isoform retains the two domains. CerSes are emerging as potential candidates to further examine how orthologs, homologs and isoforms of the same gene can influence cellular homeostasis.

5.2 BIO-INFORMATICS ANALYSIS FOR LASS 4 AND LASS 5

It has been previously shown that proteins that share high sequence similarity may be involved in similar biological functions (Zhang *et al*., 2009). Surprisingly, even though CerSes share a high sequence similarity, none of these protein-family members were revealed to interact together. This also supports reports that although CerSes share high sequence similarity, they may be involved in distinct biological functions (Levy and Futerman, 2010). Little is known about CerS4 and CerS5 and the protein-protein interactions identified in this study were identified using STRING database (showing experimentally determined and predicted interactions), BioGRID and IntAct databases, which show experimentally determined interactions. Furthermore, these results also show the interaction of CerS4 and CerS5 with proteins involved in apoptosis (SIVA1 and TMD2), cell-cycle regulation (CCND2 and CDk14) and cell proliferation (CLN8). Interestingly, CerS4 and CerS5 have also been shown to interact with proteins involved in bone and cartilage formation, and the central nervous system regulation. Furthermore, using BioGRID and IntAct databases, CerS5 was shown to interact with polyubiquitin, while CerS4 was revealed to interact with BFLP1 protein of the EBV virus, also implicated in ubiquitination (Calderwood *et al*., 2007; Whitehurst *et al*., 2009; Wagner *et al*., 2011). These results indicate that CerS4 and CerS5 may be involved in other essential cellular processes apart from apoptosis. Surprisingly, when CerS4 and/ or CerS5 were aligned with all of their potential interacting partners, no consensus sequence was revealed.

In summary, these results show that CerS4 and CerS5 are involved in apoptosis and also are very likely to be involved in other unelucidated cellular functions. However, it is not surprising to obtain predicted protein interactions for both CerS4 and CerS5, as little is known about

their fundamental structure (monomers, homodimers, heterodimers and higher order structures) (Teufel *et al*., 2009).

5.3 GENE EXPRESSION ANALYSIS

The bio-informatics analysis carried out here suggest a role for CerS4 and CerS5 in cancer biology, especially in apoptosis, as indicated in literature (Ogretmen, 2006; Schiffmann *et al*., 2009; Huang *et al*., 2011). Thus the relationship between CerS4, CerS5 and apoptosis was examined. This was further studied at a gene expression level where the possible relationship between CerS4 and or CerS5 and apoptosis inducing drugs, (5-FU in colon cells and anastrozole in endometrial cells) was investigated.

5.3.1 Induction of apoptosis by 5-FU and anastrozole in colon and endometrial cells

5-FU and anastrozole were both used at optimally defined doses as described in previous work (Thant *et al*., 2008; Matsumoto *et al*., 2008). The apoptosis percentage rate was calculated from all cells staining positive for Annexin-V and PI negative (i.e in quadrant 2). An apoptosis percentage rate of more than 24.6% was observed in the human endometrial cancerous cell line (Hec-1A), compared to the non-cancerous counterpart (GMMe), with an apoptosis percentage rate of 14.3% after 24h. In colon cells, a 5.7% apoptosis percentage rate was seen in HT-29 cells compared to 4.37% apoptosis percentage rate in Caco-2 cells after 48 h. The analysed results were shown to be statistically significant with $P < 0.05$. However, there was no significant difference between 24 h and 48 h apoptosis treatment in the Caco-2 colon cell-line. This could be that these cells (Caco-2) reached an apoptotic threshold at 24h and could not be sensitised to 5FU beyond 24 h. An increase in dosage of 5FU instead of time or an increase in both parameters of dosage and time could probably have yielded a higher apoptosis percentage rate in Caco-2 cells. Furthermore, it has been previously reported

that Caco-2 cells are more resistant to 5FU mediated apoptosis (Carnesecchi *et al*., 2002). Generally, the effectiveness of 5FU in colon cancer has been shown to be increased by other molecules such as geraniol and selenium (Carnesecchi *et al*., 2002; Thant *et al*., 2008). Both endometrial and colon cancer cell lines showed an increased apoptosis percentage rate, when compared to their non-malignant (differentiated) counterparts. The effect of 5-FU and anastrozole on the expression levels of CerS4 and CerS5 was then determined using quantitative real time-PCR.

5.3.2 The effect of 5-FU and anastrozole on the mRNA expression level of CerS4 and CerS5 in endometrial and colon cancer

Following the treatment of colon and endometrium cells with apoptosis inducing factors, sequence analysis showed that the designed primers were specific to the target sequences of LASS 4 and LASS 5. The single peaks in the melting curves demonstrate primer specificity. Subsequent to the correct sequence confirmation, both CerS4 and CerS5 were shown to be up-regulated in the cancers of colon and endometrium. The comparison was done between the cancerous cell line and the non-cancerous (differentiated) cell line, before and after apoptosis treatment. The up-regulation of CerS4 in endometrial cancer was seen before apoptosis treatment, and a down-regulation of CerS4 was observed after apoptosis treatment in endometrial cells, especially in Hec-1A cells. Furthermore, CerS4 was also found to be up-regulated in colon cancer, prior to apoptosis induction and a down-regulation of CerS4 was demonstrated after treatment for apoptosis in colon cell lines. A more significant decline (3.7 fold) was observed in HT-29 cells after 48h apoptosis treatment. CerS5 was also shown to be up-regulated in both endometrial and colon cancers prior to apoptosis induction, and was also demonstrated to decline following apoptosis treatment in endometrial and colon cancers. Both CerS4 and CerS5 showed a higher degree of down-regulation in the cancerous cell lines compared to the non-cancerous (differentiated) counterparts. This was observed in both colon

and endometrial cells, for both CerS4 and CerS5. These findings suggest a role of CerS4 and CerS5 in the apoptotic regulation of cancers of the colon and endometrial. Furthermore, CerS4 and CerS5 may be involved in similar biological functions (in colon and endometrial cancers), as they are predicted here to share some of the protein-interacting partners.

The LASS family of genes has been previously implicated in cancer biology (Ogretmen, 2006). Disruption in the synthesis of ceramide by these genes may result in disruption of apoptosis regulation (Schiffmann *et al*., 2009). The goal of this research was to determine the relationship between CerS4, CerS5 and apoptosis, in colon and endometrial cancers, especially since failure to properly regulate apoptosis (i.e. resistance to apoptosis) is one of the hallmarks of cancer (Hanahan and Weinberg, 2011). Findings in this study indicated a possible role of CerS4, CerS5 in the apoptotic regulation of colon and endometrial cancers. Schiffmann *et al*., (2009) also demonstrated a relationship between CerSes, that is, CerS2, CerS4, CerS5 and CerS6 (2, 4-6) and apoptosis in breast cancer. Their results showed elevated CerSes (2, 4-6) levels in breast cancer, which served as anti-apoptotic molecules by protecting cells from undergoing apoptosis. Furthermore, it was also shown by Karahatay *et al*., (2007) that it is not all of LASS members that have tumour protective effects. LASS1 was shown to have anti-tumour effects in head and neck squamous cell carcinoma, by inhibiting the activation of telomerase, which has tumour promotion. In contrast, CerS5 and CerS6 have been shown to activate telomerase, leading to tumour promoting properties in the breast tissue (Schiffmann *et al*., 2009). The reports implicating elevated rates of ceramide *de novo* synthesis in many tumours are growing, considering the anti-tumour properties of this SL. This was also demonstrated by Knapp *et al*., (2010), reporting high levels of CerSes in endometrial cancer, compared to normal endometrium, and their possible explanation for this double-edged SL was that activation of this pathway is required to fulfil the increased demand of proliferating cancer cells for building blocks of complex SLs such as SM and

glycosphingolipids, which are important constituents of biological membranes. However, it still remains a challenge for many studies to demonstrate which CerSes precisely play a role in the tumourigenesis of different types of cancer, as indicated by Senkal *et al*., (2007) that different CerSes can play opposing roles in the same tissue. From this investigation, it was apparent that CerS4 and CerS5 are involved in the apoptosis regulation of the endometrial and colon cells. This was apparent because induction of apoptosis in endometrial and colon cells resulted in the down-regulation of CerS4 and CerS5 in endometrial and colon cancer. However, a definite conclusive line cannot be drawn at this point, whether both these genes are pro or anti-apoptotic, or exerting opposing roles in the pathogenesis of colon and endometrial cancers.

5.4 CONCLUSION

To further understand the mechanisms of these genes in cancer biology, more future work still needs to be done. This may include the over-expression of CerS4 or CerS5 in colon and endometrial cells. This would help to determine if CerS4 or CerS5 protects the cells from undergoing apoptosis, or inhibit excessive cell growth. In addition, investigating whether the inhibition of CerS4 and CerS5 in colon and endometrial cells by si-RNA or compounds known to inhibit the synthesis of ceramide by CerSes (such as fumonisin) may lead to apoptosis or cell survival, may help better understand the biological roles of each of these CerSes. In-vitro protein assays will also aid in determining and confirming interacting partners for CerS4 and CerS5. Furthermore, determining the up-stream and down-stream targets of CerS4 and CerS5 will contribute significantly towards uncovering how exactly CerS4 and CerS5 influence the fate of a cell. Ceramide deregulation has not just been implicated in cancer development, but also in cancer progression and cancer therapy (Teufel *et al*., 2009). Therefore, targeting this family of genes and understanding their precise roles in cancer and apoptosis is a promising therapeutic tool for the discovery of new anti-cancer drugs or improving the existing ones.

REFERENCES

Abe H, Shibata M & Otsuki Y. (2006). Caspase cascade of Fas-mediated apoptosis in human normal endometrium and endometrial carcinoma cells. *Molecular Human Reproduction*, 12:535–541.

Ashktorab H, Dawkins FW & Mohamed R. (2005). Apoptosis Induced by Aspirin and 5-Fluorouracil in Human Colonic Adenocarcinoma Cells. *Digestive Diseases and Sciences*, 50:1025–1032.

Becker KP, Kitatani K & Idkowiak-Baldys J. (2005). Selective inhibition of juxtanuclear translocation of protein kinase C betaII by a negative feedback mechanism involving ceramide formed from the salvage pathway. *Journal of Biological Chemistry*, 280:2606–2612.

Becker I, Wang Eckhard L & Yaghootfam. (2008). Differential expression of (dihydro) ceramide synthases in mouse brain: oligodendrocyte-specific expression of CerS2/LASS2, *Histochemistry Cell Biology*, 129:233–241.

Birbes H, El Bawab S & Hannun A. (2001). Selective hydrolysis of a mitochondrial pool of sphingomyelin induces apoptosis. *Federation of American Societies for Experimental Biology Journal*, 15: 2669–2679.

Birbes H, Luberto C & Hsu YT. (2005). A mitochondrial pool of sphingomyelin is involved in TNFα-induced Bax translocation to mitochondria. *Biochemical Journal*, 386:445–451.

Burnett AF, Bahador A & Amezcua C. (2004). Anastrozole, an aromatase inhibitor, and medroxyprogesterone acetate therapy in premenopausal obese women with endometrial cancer: a report of two cases successfully treated without hysterectomy. *Gynecologic Oncology*, 94:832–834.

Burstein H, Prestud A & Seidenfeld J. (2010). American Society of clinical oncology clinical practice Guideline: Update on Adjuvant Endocrine therapy for women with hormone receptor-positive breast cancer. *Journal of Clinical Oncology*, 28:3784–3796.

Calderwood M, Venkatesan K & Xing L. (2007). Epstein-Barr virus and virus human protein interaction maps. *Proceedings of the National Academy of Science of the USA*, 104:7606–7611.

Carnesecchi S, Langley K & Exinger F. (2002). Geraniol, a Component of Plant Essential Oils, Sensitizes Human Colonic Cancer Cells to 5-Fluorouracil Treatment. *The Journal of Pharmacology and Experimental Therapeutics*, 301(2): 625-630.

Chaudhry P & Asselin E. (2009). Resistance to chemotherapy and hormone therapy in endometrial cancer. *Endocrine-Related Cancer*, 16:363–380.

Cheng Y, Wu J & Hertervig S. (2007). Identification of Aberrant Forms of Alkaline Sphingomyelinase (NPP7) Associated with Human Liver Tumourigenesis. *British Journal of Cancer*, 97(10):1441–1448.

Cianchi F, Papucci L & Schiavone N. (2008). Cannabinoid Receptor Activation Induces Apoptosis through Tumor Necrosis Factor β-Mediated Ceramide De novo Synthesis in Colon Cancer Cells. *Clinical Cancer Research*, 14:7691–7700.

Classon M & Harlow E. (2002). The retinoblastoma tumour suppressor in development and cancer. *Nature Reviews Cancer*, 2:910–917.

Cooper S. (2003). Reappraisal of serum starvation, the restriction point, G0, and G1 phase arrest points. *Federation of American Societies for Experimental Biology Journal*, 17:333-340.

Cowling V & Downward J. (2002). Caspase-6 is the Direct Activator of Caspase-8 in the Cytochrome c-Induced Apoptosis Pathway: Absolute Requirement for Removal of Caspase-6 Prodomain. *Cell Death and Differentiation*, 9(10):1046.

Cronje L, Paterson A & Becker P. (2009). Colorectal Cancer in South Africa: A Heritable Cause Suspected in Many Young Black Patients. *SAMJ: South African Medical Journal*, 99(2):103–106.

Cutler R, Kelly J & Storie K. (2004). Involvement of oxidative stress‐induced abnormalities in ceramide and cholesterol metabolism in brain aging and Alzheimer's disease. *Proceedings of the National Academy of Science of the USA*, 101:2070‐2075.

Davies H, Bignell G & Cox C. (2002). Mutations of the BRAF gene in human cancer. *Nature*, 417:949–954.

Deng M, Zhang K & Mehta S. (2003). Prediction of protein function using protein-protein interaction data. *Journal of Computational Biology*, 10(6):947–960.

Duan R & Nilsson A. (2009). Metabolism of sphingolipids in the gut and its relation to inflammation & cancer development, *Progress in Lipid Research*, 48:62–72.

Eto M, Bennouna J & Hunter OC. (2003). C16 ceramide accumulates following androgen ablation in LNCaP prostate cancer cells. *Prostate*, 57:66–79.

Fox TE, Finnegan CM & Blumenthal R. (2006). The clinical potential of sphingolipid- based therapeutics. *Cellular and Molecular Life Sciences*, 63:1017–1023.

Friedberg EC. (2003). DNA damage and repair. *Nature*, 421:436–440.

Fulda S. (2009). Caspase 8 in cancer biology and therapy. *Cancer Letters*, 281:128–133.

Futerman AH & Hannun YA. (2004). The complex life of simple sphingolipids. *EMBO Reports*, 5:777–782.

Futerman AH & Riezman H. (2005). The ins and outs of sphingolipid synthesis. *Trends Cellular Biology*, 15:312–318.

Garland CF, Gorham ED & Mohr SB. (2009). Vitamin D for Cancer Prevention: Global Perspective. *Annals of Epidemiology*, 19(7):468–483.

Geens MM & Niewold TA. (2010). Preliminary Characterization of the Transcriptional Response of the Porcine Intestinal Cell Line IPEC-J2 to Enterotoxigenic *Escherichia Coli*, *Escherichia Coli*, and E. Coli Lipopolysaccharide. *Comparative and Functional Genomics*, 2010:1–11.

Gehring WJ, Affolter M & Burglin T. (1994). Homeodomain proteins. *Annual Review of Biochemistry*, 63:487–526.

Göhler T, Stefan J & Gabriele W. (2005). Mutant p53 proteins bind DNA in a DNA structure-selective mode. *Nucleic Acids Research*, 33 (3), 1087–1100.

Hanahan D & Weinberg R. (2011). Hallmarks of Cancer: The Next Generation. *Cell*, 144:646–674.

Herbeuval J, Grivel J & Shearer GM. (2005). CD4 T-cell death induced by infectious and noninfectious HIV-1: role of type 1 interferon–dependent, TRAIL/DR5-mediated apoptosis. *Blood*, 106:3524–3531.

Hsieh H, Wu C & Sun C. (2006). Sphingosine-1-phosphate induces COX-2 expression via P13K/Akt and p42/p44 MAPK pathways in rat vascular smooth muscle cells. *Journal of Cell Physiology*, 207:757–766.

Huang W, Chen C & Lin Y. (2011). Apoptotic sphingolipid ceramide in cancer therapy. *Journal of Lipids*, 2011:1–15.

Huerta S, Goulet E & Livingston EH. (2006). Colon cancer and apoptosis. *The American Journal of Surgery*, 191:517–526.

Ito Y, Sato S & Ohashi T. (2004). Reduction of airway anion secretion via CFTR in sphingomyelin pathway. *Biochemical and Biophysical Research Communications*, 324:901–908.

Jana A & Pahan K. (2004). Fibrillar amyloid‐beta peptides kill human primary neurons via NADPH oxidase-mediated activation of neutral sphingomyelinase. Implications for Alzheimer's disease. *Journal of Biological Chemistry*, 279:51451–51459.

Jemal A, Bray F & Center M. (2011). Global Cancer Statistics. *A Cancer Journal for Clinicians*, 61:69–90.

Jin Z & El-Deiry WS. (2005). Overview of cell death signaling pathways. *Cancer Biology and Therapy*, 4:139–163.

Jin J, Mullen TD & Hou Q. (2009). AMPK inhibitor Compound C stimulates ceramide production and promotes Bax redistribution and apoptosis in MCF7 breast carcinoma cells. *Journal of Lipid Research*, 50:2389–2397.

Jongen VH, Thijssen JH & Hollema H. (2005). Is aromatase cytochrome P450 involved in the pathogenesis of endometrioid endometrial cancer? *International Journal Gynecological Cancer*, 15(3):529-536.

Karahatay S, Thomas K & Koybasi S. (2007). Clinical relevance of ceramide metabolism in the pathogenesis of human head and neck squamous cell arcinorma(HNSCC): attenuation of C (18)-ceramide in HNSCC tumours correlates with lymphovascular invasion and nodal metastasis. *Cancer Letters*, 256:101–111.

Kawamori T, Osta W & Johnson K. (2006). Sphingosine kinase 1 is up-regulated in colon carcinogenesis. *Federation of American Societies for Experimental Biology Journal*, 20:386–388.

King K & Cidlowski J. (1998). Cell cycle regulation and apoptosis. *Annual Review of Physiology*, 60:601–617.

Kitatani K, Idkowiak-Baldys J & Bielawski T. (2006). Protein kinase C-induced activation of a ceramide/protein phosphatase 1 pathway leading to dephosphorylation of p38 MAPK. *Journal of Biological Chemistry*, 281:36793–36802.

Knapp P, Baranowski M & Knapp M. (2010). Altered sphingolipid metabolism in human endometrial cancer. *Prostaglandins and Other Lipid Mediators*, 92:62–66.

Kronja I & Orr-Weaver. (2011). Translational regulation of the cell cycle: when, where, how and why. *Philosophical Transactions of The Royal Society Biological Sciences*, 366:3638–3652.

Lahiri S & Futerman AH. (2007). The metabolism and function of sphingolipids and glycosphingolipids. *Cellular and Molecular Life Sciences*, 64:2270–2284.

Lahiri S, Lee H & Mesicek J. (2007). Kinetic characterization of mammalian ceramide synthases: Determination of K(m) values towards sphinganine. *FEBS Letters*, 581:5289–5294.

Larrosa M, Tomas-Barberan F & Espin J. (2006). The dietary hydrolysable tannin punicalagin releases ellagic acid that induces apoptosis in human colon adenocarcinoma Caco-2 cells by using the mitochondrial pathway. *Journal of Nutritional Biochemistry*, 17:611–625.

Laviad E, Albee L & Pankova-Kholmyansky I. (2008). Characterization of ceramide Synthase 2: Tissue distribution, substrate specificity and inhibition by sphingosine 1-phosphate. *The Journal of Biological Chemistry*, 283:5677–5684.

Lee J, Xu J & Lee J. (2004). Amyloid‐beta peptide induces oligodendrocyte death by activating the neutral sphingomyelinase‐ceramide pathway. *Journal of Cell Biology*, 164:123–131.

Letovsky S & Kasif S. Predicting protein function from protein/protein interaction data: a probabilistic approach. *Bioinformatics*, 2003; 19:197–204.

Levy M & Futerman A. (2010). Mammalian Ceramide Synthases. *International Union of Biochemistry and Molecular Biology Life*, 62:347–356.

Lin C, Chen CL & Chiang W. (2007). GSK-3β acts downstream of PP2A and the PI 3-kinase-Akt pathway, and upstream of caspase-2 in ceramide-induced mitochondrial apoptosis. *Journal of Cell Science*, 120:2935–2943.

Lin S, Yan L & Liang X. (2009). A novel variant of ER-alpha, ER-alpha36 mediates testosterone-stimulated ERK and Akt activation in endometrial cancer Hec1A cells. *Reproductive Biology and Endocrinology*, **7**:1-8.

Livak K & Schmittgen T. (2001). Analysis of Relative Gene Expression Data Using Real-Time Quantitative PCR and the 2ΔΔCT Method. *Methods*, 25:402–408.

Lu Y, Zhang B & Jia Z. (2011). Hepatocellular carcinoma HepG2 cell apoptosis and caspase-8 and Bcl-2 expression induced by injectable seed extract of Coix lacryma-jobi. *Hepatobiliary Pancreatic Diseases International*, 10:303–307.

Mackenzie GG, Paola-Zago M & Keen CL. (2002). Low Intracellular Zinc Impairs the Translocation of Activated NF-κB to the Nuclei in Human Neuroblastoma IMR-32 Cells. *Journal of Biological Chemistry*, 277(37):34610–34617.

Masukawa Y, Narita H & Shimizu E. (2008). Characterization of overall Ceramide Species in Human Stratum Corneum. *Journal of Lipid Research*, 49(7):1466–1476.

Matsumoto M, Yumaguchi Y & Seino Y. (2008). Estrogen signaling ability in human endometrial cancer through the cancer–stromal interaction. *Endocrine-Related Cancer*, 15:451–463.

Meresman GF, Bilotas M & Abello V. (2005). Effects of aromatase inhibitors on proliferation and apoptosis in eutopic endometrial cell cultures from patients with endometriosis. *Fertility and Sterility*, 84(2):459–463.

Mesika A, Ben-Dor S & Laviad EL. (2007). A new functional motif in Hox domain-containing ceramide synthases: identification of a novel region flanking the Hox and TLC domains essential for activity. *Journal of Biological Chemistry*, 282:27366–27373.

Min J, Mesika A & Sivaguru M. (2007). (Dihydro)ceramide synthase 1 regulated sensitivity to cisplatin is associated with the activation of p38 mitogen-activated protein kinase and is abrogated by sphingosine kinase 1. *Molecular Cancer Research*, 5:80–112.

Mizutani Y, Kihara A & Igarashi Y. (2005). Mammalian Lass6 and its related family members regulate synthesis of specific ceramides. *Biochemical Journal*, 390:263–271.

Mizutani Y, Kihara A & Igarashi Y. (2006). LASS3 (longevity assurance homologue 3) is a mainly testis-specific (dihydro)ceramide synthase with relatively broad substrate specificity. *Biochemical Journal*, 398:531–538.

Mizutani Y, Mitsutake S & Tsuji K. (2009). Ceramide biosynthesis in keratinocyte and its role in skin function, *Biochemie*, 91:784–790.

Modrak DE, Gold DV & Goldenberg DM. (2006). Sphingolipid targets in cancer therapy. *Molecular Cancer Therapy*, 5:200–208.

Mohr A, Zwacka Rm & Jarmy G. (2005). Caspase-8L Expression Protects CD34+; Hematopoietic Progenitor Cells and Leukemic Cells from CD95-Mediated Apoptosis. *Oncogene*, 24(14):2421–2429.

Moodley J, Constant D & Williamson A. (2009). Human papillomavirus prevalence, viral load and pre-cancerous lesions of the cervix in women initiating highly active antiretroviral therapy in South Africa: a cross-sectional study. *BMC Cancer*, 9:275.

Noda S, Yoshimura S & Sawada M. (2001). Role of ceramide during cisplatin-induced apoptosis in C6 glioma cells. *Journal of Neurooncology*, 52:11–21.

Ogretmen B & Hannun YA. (2001). Updates on functions of ceramide in chemotherapy-induced cell death and in multidrug resistance. *Drug Resistance Updates*, 4:368–377.

Ogretmen B. (2006). Sphingolipids in cancer: Regulation of pathogenesis and therapy. *Federation of American Societies Experimental Biology Letters*, 580:5467–5479.

Oren M. (2003). Decision making by p53: life, death and cancer. *Cell Death Differantiation*, 10:431–442.

Ortega S, Malumbres M & Barbacid M. (2002). Cyclin D-dependent kinases, INK4 inhibitors and cancer. *Biochimica et Biophysica Acta*, 1602:73–87.

Oskouian B, Sooryiakumaran P & Borowsky A. (2006). Sphingosine-1-phosphate lyase potentiates apoptosis via-p53 and p38 dependent pathways and is down-regulated in colon cancer. *Proceedings of the National Academy of Science of the USA*, 103:17384–17389.

Panjarian S, Kozhaya L & Arayssi S. (2008). De novo N-palmitoylsphingosine synthesis is the major biochemical mechanism of ceramide accumulation following p53 up-regulation. *Prostaglandins Other Lipid Mediators*, 86:41–48.

Parkin M, Freddie B & Pisani F. (2005). Global cancer statistics, 2002. *A Cancer Journal for Clinicians*, 55:74–108.

Parkin DM, Sitas F & Phil D. (2008). Part I: Cancer in Indigenous Africans—burden, distribution, and trends. *The Lancet Oncology*, 9(7): 683-692.

Pawson T & Nash P. (2003). Assembly of cell regulatory systems through protein interaction domains. *Science*, 300:445–452.

Petrache I, Natarajan V & Zhen L (2005). Ceramide upregulation causes pulmonary cell apoptosis and emphysema‐like disease in mice. *Nature Medicine*, 11:491–498.

Petrache I, Natarajan V & Zhen L. (2006). Ceramide causes pulmonary cell apoptosis and emphysema: a role for sphingolipid homeostasis in the maintenance of alveolar cells. *Proceedings of the American Thoracic Society*, 3:510.

Pewzner-Jung Y, Ben-Dor S & Futerman AH. (2006). When Do Lasses (Longevity Assurance Genes) Become CerS (Ceramide Synthases)? *The Journal of Biological Chemistry*, 281:25001–25005.

Prieto C & De Las Rivas J. (2010). Structural domain–domain interactions: assessment and comparison with protein–protein interaction data to improve the interactome. *Proteins*, 78:109–117.

Prives C & Hall PA. (1999). The p53 pathway. *Journal of Pathology*, 187:112–126.

Rath G, Schneider C & Langlois B. (2009). De novo ceramide synthesis is responsible for the anti-tumour properties of camptothecin and doxorubicin in follicular thyroid carcinoma. *The International Journal of Biochemistry and Cell Biology*, 41:1165–1172.

Reddel RR. (2010). Senescence: an antiviral defense that is tumor suppressive? *Carcinogenesis*, 31:19–26.

Reed JC. (2000). Mechanisms of apoptosis. *American Journal of Pathology*, 157:1415–1430.

Reynolds C & Kolesnick R. (2004). Ceramide synthesis and metabolism as a target for cancer therapy. *Cancer Letters*, 206:169–180.

Saddoughi S, Song P & Ogretmen B. (2008). Roles of sphingolipids in cancer biology and therapeutics. *Subcellular Biochemistry*, 49:413–440.

Sambo L, Dangou J & Adebamowo C. (2012). Cancer in Africa: a preventable public health crisis. *African Journal of Cancer*, 4:127–136.

Sambuy Y, De Angelis & Ranaldi G. (2005). The Caco-2 cell line as a model of the intestinal barrier: influence of cell and culture-related factors on Caco-2 cell functional characteristics. *Cell Biology and Toxicology*, 21:1–26.

Sangar V, Blakenberg D & Altman N. (2007). Quantitative sequence-function relationships in proteins based on gene ontology. *BMC Bioinformatics*, 8:1–15.

Sanguinetti M, Posteraro B & Pagano L. (2003). Comparison of Real-Time PCR, Conventional PCR, and Galactomannan Antigen Detection by Enzyme-Linked Immunosorbent Assay Using Bronchoalveolar Lavage Fluid Samples from Hematology Patients for Diagnosis of Invasive Pulmonary Aspergillosis. *Journal of Clinical Microbiology*, 41:3922–3925.

Santarosa M & Ashworth A. (2004). Haploinsufficiency for tumour suppressor genes: when you don't need to go all the way. *Biochimica et Biophysica Acta*, 1654:105–122.

Schiffman S, Sander J & Birod K. (2009). Ceramide synthases and ceramide levels are increased in breast cancer tissue. *Carcinogenesis*, 30:745–752.

Schmittgen TD & Livak KJ. (2008). Analyzing Real-Time PCR data by the comparative CT method. *Nature Protocols*, 3:1101–1108.

Schröpfer A, Kammerer U & Kapp Michaela. (2010). Expression pattern of matrix metalloproteinases in human gynecological cancer cell lines. *BMC Cancer*, 10(553):1–12.

Schwarz A & Futerman A. (1997). Distinct roles for ceramide and glucosylceramide at different stages of neuronal growth. *Journal of Neuroscience*, 17:2929–2938.

Sen n, Das BB & Ganguly A. (2004). Camptothecin induced mitochondrial dysfunction leading to programmed cell death in unicellular hemoflagellate *Leishmania donovani*. *Cell Death and Differentiation*, 11: 924–936.

Senkal C, Ponnusamy S & Bielawski J. (2010). Antiapoptotic roles of ceramide-synthase-6-generated C16-ceramide via selective regulation of the ATF6/CHOP arm of ER-stress-response pathways. *Federation of American Societies Experimental Biology Journal*, 24:296–308.

Senkal C, Ponnusamy S & Rossi MJ. (2007). Role of human longevity assurance gene 1 and C18-ceramide in chemotherapy-induced cell death in human head and neck squamous cell carcinomas. *Molecular Cancer Therapy*, 6:712–722.

Sherr C. (2000). Cancer cell cycles revisited. *Cancer Research*, 60:3689–3695.

Siskind LJ, Kolesnick NR & Colombini M. (2006). Ceramide forms channels in mitochondrial outer membranes at physiologically relevant concentrations. *Mitochondrion*, 6:118–125.

Smyth MJ, Perry DK & Zhang J. (1996). prICE: a downstream target for ceramide-induced apoptosis and for the inhibitory action of Bcl-2. *Biochemical Journal*, 316:25–28, 1996.

Song J, Rutherford T & Naftolin F. (2002). Hormonal regulation of apoptosis and the Fas and Fas ligand system in human endometrial cells. *Molecular Human Reproduction*, 8(5):447–455.

Spassieva S, Seo J & Jiang J. (2006). Necessary role for the Lag1p Motif in (Dihydro) ceramide synthase activity. *Journal of Biological Chemistry*, 281:33931–33938.

Stiban J, Tidhar R & Futerman, A H. (2010). *Advances Experimental Medicine and Biology*, 688:60–71.

Summers SA. (2006). Ceramides in insulin resistance and lipotoxicity. *Progress in Lipid Research*, 45:42–72.

Teufel A, Maass T & Galle P. (2009). The longevity assurance homologue of yeast lag1 (Lass) gene family (Review). *International Journal of Molecular Medicine*, 23(2):135–140.

Thamilselvan V, Li W & Sumpio B. (2002). Sphingosine-1-phosphate stimulates human Caco-2 intestinal epithelial proliferation via p38 activation and activates ERK by an independent mechanism. *In Vitro Cellular and Developmental Biology Animal*, 38:246–253.

Thant A, Wu Y & Lee J. 2008. Role of Caspases in 5-FU and Selenium-induced Growth Inhibition of Colorectal Cancer Cells. *Anticancer Research*, 28:3579–3592.

Torkamani A, Verkhivker G & Schork NJ. (2009). Cancer driver mutations in protein kinase genes. *Cancer Letters*, 281:117–127.

Van Brocklyn JR, Jackson CA & Pearl DK. (2005). Sphingosine kinase-1 expression correlates with poor survival of patients with glioblastoma multiforme: roles of sphingosine kinase isoforms in growth of glioblastoma cell lines. *Journal of Neuropathology and Experimental Neurology*, 64:695–705.

van der Woude CJ, Moshage H and Homan M. (2005). Expression of apoptosis related proteins during malignant progression in chronic ulcerative colitis. *Journal of Clinical Pathology*, 58: 811-814.

Venkataraman K, Riebeling C & Bodennec J. (2002). Upstream of growth and differentiation factor 1 (uog1), a mammalian homolog of the yeast longevity assurance gene 1 (LAG1), regulates N-stearoyl-sphinganine (C18-(dihydro)ceramide) synthesis in a fumonisin B1-independent manner in mammalian cells. *Journal of Biological Chemistry*, 277:35642–35649.

Vilela R, Lands L & Meehan B. (2006). Inhibition of IL‐8 release from CFTR‐deficient lung epithelial cells following pretreatment with fenretinide. *International Immunopharmacology*, 6:1651–1664.

Visentin B, Vekick J & Sibbald B. (2006). Validation of an anti-sphingisine-1-phosphate antibody as a potential therapeutic in reducing growth, invasion and angiogenesis in multiple tumour lineages. *Cancer Cell*, 9:225–238.

Vogelstein B & Kinzler K. (2004). Cancer genes and the pathways they control. *Nature Medicine*, 10:789–799.

Vogelstein B, Lane D & Levine A. (2000). Surfing the p53 network. *Nature*, 408:307–310.

Wagner S, Beli P & Weiner B. (2011). A Proteome-wide, Quantitative Survey of In Vivo Ubiquitylation Sites Reveals Widespread Regulatory Roles. *Molecular and Cellular Proteomics*, 10:1–13.

Wang JC. (1991). DNA topoisomerases: why so many? *Journal of Biological Chemistry*, 266: 6659–6662.

Wang S, Pudney J & Song J. (2003). Mechanisms involved in the evolution of progestin resistance in human endometrial hyperplasia – precursor of endometrial cancer. *Gynecologic Oncology*, 88:108–117.

Wang X & Chen S. (2006). Aromatase Destabalizer: Novel Action of Exemestane, a food and drug Administration-Approved Aromatase Inhibitor. *Cancer Research*, 66(21): 10280-10286.

Wang G, Silva J & Dasgupta S. (2008) Long‐chain ceramide is elevated in presenilin 1 (PS1M146V) mouse brain and induces apoptosis in PS1 astrocytes. *Glia*, 56:449–456.

Wang Y, An L & Jiang Y. (2011). Effects of Simulated Microgravity on Embryonic Stem Cells. *PLoS ONE*, 6(12): e29214.

Wei C, Wu Q & Vega VB. (2006). A global map of p53 transcription-factor binding sites in the human genome. *Cell*, 124:207–219.

Whitehurst C, Ning S & Bentz G. (2009). The Epstein-Barr Virus (EBV) Deubiquitinating Enzyme BPLF1 Reduces EBV Ribonucleotide Reductase Activity. *Journal of Virology*, 83:4345–4353.

Wu J, Cheng Y & Nilsson A. (2004). Identification of one exon deletion of intestinal alkaline sphingimyelase in colon cancer HT-29 cells and a differentiation-related expression of the wild-type enzyme in Caco-2 cells, *Carcinogenesis*, 25(8):1327–1333.

Xu Z, Zhou J & McCoy DM. (2005). LASS5 is the predominant ceramide synthase isoform involved in *de novo* sphingolipid synthesis in lung epithelia. *Journal of Lipid Research*, 46:1229–1238.

Yu Z, Nikolova‐Karakashian M & Zhou D. (2000). Pivotal role for acidic sphingomyelinase in cerebral ischemia‐induced ceramide and cytokine production and neuronal apoptosis. *Journal of Molecular Neuroscience*, 15:85–97.

Zalatan J, Fenn T & Herschlag D. (2006). Structural and functional comparisons of nucleotide pyrophosphatase/phosphodiesterase and alkaline phosphatase: implications for mechanism and evolution. *Biochemistry*, 45:9788–9803.

Zhang S, Chen H & Liu K. (2009). Inferring protein function by domain context similarities in protein-protein interaction networks. *BMC Bioinformatics*, 10:1–6.

Websites:

http://multalin.toulouse.inra.fr/multalin/

http://string-db.org/

http://thebiogrid.org/

http://www.clustal.org/omega/

http://www.ncbi.nlm.nih.gov/tools/cobalt/

www.atcc.org

www.cansa.org.za

www.drugbank.ca.za

www.ebi.ac.uk/intact/

www.ncbi.nlm.nih.gov

www.promega.com

APPENDICES

APPENDIX 1

10X PBS

Reagents (for 1 L):

- NaCl – 80 g
- KCl – 2.0g
- Na_2HPO_4:7H2O – 14.4 g
- KH_2PO4 - 2.4 g
- Pure Water H_2O – 1 L

Procedure:

1. Add each of reagents to 800 ml of pure water.
2. Adjust by adding enough pure water to make 1000 ml of solution.
3. Adjust pH between 7.2 and 7.6
4. Autoclave and Store at room temperature

1X PBS (1L)

100 ml of 10X PBS and 900 ml of water

10X TE

- 100 ml 1 M Tris-HCl pH 7.5
- 20 ml 500 mM EDTA pH 8.0
- 880 ml pure water

1X TE (100 ml)

10 ml 10X TE and 90 ml pure water

10X TBE

Reagents (for 1L):

- 108 g of Tris base [tris(hydroxymethyl)aminomethane]
- 55 g of boric acid
- 7.5 g of EDTA, disodium salt
- deionised water

Procedure:

1. Dissolve the Tris, boric acid and EDTA in 800 ml of pure water.
2. Dilute the buffer to 1 L. Undissolved white clumps may be made to dissolve by placing the bottle of solution in a hot water bath, and store at room temperature.

1X TBE

100 ml of 10X TBE and 900 ml of pure water

Calculations of concentrations for apoptosis inducing drugs:

1. C = concentration
2. N = moles
3. M = mass
4. V = volume

MM = molecular mass

5 Flourouracil (5FU):

50 mg of 5FU was dissolved in 1 ml PBS = 50 mg/ml

5 µM 5FU = 0.065 mg in 100 ml

5 µM = 5 µmol/L

Molecular mass (MM) 5FU = 130.08 g/mol

C = n/V

N = CV

= 5 µmol/L X 0.1 L

= 0.5 µmol

N = m/MM

M = nMM

= 0.5 µmol X 130.08 g/mol

= 0.065 mg

Anastrozole:

40 mg dissolved in 1 ml DMSO (Sigma-Aldrich, USA) = 40 mg/ml

2 µM anastrozole = 0.0587mg in 100 ml

2 µM = 2 µmol/L

Molecular mass (MM) anastrozole = 293.4 g/mol

C = n/V

N = CV

= 2 µmol/L X 0.1 L

= 0.2 µmol

N = m/MM

M = nMM

= 0.2 µmol X 293.4 g/mol

= 0.0587 mg

APPENDIX 2

Table 2a: Shows the Reverse transcription composition

Reagents	Volume (µl)
iScript-Buffer	4
RNA	2
Reverse transcriptase	1
Nuclease-Free H_2O	13
Total volume	**20**

Table 2b: cDNA synthesis cycling conditions

Temperature (ºC)	Time (min)
25	5
42	30
85	5

Table 2c: Shows the composition of Polymerase Chain Reaction (PCR) Reaction

Reagents	Experiment	Negative Control
2X PCR Master Mix (Promega,USA)	10	10
Forward Primer	1	1
Reverse Primer	1	1
Nuclease Free H_2O	6	8
Template (cDNA)	2	0
Total volume	**20**	**20**

Table 2d: Shows the PCR Conditions used to amplify the region of interest

Step	Temperature (ºC)	Time (min)
Initial Denaturation	95	2
Denaturation	94	0.5
Annealing	x	1
Extension	72	1
Final extension	72	10
Hold	4	∞

x represents the annealing temperature of either LASS4 or LASS5 which was 53 ºC for LASS4, 55 ºC for LASS5 and 54 ºC for β-actin.

NB: 35 cycles were run and the results were analysed by agarose gel electrophoresis

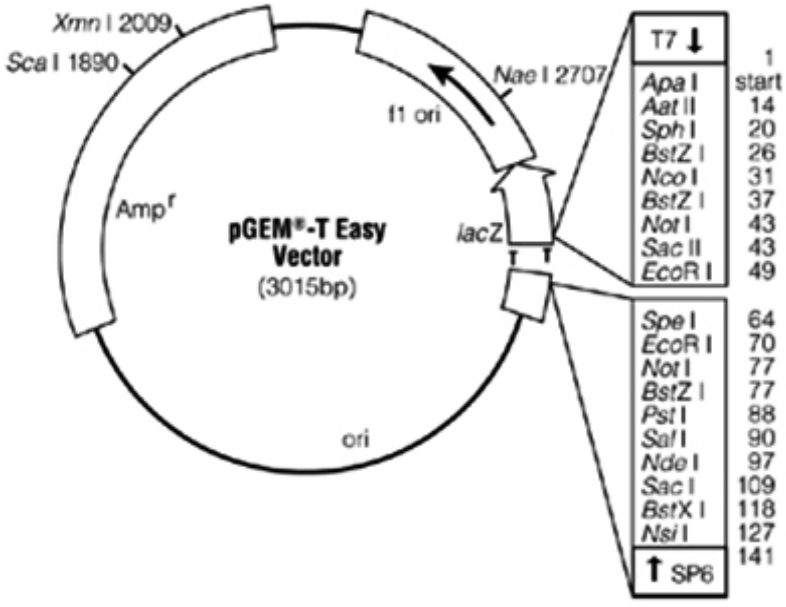

Figure 2a – A diagrammatic representation of p-GEM-T-Easy cloning vector: The PCR insert is ligated into the multiple cloning site, between 49 and 64 (www.promega.com).

Table 2e: Shows the ligation system using the p-GEM-T-easy vector

Reagents	Experimental Samples (µl)	Negative control (µl)
2X Ligation Buffer	5	5
p-GEM-T-easy vector (10ng/µl)	1	1
T4 ligase	1	1
PCR product	2	-
sd H_2O	1	3
Total	**20**	**20**

sdH_2O = sterile distilled water

Tfb solutions

Tfb1

30 mM KAc (Fluka Chemie Gmbh, Sigma-Aldrich Chemie

GmbH, Steinheim, Switzerland)

50 mM MnCl2 (Riedel-de-Haën, Sigma-Aldrich

Laborchemikalien GmbH, Seelze)

100 mM KCl (Riedel-de-Haën, Sigma-Aldrich

Laborchemikalien GmbH, Seelze)

10 mM Calcium Chloride (CaCl2) (Riedel-de-Haën, Sigma-

Aldrich Laborchemikalien GmbH, Seelze)

15% (v/v) Glycerol

Solution was sterilised by filtration

Tfb2 10 mM MOPS, pH7.0

109

75 mM CaCl2

10 mM KCl

15% (v/v) Glycerol

Solution was sterilised by filtration

APPENDIX 3

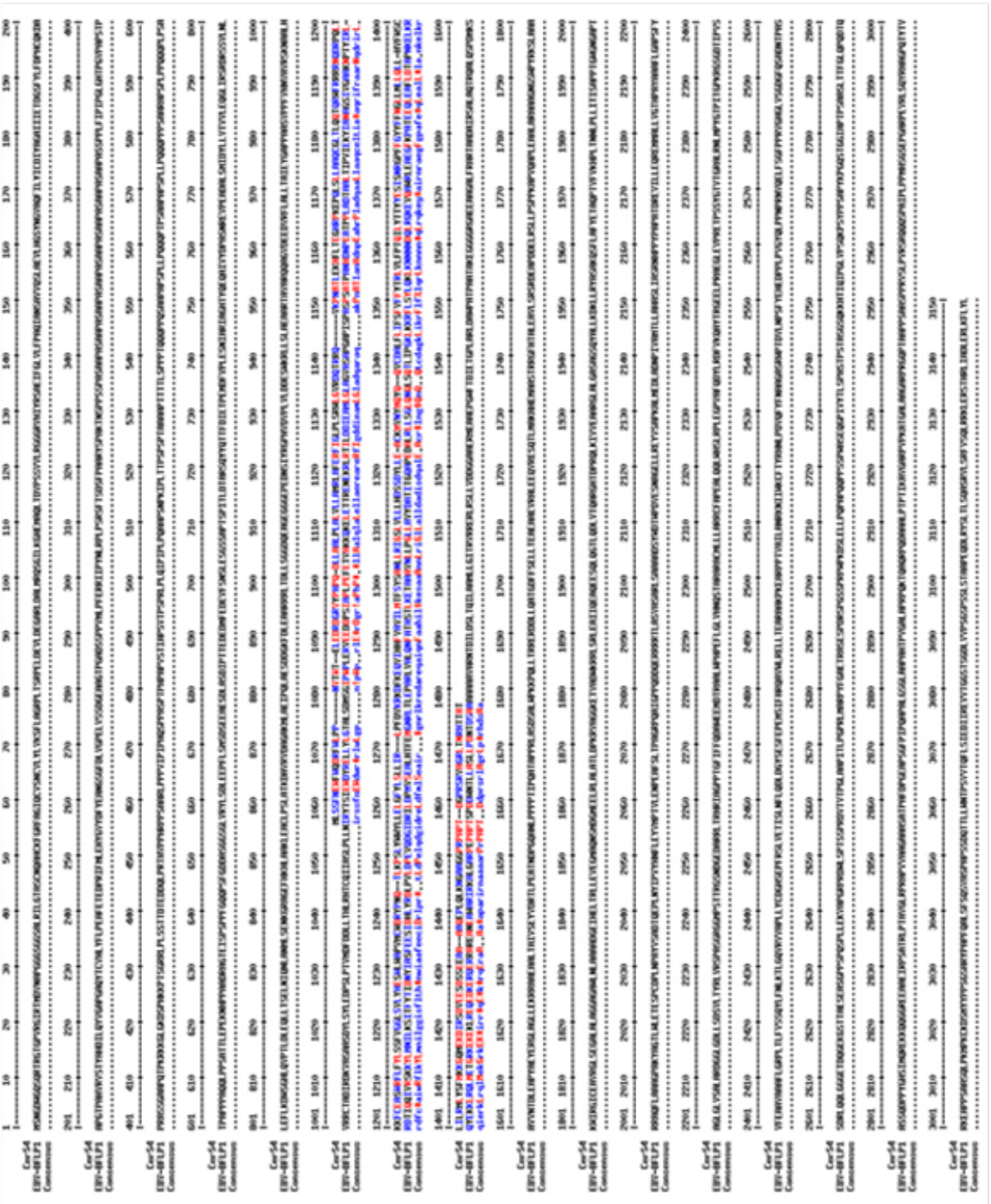

Figure 3a – The sequence alignment between CerS4 and EBV-BFLP1 protein using MultiAlign database: This interaction was determined using the IntAct protein-protein interaction database and the EBV-BFLP1 sequence was obtained from NCBI. Red residues show high consensus while blue residues show low consensus.

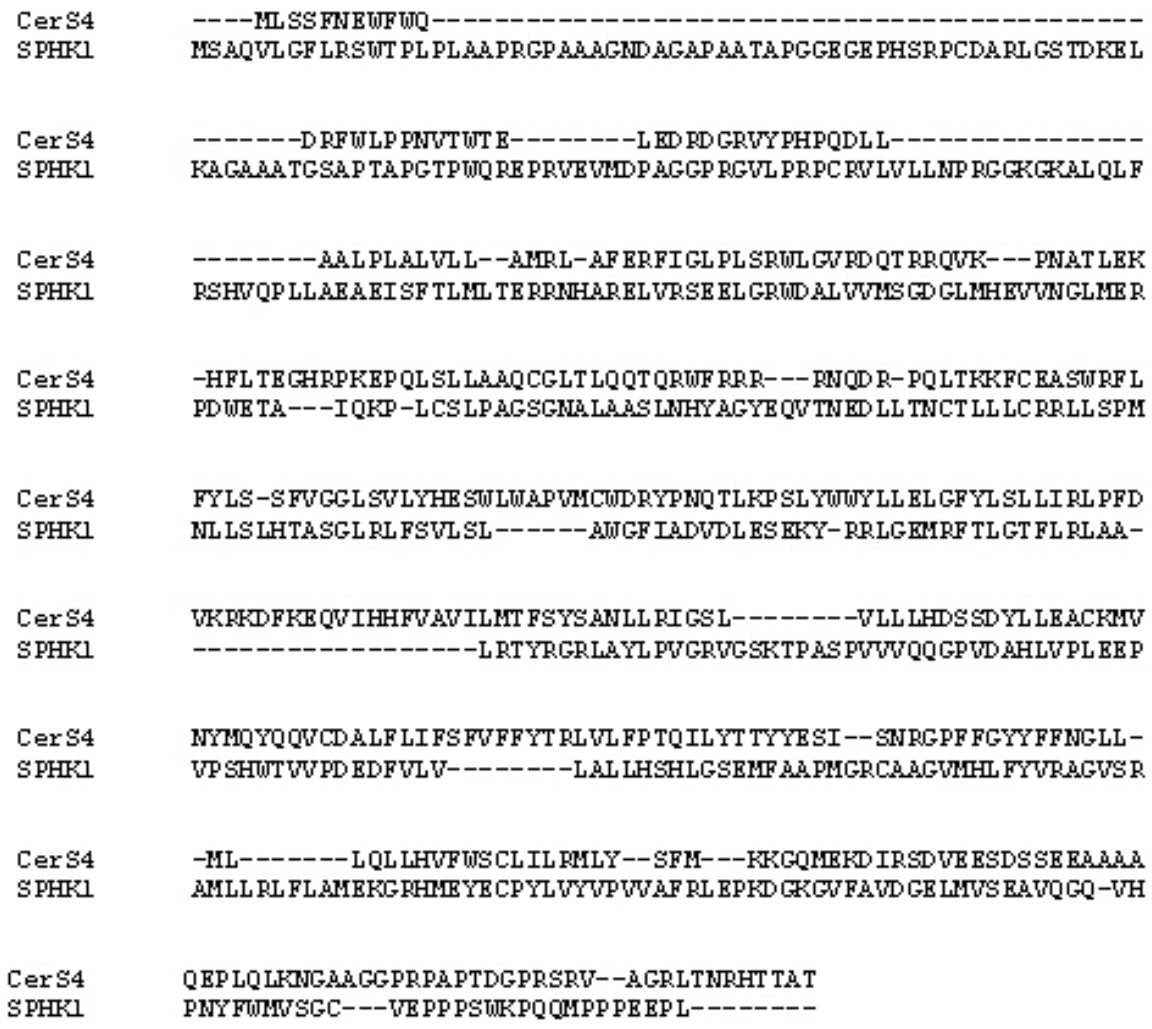

Figure 3b – The sequence alignment between CerS4 and SPHK1 using Clustal Omega: No consensus sequence was revealed, especially when CerS4 sequence was aligned with all of its protein interacting partners.

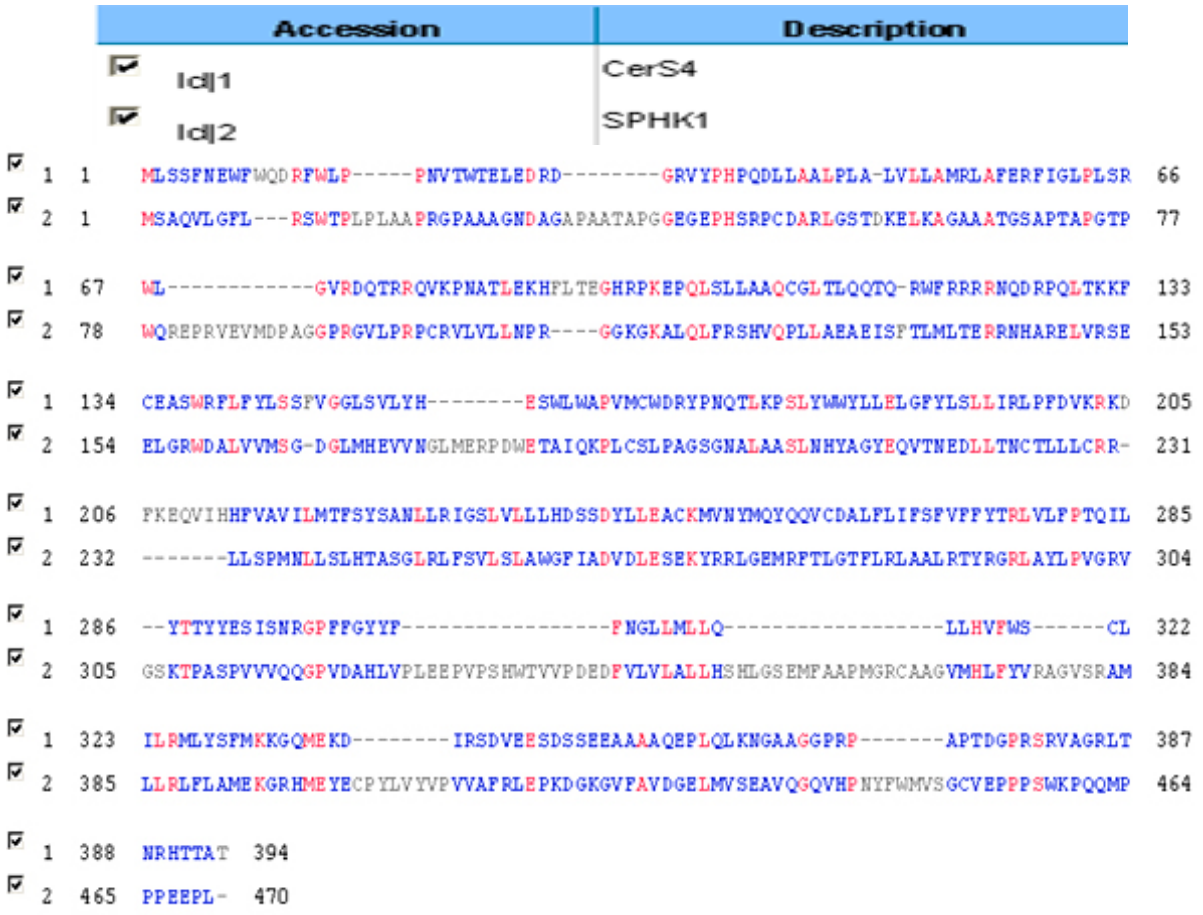

Figure 3c – The sequence alignment between CerS4 and SPHK1 using COBALT: Sequence similarity between the two sequences is shown in red, whereas non-identical amino acids are shown in blue.

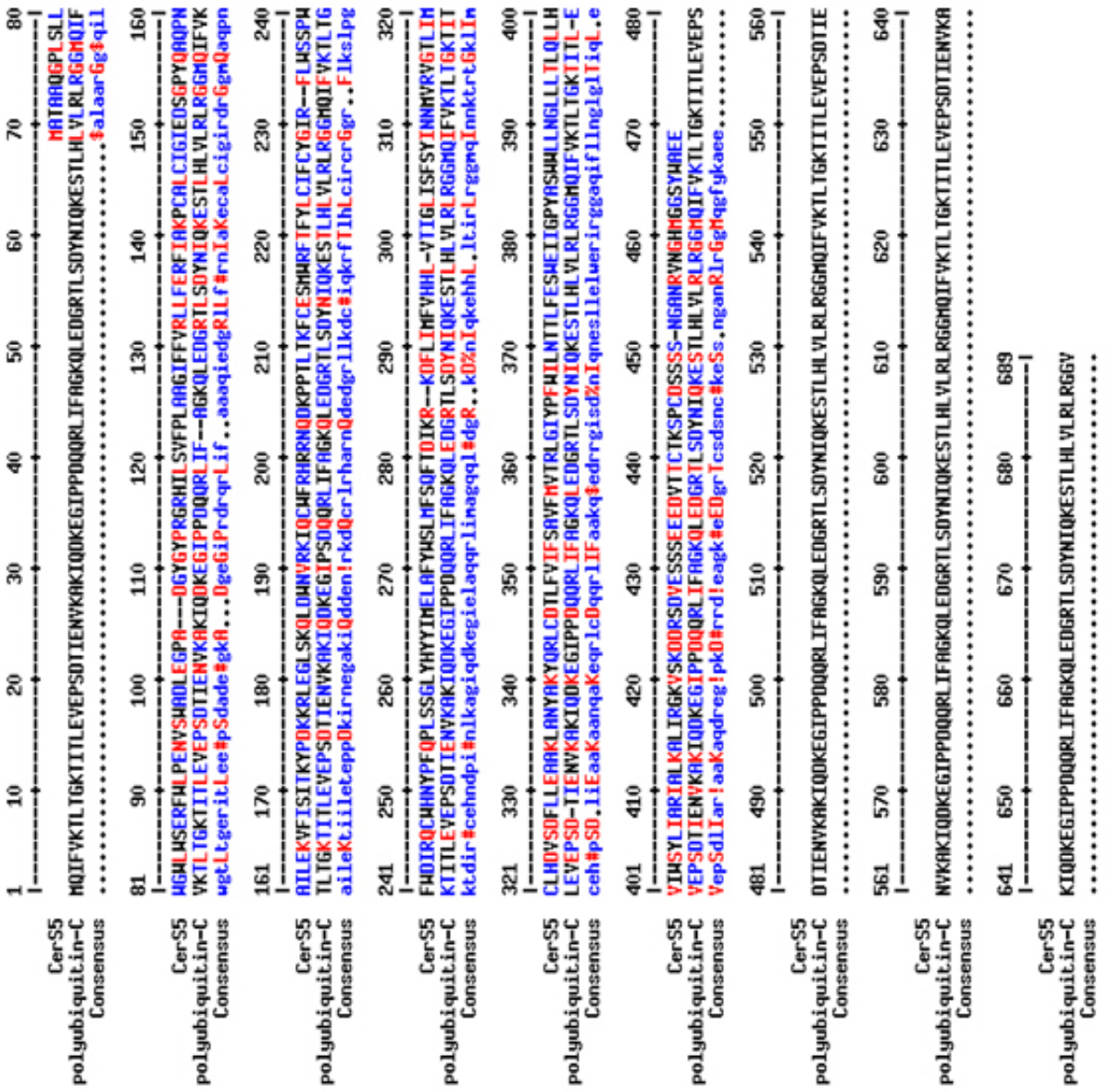

Figure 3d – The sequence alignment between CerS5 and polyubiquitin-C (UBC) using MultiAlign database: This protein interaction was obtained from BioGRID and the UBC amino acid sequence was obtained from NCBI. The high consensus is shown in red and the low consensus is shown in blue.

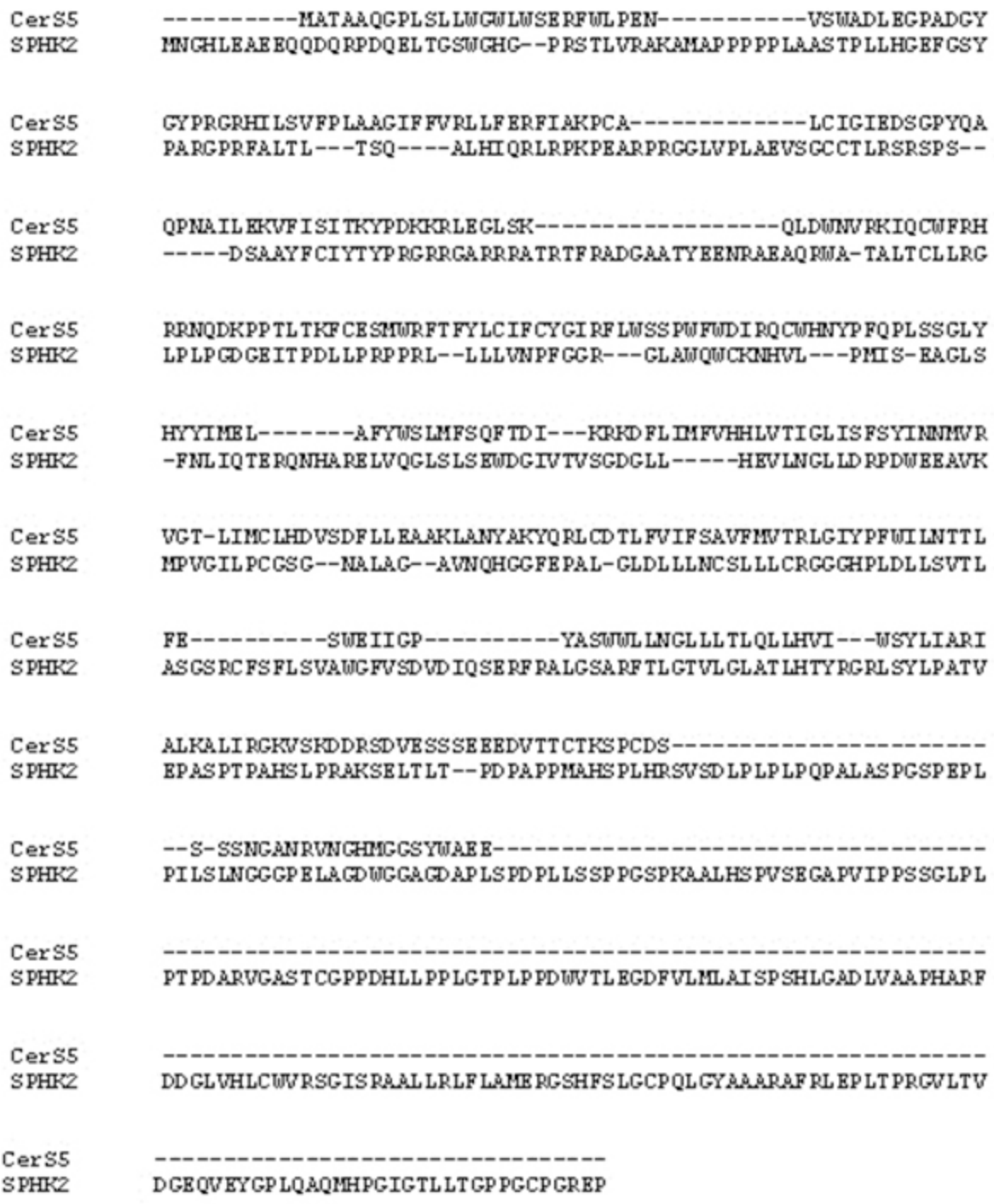

Figure 3e – The sequence alignment between CerS5 and SPHK2 using Clustal Omega: No consensus sequence was revealed, especially when CerS5 sequence was aligned with all of its protein interacting partners.

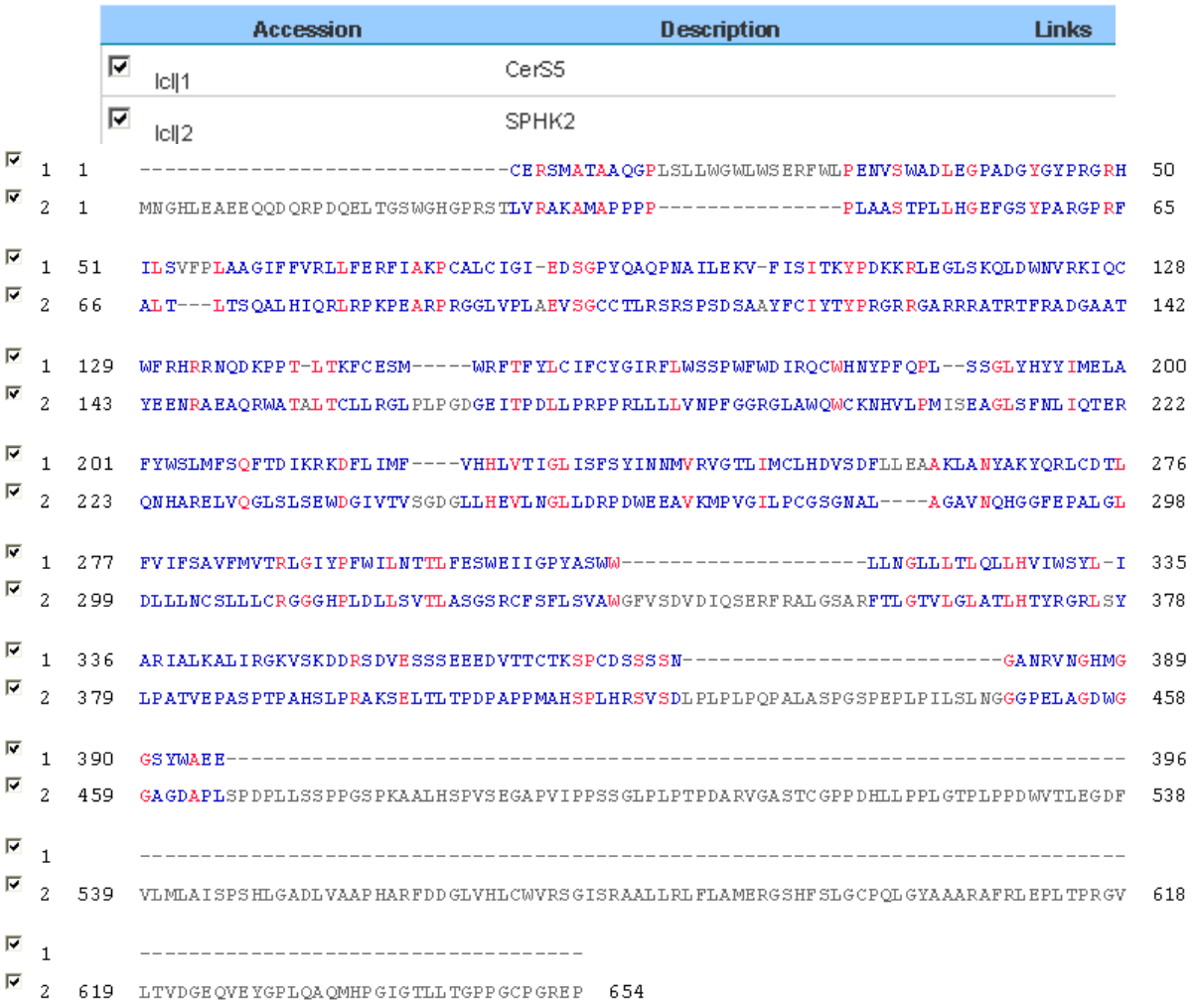

Figure 3f – The sequence alignment between CerS5 and SPHK2 using COBALT: Sequence similarity between the two sequences is shown in red, whereas non-identical amino acids are shown in blue.

APPENDIX 4

Flow Cytometry/FACS analysis

Endometrial cell lines

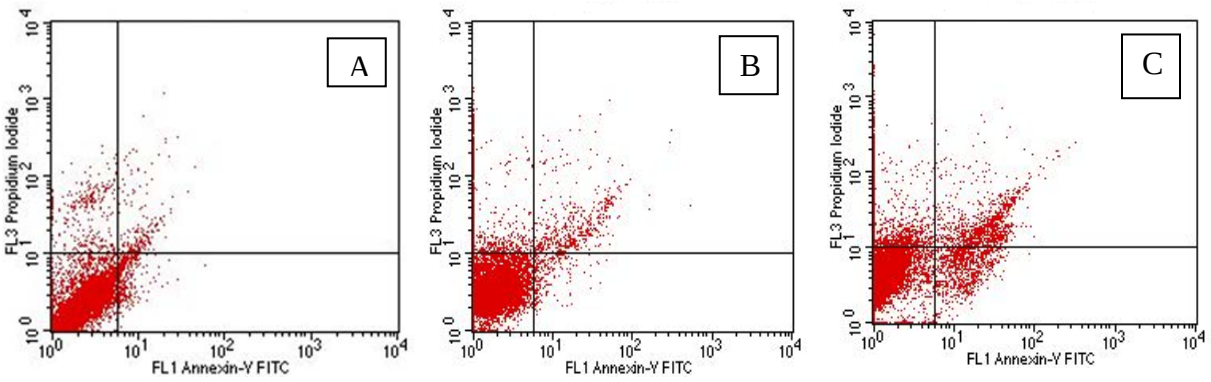

Figure 4a – The cytograms illustrating the endometrial GMMe cell line undergoing apoptosis: (a) The viable cell population (blank), (b) The negative control and (c) The experiment-apoptosis induced. The gates of the controls and the experiment are the same. A 15% apoptosis was seen.

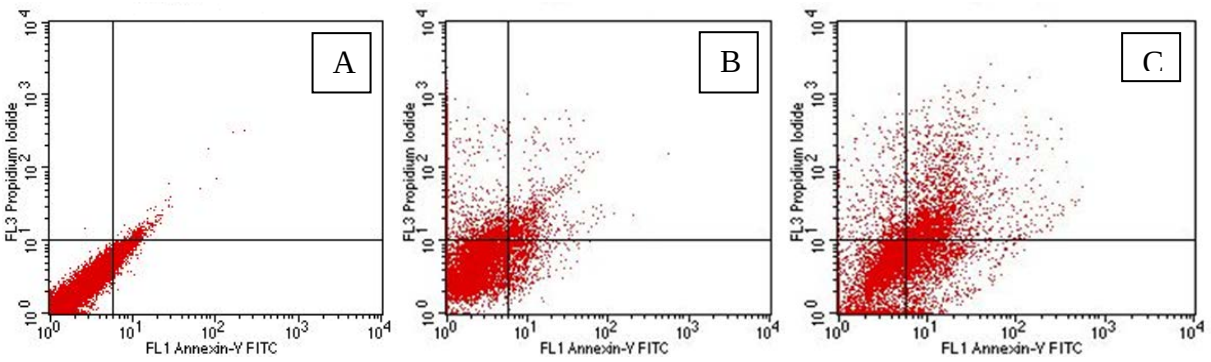

Figure 4b – The cytograms illustrating the endometrial Hec-1A cell line undergoing apoptosis: (a) The viable cell population (blank), (b) The negative control and (c) The experiment- apoptosis induced. The experiment's apoptosis signal was subtracted from the positive control, to get the true apoptosis signal, and a 33% apoptosis signal was seen. The experiments were done in triplicate for each cell-line.

Colon cell lines

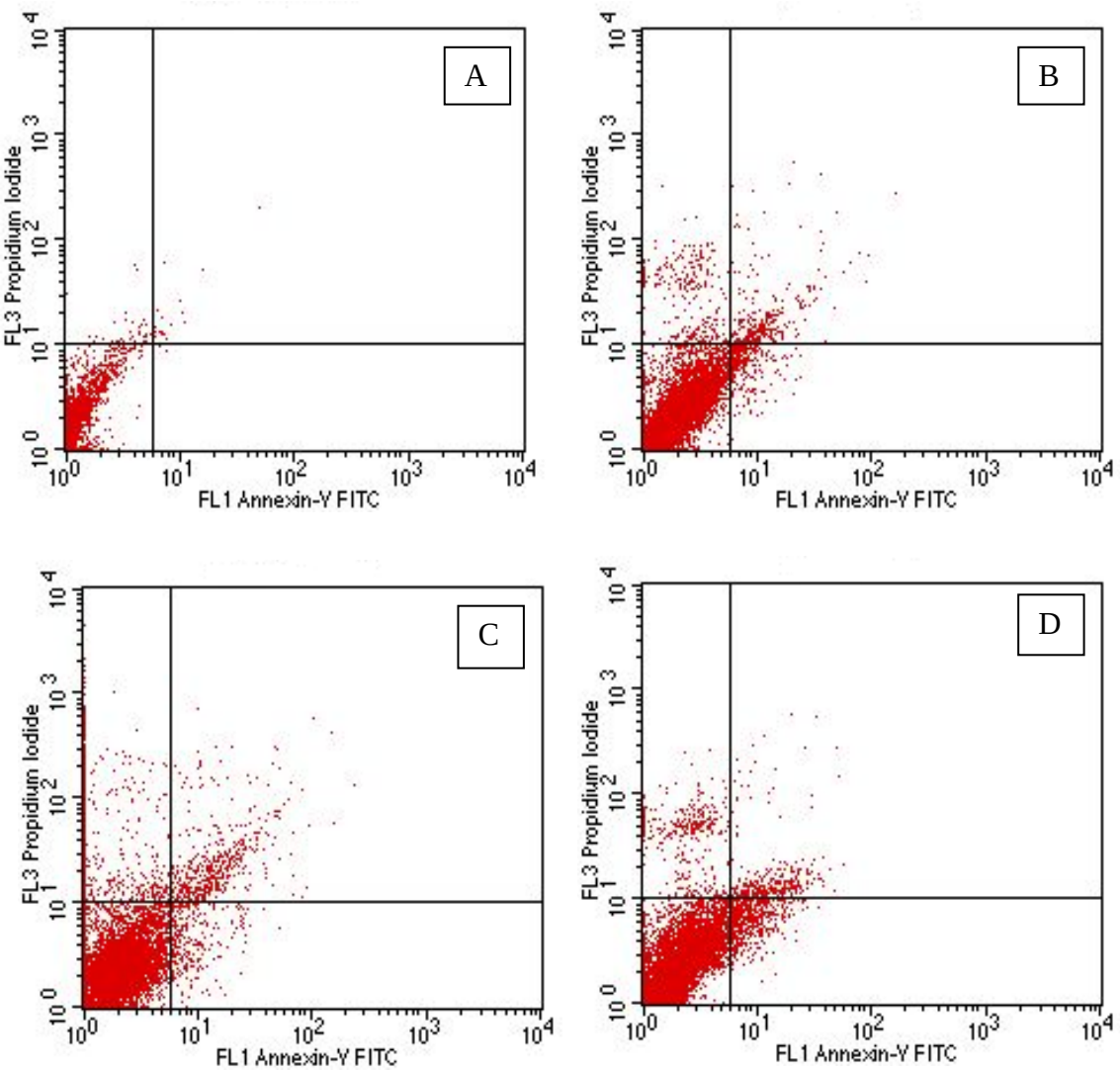

Figure 4c – Diagrammatic representations (cytograms) of the Caco-2 cell line undergoing apoptosis: (a) Showing the viable population (blank), (b) the negative control, (c) 24 hrs-treatment and (d) 48 hrs treatment. The horizontal and the vertical gates of the controls is the same as the experiments. A 6% apoptosis signal was seen in Caco-2 cells after 24 hrs, and 7.8% after 48 hrs.

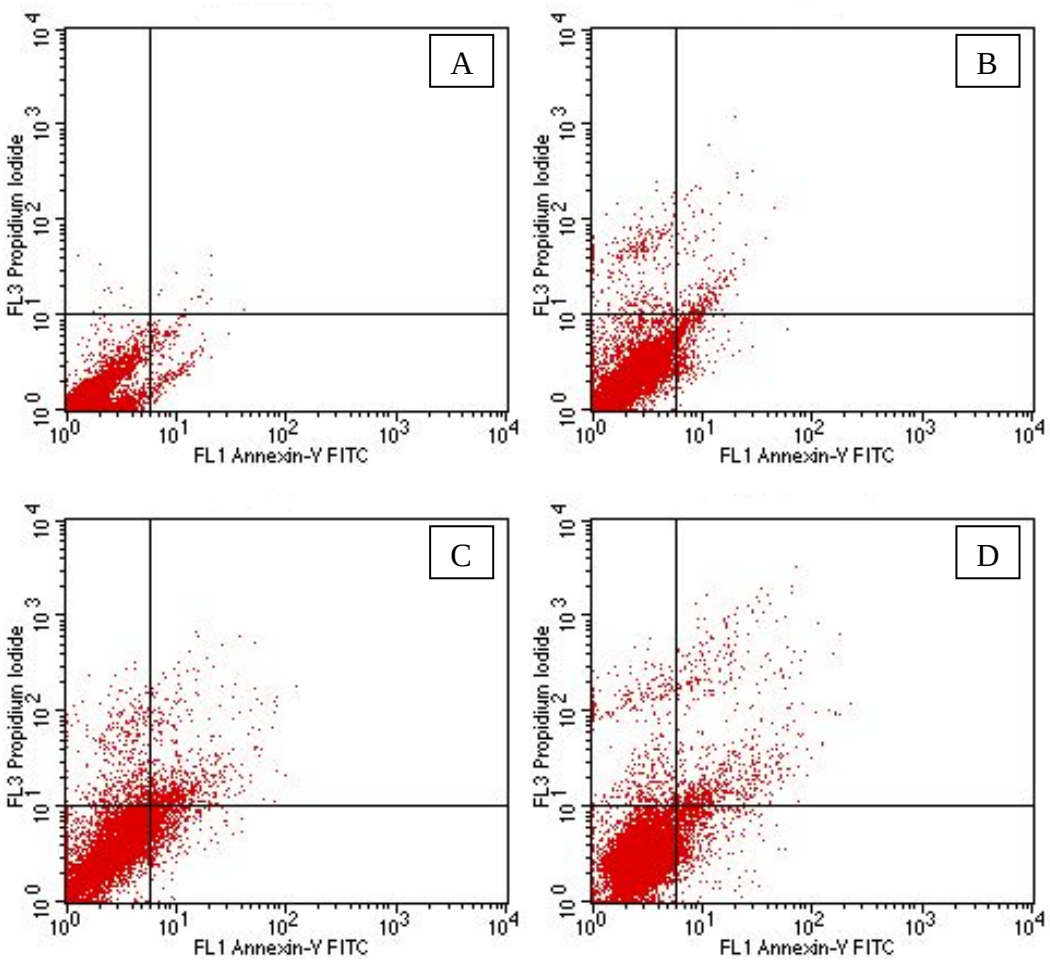

Figure 4d – The Flow cytometric representation of the HT-29 cell line undergoing apoptosis: The viable cell population (blank), (b) the negative control, (c) the 24 hrs treatment and (d) the 48 hrs treatment. A 11% for 24 hrs and 14% for 48 hrs apoptosis signal was observed.

Tables 4a and 4b show the FACS analysis for GMMe cell-line and Hec-1A and table 4c and 4d show the statistical analysis of GMMe and Hec-1A. Table 4e and 4f show the FACS analysis for Caco-2 and HT-29, while table 4g and 4h show the statistical analysis for Caco-2 and HT-29 colon cell lines.

NB: Values in the experiment column denote those in the apoptosis quadrant (2), staining Annexin V positive and PI negative.

Table 4a: FACS analysis of GMMe endometrial cell-line

GMMe	Blank	Negative Control	GMMe experiment
	0.24	4.26	14.77
	0.72	3.86	13.97
	0.63	4.01	14.15

Table 4b: FACS analysis for Hec-1A endometrial cell-line

Hec-1A	Blank	Negative Control	Hec-1A experiment
	2.36	5.86	25.51
	1.98	4.98	24.59
	2.02	5.32	23.68

Table 4c: GMMe cell line statistical analysis

Table Analysed	Data 1				
One-way analysis of variance					
P value	P <0.0001				
P value summary	***				
Are means signif. different? (P <0.05)	Yes				
Number of groups	3				
F	1633				
R squared	0.9982				

ANOVA Table	SS	df	MS		
Treatment (between columns)	307.0	2	153.5		
Residual (within columns)	0.5641	6	0.09402		
Total	**307.6**	**8**			
Tukey's Multiple Comparison Test	**Mean Diff.**	**q**	**Significant? P <0.05?**	**Summary**	**95% CI of diff**
Blank vs Negative control	-3.513	19.85	Yes	***	-4.281 to -2.745
Blank vs GMMe experiment	-13.77	77.76	Yes	***	-14.53 to -13.00
Negative control vs GMMe experiment	-10.25	57.92	Yes	***	-11.02 to -9.485

Table 4d: Hec-1A cell line statistical analysis

Table Analysed	Data 1				
One-way analysis of variance					
P value	P <0.0001				
P value summary	***				
Are means signif. different? (P <0.05)	Yes				
Number of groups	3				
F	1231				
R squared	0.9976				

ANOVA Table	SS	df	MS		
Treatment (between columns)	884.6	2	442.3		
Residual (within columns)	2.156	6	0.3593		
Total	**886.8**	**8**			
Tukey's Multiple Comparison Test	**Mean Diff.**	**q**	**Significant? P <0.05?**	**Summary**	**95% CI of diff**
Blank vs Negative control	-3.267	9.440	Yes	**	-4.768 to -1.765
Blank vs Hec-1A Experiment	-22.47	64.94	Yes	***	-23.97 to -20.97
Negative control vs Hec-1A Experiment	-19.21	55.50	Yes	***	-20.71 to -17.71

Table 4e: FACS analysis for the Caco-2 colon cell-line

Caco-2	Blank	Negative Control	24-hr	48-hr
	0.32	1.39	4.09	3.63
	0.25	1.93	4.92	4.52
	0.46	1.61	5.01	4.97

Table 4f: FACS analysis for the HT-29 colon cell-line

HT-29	Blank	Negative Control	24-hr	48-hr
	0.63	1.24	4.05	60.2
	0.35	0.92	5.06	5.95
	0.42	0.78	4.86	5.14

Table 4g: Caco-2 cell line statistical analysis

Table Analysed	Data 1				
One-way analysis of variance					
P value	P <0.0001				
P value summary	***				
Are means signif. different? (P <0.05)	Yes				
Number of groups	4				
F	66.14				
R squared	0.9612				
ANOVA Table	**SS**	**df**	**MS**		
Treatment (between columns)	40.05	3	13.35		
Residual (within columns)	1.615	8	0.2019		
Total	**41.67**	**11**			

Tukey's Multiple Comparison Test	Mean Diff.	q	Significant? P <0.05?	Summary	95% CI of diff
Blank vs Negative control	-1.300	5.012	Yes	*	-2.475 to -0.1252
Blank vs Caco-2 24h treatment	-4.330	16.69	Yes	***	-5.505 to -3.155
Blank vs Caco-2 48h treatment	-4.030	15.54	Yes	***	-5.205 to -2.855
Negative control vs Caco-2 24h treatment	-3.030	11.68	Yes	***	-4.205 to -1.855
Negative control vs Caco-2 48h treatment	-2.730	10.52	Yes	***	-3.905 to -1.555
Caco-2 24h treatment vs Caco-2 48h treatment	0.3000	1.157	No	ns	-0.8748 to 1.475

Table 4h: HT-29 cell line statistical analysis

Table Analysed	Data 1				
One-way analysis of variance					
P value	P <0.0001				
P value summary	***				
Are means signif. different? (P <0.05)	Yes				

Number of groups	4				
F	136.5				
R squared	0.9808				
ANOVA Table	**SS**	**df**	**MS**		
Treatment (between columns)	61.62	3	20.54		
Residual (within columns)	1.204	8	0.1505		
Total	**62.83**	**11**			
Tukey's Multiple Comparison Test	**Mean Diff.**	**q**	**Significant? P <0.05?**	**Summary**	**95% CI of diff**
Blank vs Negative control	-0.5133	2.292	No	ns	-1.528 to 0.5012
Blank vs HT-29 24h treatment	-4.190	18.71	Yes	***	-5.204 to -3.176
Blank vs HT-29 48h treatment	-5.237	23.38	Yes	***	-6.251 to -4.222
Negative control vs HT-29 24h treatment	-3.677	16.41	Yes	***	-4.691 to -2.662
Negative control vs HT-29 48h treatment	-4.723	21.09	Yes	***	-5.738 to -3.709
HT-29 24h treatment vs HT-29 48h treatment	-1.047	4.673	Yes	*	-2.061 to -0.03218

APPENDIX 5

Real-Time PCR

Table 5a: Shows a 5X dilution series of HT-29 for constructing the STD-curve

Dilution	HT-29 (ng/µl)
Undiluted	245
1:5	49
1:25	9.8
1:125	1.96
1:625	0.39

NB: Different dilutions were run in duplicates, each cell line was diluted.

Table 5b: Shows a 5X dilution series of Caco-2 for constructing the STD-curve

Dilution	Caco-2 (ng/µl)
Undiluted	131.9
1:5	26.38
1:25	5.28
1:125	1.06
1:625	0.21

Table 5c: Shows a 5X dilution series of GMMe for constructing the STD-curve

Dilution	GMMe (ng/µl)
Undiluted	168.5
1:5	33.7
1:25	6.74
1:125	1.35
1:625	0.27

Table 5d: Shows the qRT-PCR protocol for LASS4, LASS5 and β-actin

Reagents	Exp (µl)	Neg. control (µl)
SYBR Green	10	10
Fw primer	0.5	0.5
Rv primer	0.5	0.5
Nuclease Free H2O	7	9
cDNA	2	–
Total	**20**	**20**

The cancer cell-line was compared to a normal cell line, with the initial concentration of both cell lines being the same.

Table 5e: Shows the qRT-PCR incubation using the Mini-Opticon (Bio-Rad)

Step (Incubation ºC)	Time (min)
95	2
94	0.5
x*	0.5
72	1
Plate Read	–
Go to line 2, 39 times	–
72	10
Melting Curve from x to y, 1 °C	0.17

x* depends on the annealing temperatures, i.e. LASS4 is 53 ºC and LASS5 is 55 ºC and 54 ºC for β-actin.

Results were analysed using the Opticon-Monitor, Bio-Rad, Version 3.1

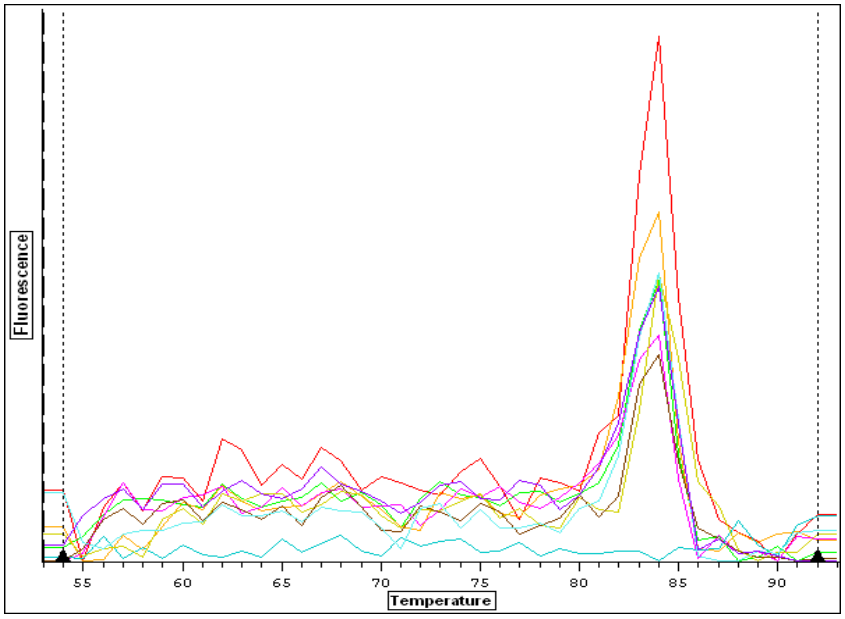

Figure 5a – LASS5 melting curve with a melting temperature of 84°C: The single peak illustrates the specificity of primers, yielding one product. There was no product amplified in the negative control (---) as there was no template added.

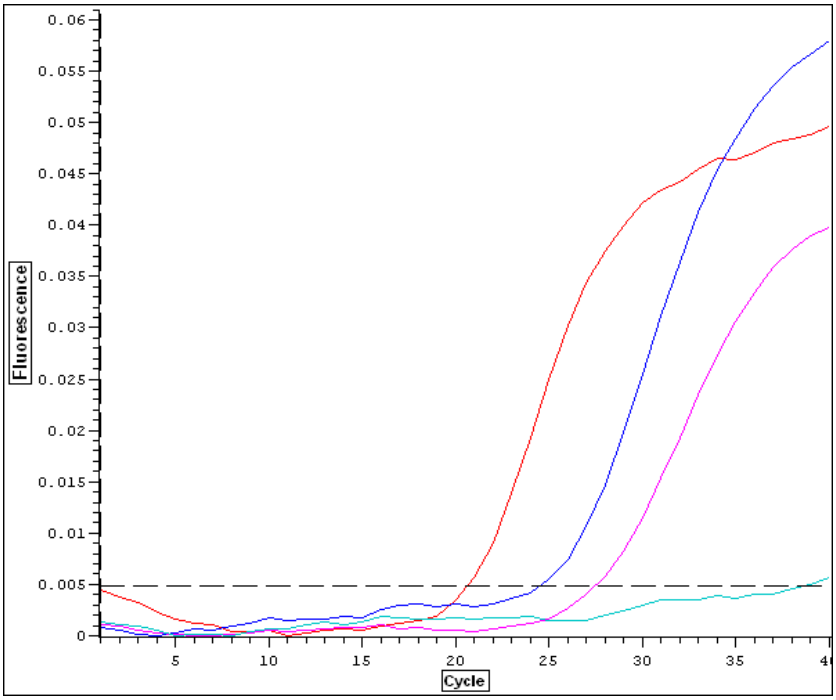

Figure 5b – Amplification curves for LASS5, for standard curve construction of LASS5: The 5X dilution was used to construct a standard curve from the 131.9 ng/µl of Caco-2 cell line synthesised cDNA.

Table 5f: Shows the log concentrations with the corresponding threshold cycle for LASS5

Log Concentration	Threshold Cycle
2.12	20.62
1.42	23.31
0.7	25.80

NB: For β-actin, the HT-29 cDNA synthesised from RNA was used, the concentration was 245ng/µl

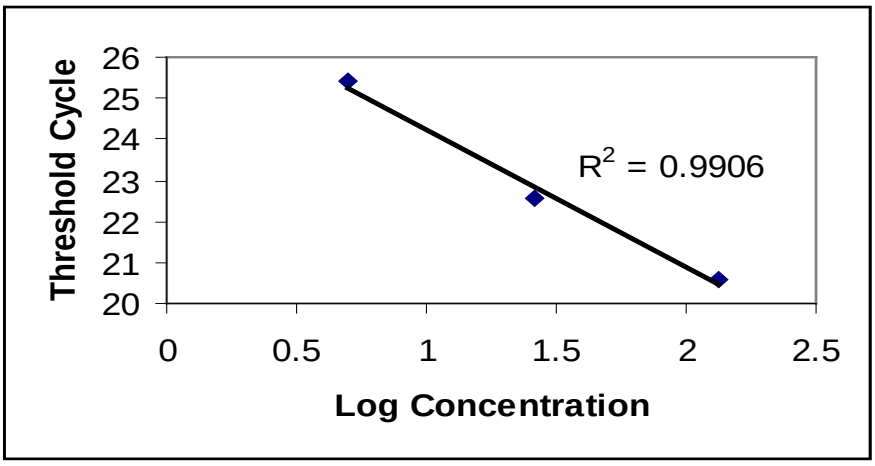

Figure 5c – Standard curve for LASS5: The slope was calculated to be -3.39 and r^2 value is 0.9906.

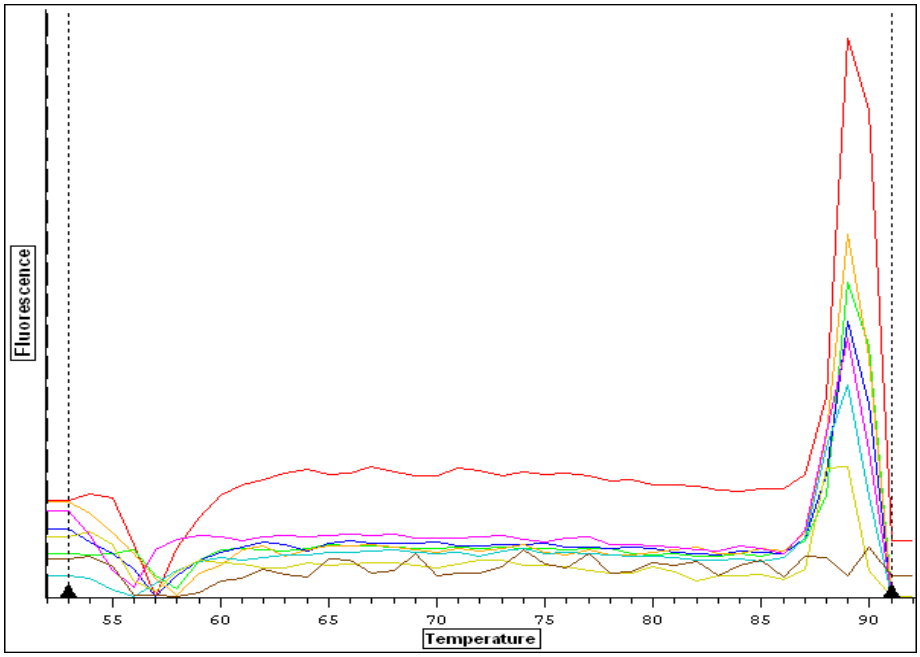

Figure 5d – β-actin melting-curve with melting temperature of 89 °C: The primers are shown to be specific, yielding only one product. The negative control (---) yielded no product as there was no template added to the reaction mixture.

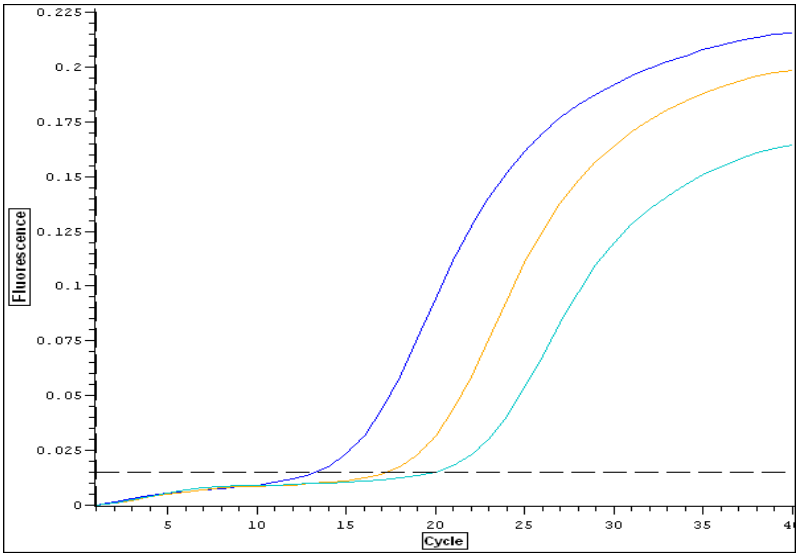

Figure 5e – Amplification curves for β-actin used for standard curve construction: The CT values of these amplification curves together with the log-concentrations, (from initial 245ng/µl HT-29 cDNA) were used to construct a standard curve.

Table 5g: Shows the Log Concentrations of the corresponding threshold cycles for β-actin

Log Concentration	Threshold Cycle
2.39	13.89
1.69	16.72
0.99	18.82

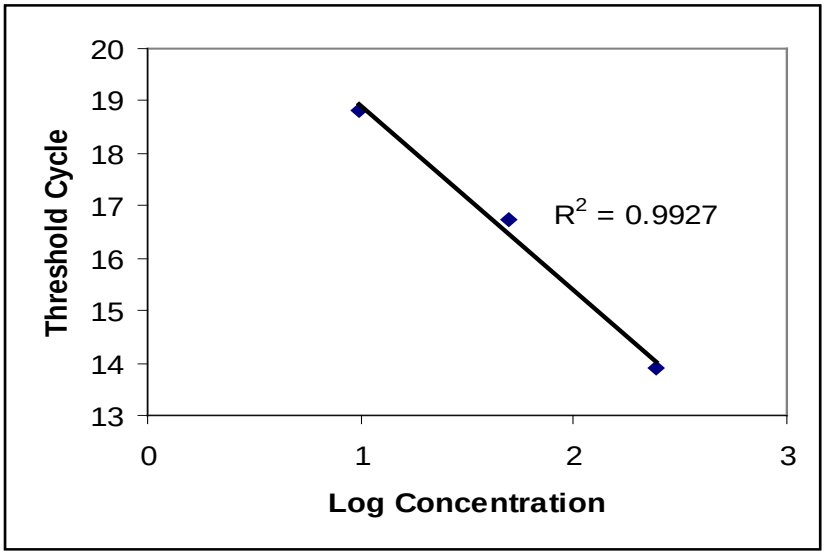

Figure 5f – Standard curve for β-actin: It was constructed using the 5X dilution of HT-29 cDNA. Slope = -3.5 and r^2 = 0.9927

The percentage efficiency were calculated as follows; for LASS4, LASS5 and β-actin:

LASS4

Slope = -3.6

$E = 10^{(-1/slope)}$

= 1.9

% Efficiency = (E – 1) X 100%

= 90%

LASS5

Slope = -3.39

$E = 10^{(-1/slope)}$

= 1.97

% Efficiency = (E -1) X 100%

= 97%

β-actin

Slope = -3.5

$E = 10^{(-1/slope)}$

$= 1.93$

% Efficiency = (E -1) X 100%

= 93%

Each experiment was done in triplicate and the readings for LASS 4 and LASS 5 are represented in tables below:

Tables for LASS4

Table 5h: LASS 4 mRNA expression levels in endometrial cell lines before apoptosis treatment

LASS 4 ($2^{-\Delta\Delta CT}$)	GMMe	β-actin	Hec-1A	β-actin
6.73	21.93	16.59	18.96	16.37
3.36	21.04	16.06	19.12	15.89
3.2	20.98	16.74	18.58	16.02

Table 5i: LASS 4 mRNA expression level in GMMe apoptosis treatments

LASS 4 ($2^{-\Delta\Delta CT}$)	GMMe 24h	β-actin 24h	GMMe 0h	β-actin 0h
0.37	26.63	16.47	24.49	15.76
0.4	26.14	16.31	24.08	15.58
0.35	26.21	16.01	24.77	16.10

Table 5j: LASS 4 mRNA expression level in Hec-1A apoptosis treatments

LASS 4 ($2^{-\Delta\Delta CT}$)	Hec-1A 24h	β-actin 24h	Hec-1A 0h	β-actin 0h
0.24	25.98	16.19	23.32	15.6
0.27	25.46	16.39	22.86	15.69
0.16	25.17	15.98	22.25	16.18

Colon cell lines

Table 5k: LASS 4 mRNA in colon cell lines Caco-2 and HT-29 before apoptosis treatment

LASS 4 ($2^{-\Delta\Delta CT}$)	Caco-2	β-actin	HT-29	β-actin
10.63	25.27	16.74	21.41	16.29
10.78	25.03	16.13	20.96	15.49
4.69	24.46	16.41	21.72	15.9

Table 5l: LASS 4 mRNA expression level in Caco-2 24h apoptosis treatments

LASS4 ($2^{-\Delta\Delta CT}$)	Caco-2 24h	β-actin 24h	Caco-2 0h	β-actin 0h
0.56	27.82	16.7	26.43	16.15
0.28	27.13	16.41	25.12	16.26
0.66	26.93	16.23	25.81	15.72

Table 5m: LASS 4 mRNA expression level in Caco-2 48h apoptosis treatments

LASS4 ($2^{-\Delta\Delta CT}$)	Caco-2 48h	β-actin 48h	Caco-2 0h	β-actin 0h
0.23	26.6	16.17	24.73	16.39
0.51	25.83	16.72	24.33	16.19
0.28	26.08	16.56	24.14	16.48

Table 5n: LASS 4 mRNA expression level in HT-29 24h apoptosis treatments

LASS 4 ($2^{-\Delta\Delta CT}$)	HT-29 24h	β-actin 24h	HT-29 0h	β-actin 0h
0.45	23.33	16.53	21.99	16.35
1.65	22.62	16.72	22.5	15.88
0.30	22.91	16.11	21.73	16.66

Table 5o: LASS 4 mRNA expression levels in HT-29 48h apoptosis treatment

LASS 4 ($2^{-\Delta\Delta CT}$)	HT-29 48h	β-actin 48h	HT-29 0h	β-actin 0h
0.19	22.16	16.32	19.67	16.2
0.10	23.01	16.12	19.28	15.77
0.51	22.57	16.35	20.56	15.31

Tables for LASS 5

Endometrial cell lines

Table 5p: LASS 5 mRNA expression level in endometrial cell lines GMMe and Hec-1A

LASS5 ($2^{-\Delta\Delta CT}$)	GMMe	β-actin	Hec-1A	β-actin
38.05	26.48	16.41	20.71	15.89
51.98	26.12	16.34	19.79	16.16
39.67	25.82	15.65	21.02	15.71

Table 5q: LASS 5 mRNA expression level in GMMe apoptosis treatments

LASS5 ($2^{-\Delta\Delta CT}$)	GMMe 24h	β-actin 24h	GMMe 0h	β-actin 0h
0.13	26.03	16.48	22.89	16.27
0.14	25.26	15.97	22.2	15.75
0.16	25.75	16.14	22.57	15.58

Table 5r: LASS 5 mRNA expression level in Hec-1A apoptosis treatments

LASS5 ($2^{-\Delta\Delta CT}$)	Hec-1A 24h	β-actin 24	Hec-1A 0h	β-actin 0h
0.08	24.89	16.31	20.83	15.81
0.05	24.38	16.04	20.15	16.09
0.08	25.07	16.61	20.52	15.76

Colon cell lines

Table 5s: LASS 5 mRNA expression level in colon cell lines Caco-2 and HT-29 before apoptosis treatment

LASS5 ($2^{-\Delta\Delta CT}$)	Caco-2	β-actin	HT-29	β-actin
33.82	25.77	16.14	20.62	16.07
21.11	25.16	16.5	19.81	15.55
20.68	24.96	16.73	20.15	16.29

Table 5t: LASS 5 mRNA expression level in Caco-2 24h apoptosis treatment

LASS5 ($2^{-\Delta\Delta CT}$)	Caco-2 24h	β-actin 24h	Caco-2 0h	β-actin 0h
0.57	24.93	16.07	24.09	16.03
0.37	25.22	16.56	23.64	16.43
1.05	24.61	16.77	24.41	16.18

Table 5u: LASS 5 mRNA expression level in Caco-2 48h apoptosis treatment

LASS5 ($2^{-\Delta\Delta CT}$)	Caco-2 48h	β-actin 48h	Caco-2 0h	β-actin 0h
0.22	24.26	16.48	21.82	16.23
0.11	24.37	15.84	21.15	15.8
0.07	24.85	16	21.53	16.55

Table 5v: LASS5 mRNA expression level in HT-29 24h apoptosis treatments

LASS5 ($2^{-\Delta\Delta CT}$)	HT-29 24h	β-actin 24h	HT-29 0h	β-actin 0h
0.04	24.78	15.62	19.84	15.44
0.06	24.41	16.05	20.39	16.11
0.07	23.94	15.91	20.61	16.32

Table 5w: LASS 5 mRNA expression level in HT-29 48h apoptosis treatment

LASS5 ($2^{-\Delta\Delta CT}$)	HT-29 48h	β-actin 48h	HT-29 0h	β-actin 0h
0.03	24.18	16.31	18.08	15.46
0.01	24.52	16.15	17.96	16.03
0.01	24.8	15.93	18.36	15.99

Statistical Analysis using the ANOVA test

LASS4 endometrial cell lines

Table 5i: Statistical analysis using ANOVA test for LASS4 endometrial cells

Table Analysed	Data 1
Column A	GMMe
vs	vs
Column B	Hec-1A

Unpaired t test	
P value	0.0409
P value summary	*
Are means signif. different? (P <0.05)	Yes
One- or two-tailed P value?	Two-tailed
t, df	t = 2.976, df = 4
How big is the difference?	
Mean ± SEM of column A	1.000 ± 0.05774 N = 3
Mean ± SEM of column B	4.430 ± 1.151 N = 3
Difference between means	-3.430 ± 1.152
95% confidence interval	-6.629 to -0.2310
R squared	0.6889
F test to compare variances	
F, DFn, Dfd	397.4, 2, 2
P value	0.0050
P value summary	**
Are variances significantly different?	Yes

Table 5ii: Statistical analysis using ANOVA test for LASS4 in GMMe 24h apoptosis treated cells

Table Analysed	**Data 1**
Column A	L4 GMMe 0h
vs	vs
Column B	L4 GMMe 24h
Unpaired t test	
P value	0.0005
P value summary	***
Are means signif. different? (P <0.05)	Yes
One- or two-tailed P value?	Two-tailed
t, df	t = 10.53, df = 4
How big is the difference?	
Mean ± SEM of column A	1.000 ± 0.05774 N=3
Mean ± SEM of column B	0.3733 ± 0.01453 N=3
Difference between means	0.6267 ± 0.05954
95% confidence interval	0.4614 to 0.7919
R squared	0.9652
F test to compare variances	
F, DFn, Dfd	15.79, 2, 2
P value	0.1191
P value summary	ns
Are variances significantly different?	No

Table 5iii: Statistical analysis using ANOVA for LASS4 in 24h apoptosis treated Hec-1A cells

Table Analysed	**Data 1**
Column A	L4 Hec-1A 0h
vs	vs
Column B	L4 Hec-1A 24h
Unpaired t test	
P value	0.0003
P value summary	***
Are means signif. different? (P <0.05)	Yes
One- or two-tailed P value?	Two-tailed
t, df	t = 11.69, df = 4
How big is the difference?	
Mean ± SEM of column A	1.000 ± 0.05774 N=3
Mean ± SEM of column B	0.2233 ± 0.03283 N=3
Difference between means	0.7767 ± 0.06642
95% confidence interval	0.5923 to 0.9610
R squared	0.9716
F test to compare variances	
F, DFn, Dfd	3.093, 2, 2
P value	0.4887
P value summary	ns
Are variances significantly different?	No

LASS4 colon treatments

Table 5iv: Statistical analysis for LASS4 in Caco-2 cells after 24h apoptosis treatment using ANOVA test

Table Analysed	**Data 1**
Column A	L4 Caco-2 oh
vs	vs
Column B	L4 Caco-2 24h
Unpaired t test	
P value	0.0172
P value summary	*
Are means signif. different? (P <0.05)	Yes
One- or two-tailed P value?	Two-tailed
t, df	t = 3.920, df = 4
How big is the difference?	
Mean ± SEM of column A	1.000 ± 0.05774 N=3
Mean ± SEM of column B	0.5000 ± 0.1137 N=3
Difference between means	0.5000 ± 0.1275
95% confidence interval	0.1459 to 0.8541
R squared	0.7935
F test to compare variances	
F, DFn, Dfd	3.880, 2, 2
P value	0.4098
P value summary	ns
Are variances significantly different?	No

Table 5v: Statistical analysis for LASS4 in Caco-2 cells after 48h apoptosis treatment using ANOVA test

Table Analysed	**Data 1**
Column A	L4 Caco-2 0h
vs	vs
Column B	L4 Caco-2 48h
Unpaired t test	
P value	0.0031
P value summary	**
Are means signif. different? (P <0.05)	Yes
One- or two-tailed P value?	Two-tailed
t, df	t = 6.361, df = 4
How big is the difference?	
Mean ± SEM of column A	1.000 ± 0.05774 N=3
Mean ± SEM of column B	0.3400 ± 0.08622 N=3
Difference between means	0.6600 ± 0.1038
95% confidence interval	0.3720 to 0.9480
R squared	0.9100
F test to compare variances	
F, DFn, Dfd	2.230, 2, 2
P value	0.6192
P value summary	ns
Are variances significantly different?	No

Table 5vi: Statistical analysis for LASS4 in HT-29 cells after 24h apoptosis treatment using ANOVA test

Table Analysed	**Data 1**
Column A	L4 HT-29 0h
vs	vs
Column B	L4 HT-29 24h
Unpaired t test	
P value	0.6668
P value summary	ns
Are means signif. different? (P <0.05)	No
One- or two-tailed P value?	Two-tailed
t, df	t = 0.4639, df = 4
How big is the difference?	
Mean ± SEM of column A	1.000 ± 0.05774 N=3
Mean ± SEM of column B	0.8000 ± 0.4272 N=3
Difference between means	0.2000 ± 0.4311
95% confidence interval	-0.9967 to 1.397
R squared	0.05106
F test to compare variances	
F, DFn, Dfd	54.75, 2, 2
P value	0.0359
P value summary	*
Are variances significantly different?	Yes

Table 5vii: Statistical analysis for LASS4 in HT-29 cells after 48h apoptosis treatment using ANOVA test

Table Analysed	**Data 1**
Column A	L4 HT-29 0h
vs	vs
Column B	L4 HT-29 48h
Unpaired t test	
P value	0.0059
P value summary	**
Are means signif. different? (P <0.05)	Yes
One- or two-tailed P value?	Two-tailed
t, df	t = 5.347, df = 4
How big is the difference?	
Mean ± SEM of column A	1.000 ± 0.05774 N=3
Mean ± SEM of column B	0.2667 ± 0.1244 N=3
Difference between means	0.7333 ± 0.1372
95% confidence interval	0.3526 to 1.114
R squared	0.8773
F test to compare variances	
F ,DFn, Dfd	4.643, 2, 2
P value	0.3544
P value summary	ns
Are variances significantly different?	No

Tables for LASS5

LASS5 endometrium

Table 5viii: ANOVA test for LASS5 in endometrial cells

Table Analysed	Data 1
Column A	L5 GMMe
vs	vs
Column B	L5 Hec-1A
Unpaired t test	
P value	0.0007
P value summary	***
Are means signif. different? (P <0.05)	Yes
One- or two-tailed P value?	Two-tailed
t, df	t = 9.589, df = 4
How big is the difference?	
Mean ± SEM of column A	1.000 ± 0.05774 N=3
Mean ± SEM of column B	43.24 ± 4.405 N=3
Difference between means	-42.24 ± 4.405
95% confidence interval	-54.47 to -30.01
R squared	0.9583
F test to compare variances	
F, DFn, Dfd	5821, 2, 2
P value	0.0003
P value summary	***
Are variances significantly different?	Yes

Table 5ix: ANOVA test for LASS5 in GMMe cells after 24h apoptosis treatment

Table Analysed	**Data 1**
Column A	L5 GMMe 0h
vs	vs
Column B	L5 GMMe 24h
Unpaired t test	
P value	0.0001
P value summary	***
Are means signif. different? (P <0.05)	Yes
One- or two-tailed P value?	Two-tailed
t, df	t = 14.67, df = 4
How big is the difference?	
Mean ± SEM of column A	1.000 ± 0.05774 N=3
Mean ± SEM of column B	0.1433 ± 0.008819 N=3
Difference between means	0.8567 ± 0.05840
95% confidence interval	0.6945 to 1.019
R squared	0.9817
F test to compare variances	
F, DFn, Dfd	42.86, 2, 2
P value	0.0456
P value summary	*
Are variances significantly different?	Yes

Table 5x: ANOVA test for LASS5 in Hec-1A cells after 24h apoptosis treatment

Table Analysed	**Data 1**
Column A	L5 Hec-1A oh
vs	vs
Column B	L5 Hec-1A 24h
Unpaired t test	
P value	P <0.0001
P value summary	***
Are means signif. different? (P <0.05)	Yes
One- or two-tailed P value?	Two-tailed
t, df	t = 15.87, df=4
How big is the difference?	
Mean ± SEM of column A	1.000 ± 0.05774 N=3
Mean ± SEM of column B	0.0700 ± 0.01000 N=3
Difference between means	0.9300 ± 0.05859
95% confidence interval	0.7673 to 1.093
R squared	0.9844
F test to compare variances	
F, DFn, Dfd	33.33, 2, 2
P value	0.0583
P value summary	ns
Are variances significantly different?	No

LASS5 colon cells

Table 5xi: ANOVA test for LASS5 in colon cells

Table Analysed	**Data 1**
Column A	L5 Caco-2
vs	vs
Column B	L5 HT-29
Unpaired t test	
P value	0.0050
P value summary	**
Are means signif. different? (P <0.05)	Yes
One- or two-tailed P value?	Two-tailed
t, df	t = 5.612, df = 4
How big is the difference?	
Mean ± SEM of column A	1.000 ± 0.05774 N=3
Mean ± SEM of column B	25.20 ± 4.312 N=3
Difference between means	-24.20 ± 4.312
95% confidence interval	-36.17 to -12.23
R squared	0.8873
F test to compare variances	
F, DFn, Dfd	5577, 2, 2
P value	0.0004
P value summary	***
Are variances significantly different?	Yes

Table xii: ANOVA test for LASS5 in Caco-2 cells after 24h apoptosis treatment

Table Analysed	**Data 1**
Column A	L5 Caco-2 oh
vs	vs
Column B	L5 Caco-2 24h
Unpaired t test	
P value	0.1839
P value summary	ns
Are means signif. different? (P <0.05)	No
One- or two-tailed P value?	Two-tailed
t, df	t = 1.604, df = 4
How big is the difference?	
Mean ± SEM of column A	1.000 ± 0.05774 N=3
Mean ± SEM of column B	0.6633 ± 0.2018 N=3
Difference between means	0.3367 ± 0.2099
95% confidence interval	-0.2459 to 0.9193
R squared	0.3915
F test to compare variances	
F, DFn, Dfd	12.21, 2, 2
P value	0.1514
P value summary	ns
Are variances significantly different?	No

Table xiii: ANOVA test for LASS5 in Caco-2 cells after 48h apoptosis treatment

Table Analysed	**Data 1**
Column A	L5 Caco-2 oh
vs	vs
Column B	L5 Caco-2 48h
Unpaired t test	
P value	0.0003
P value summary	***
Are means signif. different? (P <0.05)	Yes
One- or two-tailed P value?	Two-tailed
t, df	t = 11.85, df = 4
How big is the difference?	
Mean ± SEM of column A	1.000 ± 0.05774 N=3
Mean ± SEM of column B	0.1333 ± 0.04485 N=3
Difference between means	0.8667 ± 0.07311
95% confidence interval	0.6637 to 1.070
R squared	0.9723
F test to compare variances	
F, DFn, Dfd	1.657, 2, 2
P value	0.7526
P value summary	ns
Are variances significantly different?	No

Table xiv: ANOVA test for LASS5 in HT-29 cells after 24h apoptosis treatment

Table Analysed	**Data 1**
Column A	L5 HT-29 oh
vs	vs
Column B	L5 HT-29 24h
Unpaired t test	
P value	P <0.0001
P value summary	***
Are means signif. different? (P <0.05)	Yes
One- or two-tailed P value?	Two-tailed
t, df	t = 16.15, df = 4
How big is the difference?	
Mean ± SEM of column A	1.000 ± 0.05774 N=3
Mean ± SEM of column B	0.05667 ± 0.008819 N=3
Difference between means	0.9433 ± 0.05840
95% confidence interval	0.7812 to 1.105
R squared	0.9849
F test to compare variances	
F, DFn, Dfd	42.86, 2, 2
P value	0.0456
P value summary	*
Are variances significantly different?	Yes

Table xv: ANOVA test for LASS5 in HT-29 cells after 48h apoptosis treatment

Table Analysed	Data 1
Column A	L5 HT-29 oh
vs	vs
Column B	L5 HT-29 48h
Unpaired t test	
P value	P <0.0001
P value summary	***
Are means signif. different? (P <0.05)	Yes
One- or two-tailed P value?	Two-tailed
t, df	t = 16.92, d f= 4
How big is the difference?	
Mean ± SEM of column A	1.000 ± 0.05774 N=3
Mean ± SEM of column B	0.01667 ± 0.006667 N=3
Difference between means	0.9833 ± 0.05812
95% confidence interval	0.8220 to 1.145
R squared	0.9862
F test to compare variances	
F, DFn, Dfd	75.00, 2, 2
P value	0.0263
P value summary	*
Are variances significantly different?	Yes